Functional Role of New Aldosterone Regulated Gene Products

Dissertation

zur

Erlangung der naturwissenschaftlichen Doktorwürde
(Dr. sc. nat.)

vorgelegt der

Mathematisch-naturwissenschaftlichen Fakultät

der
Universität Zürich

von

Gabriele Adam

aus
Deutschland

Promotionskomitee

Prof. Dr. François Verrey
Prof. Dr. Olivier Staub
Prof. Dr. Thomas Lutz

Zürich, 2008

From June 2005 until May 2008 I was member of the PhD-Program
in integrative and molecular physiology of the

Zurich Center for Integrative Human Physiology (ZIHP)

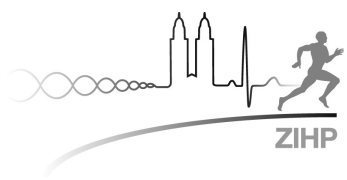

INDEX

1 Summary

The kidney regulates the body's fluid volume, mineral composition and acidity by excretion and reabsorption of electrolytes and water. The ability of the kidney to regulate salt homeostasis and extracellular fluid volume is crucial for blood pressure maintenance. The mineralocorticoid hormone aldosterone adjusts salt homeostasis largely by regulating sodium reabsorption across principal cells of the aldosterone-sensitive distal nephron (ASDN). The stimulatory action of aldosterone on sodium reabsorption in the distal nephron has been shown to depend mainly on transcriptional regulation that is mediated by the activation of the mineralocorticoid receptor, a member of the family of nuclear receptors. Early genomic effects on sodium reabsorption are thought to be mediated mostly by the induction or repression of elements of the regulatory pathways that control the function of preexisting epithelial sodium channel (ENaC), sodium potassium pump (Na^+-K^+-ATPase) and potassium channel (ROMK). Aldosterone regulates the cell-surface expression and function and subsequent internalization of ENaC in its target cells partly by the transcriptional induction of the serum- and glucocorticoid-regulated kinase 1 (Sgk1). This kinase prevents the ubiquitylation of ENaC by phosphorylating the ubiquitin ligase Nedd4-2.

The aim of my project was to investigate the mechanism by which the early aldosterone-induced changes in gene expression impact on sodium and potassium transport in aldosterone target cells in the kidney. A microarray of RNA extracted from mouse epithelial cells of the ASDN had identified 22 significantly and more than two-fold early aldosterone-regulated RNA *in vivo*. The focus of this work was on three of these significantly up-regulated gene products: the ubiquitin-specific proteases Usp2 and Usp53 and the voltage gated proton channel H_v1. In exogenous gene expression systems like *Xenopus laevis* oocytes and cultured mouse cortical collecting duct cells their impact on channels and transporters involved in the sodium absorption in the collecting duct was investigated using electrophysiological techniques.

A pronounced induction of ENaC mediated currents by the co-expression of the Usp2 isoform Usp2-45 was detected using two-electrode voltage-clamp recordings. The stimulatory effect on ENaC was not additive to that of Sgk1. This suggests that Usp2-45

acts on the same regulatory pathway as Sgk1, namely the ubiquitylation/deubiquitylation of ENaC. The stimulation of ENaC is further due to the catalytic action of Usp2-45 since substitution of Cys67 with Ala within the catalytic site of Usp2-45 abolished its effect. Further experiments performed in cultured human embryonic kidney cells showed that indeed Usp2-45 deubiquitylates and thereby activates ENaC.

Another ubiquitin-specific protease, Usp53 was significantly up-regulated in the mouse distal nephron. Experiments aiming at investigating the possible impact of Usp53 on sodium transport molecules (ENaC, Na^+-K^+-ATPase) expressed in *Xenopus laevis* oocytes were inconclusive and the role of Usp53 in regulating salt reabsorption remains elusive.

The third investigated gene product, a voltage gated proton channel (H_v1) structurally resembles the voltage sensor of typical voltage gated channels of the S4-family. H_v1 substantially decreases ENaC and ROMK function in oocytes which appears contradictory to the fact that it is up-regulated by aldosterone. However, early up-regulation of a voltage gated proton channel in the ASDN could be essential in the regulatory control of salt reabsorption fine tuning by aldosterone.

2. Zusammenfassung

Die Nieren sind für die Aufrechterhaltung des Flüssigkeitsvolumens, der Salzzusammensetzung und des Säure-Base-Haushaltes des Körpers zuständig. Dies geschieht durch Ausscheidung und Reabsorption von Elektrolyten und Wasser. Die Regulierung des Salzhaushaltes und des Volumens der extrazellulären Flüssigkeit ist für die Aufrechterhaltung des Blutdrucks essentiell. Das Mineralokortikoidhormon Aldosteron regelt den Salzhaushalt vor allem durch die Stimulation der Natriumrückresorption durch die Hauptzellen des Aldosteron sensitiven distalen Nephrons (ASDN).

Die Wirkung von Aldosteron auf die Rückresorption von Natrium im distalen Nephron hängt vor allem von der Regulierung der Transkription ab. Diese Aufgabe übernimmt der Mineralokortikoidrezeptor, der zur Familie der nukleären Rezeptoren gehört und durch Aldosteron aktiviert wird. Rasche Änderungen der Transkription wirken sich innerhalb kurzer Zeit auf die Natriumrückresorption aus. Dies wird grösstenteils durch die transkriptionelle Aktivierung und Repression von regulatorischen Faktoren erreicht, die die Funktion von bereits vorhandenen Natriumkanälen (ENaC), Natriumpumpen (Na^+-K^+-ATPase) und Kaliumkanälen (ROMK) regulieren. Es ist bekannt, dass die Oberflächenexpression und die Funktion von ENaC teilweise durch die transkriptionelle Aktivierung von Sgk1 gesteigert werden. Sgk1 ist eine Kinase, welche die Ubiquitylierung von ENaC verhindert, indem sie die Ubiquitin Ligase Nedd4-2 phosphoryliert und so deren Funktion inhibiert. Das Ziel meines Projektes war es, Mechanismen zu untersuchen, durch welche frühe Aldosteron-induzierte Veränderungen der Genexpression zur Regulation von Natrium und Kalium Transport in Aldosteron Zielzellen führen.

Mit Hilfe eines RNA-Microarrays konnten 22 mRNAs identifiziert werden, die in Epithelialzellen des ASDN durch Aldosteron mehr als zweifach hochreguliert sind. Im Fokus dieser Arbeit lagen drei dieser Genprodukte: Die Ubiquitinproteasen Usp2 und Usp53 und ein spannungsabhängiger Protonenkanal (H_v1). Ihr Einfluss auf Kanäle und Transporter, die bei der Natriumrückresorption wichtig sind, wurde vor allem anhand von elektrophysiologischen Methoden an Expressionsystemen wie *Xenopus laevis* Oozyten

und kultivierten Sammelrohrzellen aus der Maus untersucht. Elektrophysiologische Messungen an koexprimierenden *X. laevis* Oozyten zeigten, dass die Funktion von ENaC durch eine Isoform von Usp2 (Usp2-45) signifikant verstärkt wird. Dieser stimulierende Effekt von Usp2-45 auf ENaC ist nicht additiv zu dem bereits beschriebenen Effekt von Sgk1. Das bedeutet, dass Usp2-45 in dem Selben Regulationsmechanismus eingebunden ist wie Sgk1, nämlich Ubiquitylierung / Deubiquitylierung. Es konnte weiterhin gezeigt werden, dass die Stimulierung von ENaC auf die katalytische Aktivität von Usp2-45 zurückzuführen ist, da durch die Cys67Ala Substitution im katalytischen Zentrum der stimulatorische Effekt von Usp2-45 ausblieb. Weitere Experimente mit kultivierten menschlichen embryonalen Nierenzellen wiesen darauf hin, dass Usp2-45 ENaC in der Tat deubiquityliert und dadurch aktiviert.

Im distalen Nephron der Maus ist die mRNA Expression von Usp53, einer weiteren Ubiquitinprotease, ebenfalls durch Aldosteron signifikant hochreguliert. Experimente zur Erforschung ihres möglichen Einflusses auf Natriumtransportmoleküle wurden in *X. laevis* Oozyten durchgeführt. Die Ergebnisse waren jedoch kontrovers und es bleibt unklar, welche Rolle Usp53 bei der Regulation der Salzrückresorption spielt.

Ferner wurde ein Genprodukt untersucht, welches einen spannungsabhängigen Protonenkanal (H_v1) kodiert. Dieser weist eine strukturelle Ähnlichkeit zu dem Sensordomäne von typischen spannungsabhängigen Ionenkanälen der S4 Familie auf. Werden die beiden Ionenkanäle ENaC und ROMK zusammen mit H_v1 exprimiert, verringert sich deren Funktion signifikant. Dieser Effekt steht im Widerspruch zur Aktivierung von H_v1 durch Aldosteron. Die frühe Regulation eines spannungsabhängigen Protonenkanals im ASDN könnte allerdings für die Feinabstimmung der Salzrückresorption durch Aldosteron bedeutungsvoll sein.

3 Introduction

3.1 Structure and function of the kidney

The kidneys are a pair of vertebrate organs situated in the body cavity near the spinal column. They are responsible for removal of toxic substances from the body and are involved in the maintenance of water and electrolyte balance of the whole body. In addition kidneys are endocrine organs which produce and secrete hormones that are involved in the regulation of erythrogenesis, calcium metabolism and the regulation of blood pressure. The functional unit of the kidney is the nephron, the structure of which is crucial to accomplish multiple functions of the kidney (Boron W F 2005).

3.1.1 The nephron

The nephron is the functional unit of the kidney. One human kidney consists of around one million nephrons. A nephron is divided in different segments that can be distinguished by function and ultrastructure.

Table 1

Segment	**Abbreviation**
Glomerulus	
Proximal convoluted tubule	PCT
Proximal straight tubule	PST
Thin descending limb of the loop of Henle	tDLH
Thin ascending limb of the loop of Henle	tALH
Thick ascending limb of the loop of Henle	TAL
Distal convoluted tubule	DCT
Connecting tubule	CNT
Cortical collecting duct	CCD
Outer medullary collecting duct	OMCD
Inner medullary collecting duct	IMCD

Some of the mentioned segments can further be divided into subsegments, which is explained more in detail in the following section.

In the **glomerulus** primary urine is produced from the blood by filtration across the wall of small capillaries that are set up in a tuft like structure within the surrounding Bowman's space which leads the primary urine to the tubular lumen. Solute concentrations in the ultrafiltrate are similar to the concentrations in the plasma. The main task of the glomerular filter is to prevent red and white blood cells and large proteins to enter the tubular lumen. The passage of proteins through the filter depends on their size and charge. The ultrafiltrate is subsequently processed to final urine while flowing through the following nephron segments. The main bulk of the filtered fluid and solutes is then reabsorbed by the epithelial cells of the nephron tubules.

Figure 1

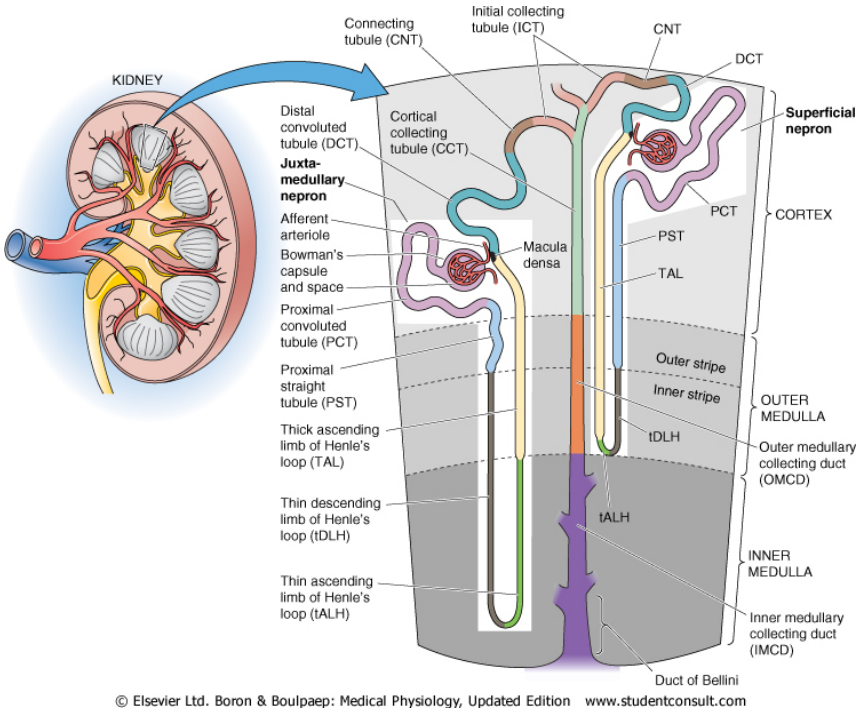

Figure 1: *Anatomy of the kidney*. On the left side of the figure, an anatomical view of the kidney is shown. The right side illustrates the structure of two nephrons. A juxtamedullary nephron is shown on the left side and a superficial one on the right side. Different colours depict the different segments of the nephrons. This figure was taken from Boron and Boulpaep: Medical Physiology (Boron W F 2005).

Following the glomerulus the largest fraction of the ultrafiltrate is retrieved by the **proximal tubule** (PT). It reabsorbs nearly 100 % of the most important nutrients like amino acids or glucose and the biggest portion of solutes and water without changing the osmolality of the filtrate. Together with two third of the filtered fluid a large fraction of NaCl, $NaHCO_3$ as well as divalent ions are reabsorbed and delivered back to the body. Structurally the PT can be divided into three distinct segments: S1, S2 and S3. These segments mainly differ in their ultrastructure and particular function. The S1 segment is located directly after the glomerulus and belongs to the proximal convoluted tubule (PCT). The S2 segment is also part of the PCT but differs from S1 in terms of specific functional issues. The proximal straight tubule (PST) which is following the PCT can be equated to S3 and recognized by its distinct structure (Boron W F 2005).

The S3 segment of the PT is followed by the **loop of Henle** that is divided into the tDLH, tALH and the TAL (Table 1). The main function of the loop of Henle is to participate in the formation of concentrated urine. To accomplish the formation of urine concentration the subsegments of the loop of Henle have distinct functional features. The function of the loop of Henle is to produce an increasing osmotic gradient from the cortex to the tip of the renal papilla by the *counter-current multiplier* mechanism. The thin limbs are lined with epithelium which has no capacity for active transport but allows diffusion. The tDLH has a great permeability for water but only low permeability for ions and urea. This leads to an increased osmolarity of the tubular fluid since the surrounding interstitial fluid is highly osmolar. In contrast the tALH and the TAL are not permeable to water. The **TAL** (Table 1) is very important for setting a concentration gradient between the interstitium and the tubular lumen by actively pumping ions against its gradient from the lumen into the interstitium. Since the TAL is water impermeable it is creating a hypotonic tubular fluid. As a result urine osmolality in the following collecting ducts can far exceed that of the plasma considering that water can cross their epithelia driven by the high osmolarity in the surrounding interstitium. The region where the TAL “contacts” the glomerulus is called **juxtaglomerular apparatus** (JGA). The JGA is important for giving regulatory feedback from the TAL directly towards the glomerulus. Parts of the JGA are in charge to sense the current NaCl concentration in the tubular lumen and to provide

specific signals to start regulatory mechanisms as described later more in detail (Boron W F 2005).

The **classic distal tubule** can be divided into three different parts: the distal convoluted tubule (DCT), the connecting tubule (CNT) and the initial collecting duct. The classical distal tubule and the collecting duct system (CCD, OMCD, IMCD) are primarily sites for the fine tuning of salt and water excretion (Table 1). Several hormones carry out their main effects on electrolyte and water excretion at these sites, including the mineralocorticoid hormone aldosterone and vasopressin (Boron W F 2005). Aldosterone action in the kidney is mainly taking place in the aldosterone sensitive distal nephron (ASDN) which consists of the second part of the DCT, the CNT, the CCD and the medullary collecting ducts (OMCD and IMCD) (Table 1). These nephron segments exhibit distinct structural and functional features that allow the reabsorption of salt and water under strict regulation. The DCT, CNT, CCD and medullary collecting ducts are composed of two different cell types (principal cells and intercalated cells) that show striking differences in function and morphology (Wall 2005). One third of the cell population consists of intercalated cells and two thirds of principal cells. Intercalated cells are separated in two subpopulations: α and β intercalated cells. Each of these cell types exhibits a specialized morphology and function. Principle cells are the classical target cells of the mineralocorticoid hormone aldosterone that triggers the salt and water reabsorption in the ASDN (Boron W F 2005).

3.2 Blood pressure is regulated by the kidney

The kidneys regulate the body's fluid volume, mineral composition and acidity by excreting and reabsorbing water and inorganic electrolytes. They help to balance these solutes (which include Na^+, K^+, Cl^-, Ca^{2+}, Mg^{2+}, phosphate and protons) in the body and keep their normal concentrations in the extracellular fluid. Body fluid volume is directly associated to blood volume and the arterial blood pressure. The ability of the kidney to regulate salt homeostasis and extracellular fluid volume within the whole body is crucial for blood pressure maintenance. Changes in blood pressure are sensed by receptors which generate distinct hormonal and neuronal signals. The kidney has the ability to adjust body fluid volume and its osmolality in response to these signals. For instance, a decrease of the extracellular fluid volume is followed immediately by the stimulation of hormonal effector pathways, such as the renin-angiotensin-aldosterone system (RAAS) and the inhibition of Atrial Natriuretic Peptide (ANP) (Boron W F 2005).

Since the extracellular osmolality has per se to be kept constant and also may reflect the status of general body water content it is an important issue to regulate it as tightly as possible. Dehydration of the body leads to an increased plasma osmolality that is sensed by special receptors in the hypothalamus. The activation of these osmoreceptors subsequently leads to the release of the neuropeptide hormone arginine vasopressin (AVP, antidiuretic hormone) that is synthesized in the hypothalamus. AVP acts in the collecting duct where it increases water reabsorption via the regulation of water channel trafficking (Boron W F 2005).

3.2.1 Atrial Natriuretic Peptide (ANP)

ANP promotes natriuresis (Na^+-excretion) in response to an increase in blood pressure. Stretch receptors located in the atrial myocytes sense high blood pressure and release signals that lead to liberation of ANP from intracellular stores into the circulation (Boron W F 2005). ANP has synergistic effects that activate renal Na^+ and water excretion. It directly inhibits Na^+ transport in the medullary collecting ducts, decreases the release of

renin and increases the glomerular flitration rate. However the major effect of ANP is hemodynamic, because it triggers renal vasodilatation and massively increases renal blood flow which supports the activation of salt and water secretion (Boron W F 2005).

3.2.2 The Renin Angiotensin Aldosterone System RAAS

The RAAS is an integrative system that links the cardiovascular system to the renal functions by regulating salt and water homeostasis and therefore the blood pressure. Renin is an endopeptidase that had first been identified in the kidney, specifically in the cells of the JGA. It cleaves the circulating alpha 2 globulin angiotensinogen that is mainly synthesized in the liver and fat tissue and generates the dekapeptide angiotensin I (Williams 2005). Angiotensin I is an inactive molecule that is converted to the active octapeptide angiotensin II (AngII) by the angiotensin converting enzyme (ACE), which is localized in vascular endothelial cells in many tissues of the body (Williams 2005) (Boron W F 2005). AngII has two main distinct effects on the regulation of blood pressure: It directly mediates vasoconstriction and it regulates production and release of aldosterone (Figure 2) (Boron W F 2005).

Figure 2

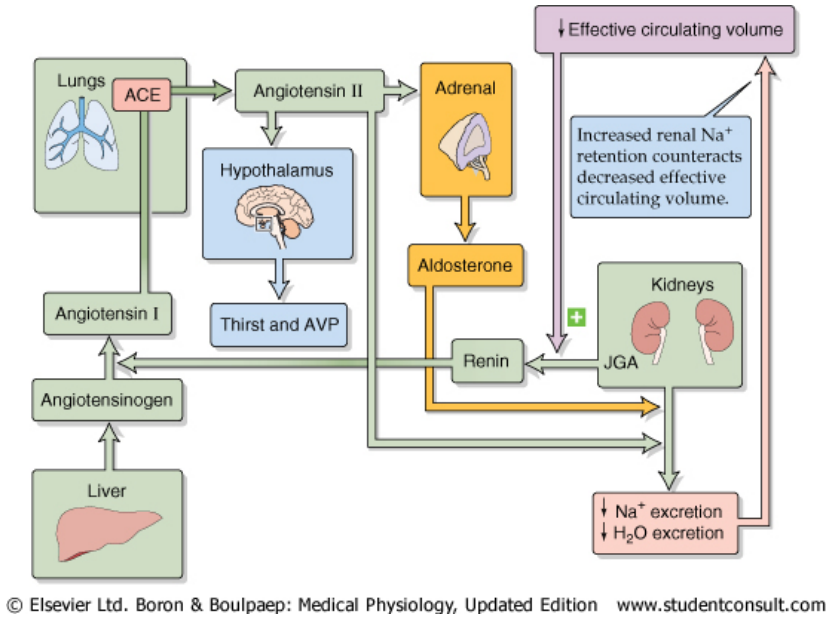

Figure 2: *The Renin-Angiotensin-Aldosterone System*. This hormonal pathway integrates different organs and exhibits some important feedback mechanisms. JGA = juxtaglomerular apparatus, ACE = angiotensin converting enzyme. This figure was adopted from Boron and Boulpaep: Medical Physiology (Boron W F 2005).

The release of renin from specialized granular cells in the JGA is regulated by several factors including renal perfusion pressure, beta adrenergic stimulation, potassium, AngII and ANP (Williams 2005). The most important regulatory mechanism is triggered by the renal perfusion pressure. Changes in perfusion pressure are sensed by baroreceptors located in the afferent arteriole that send signals to the granular cells modifying the level of renin release. A decrease in blood pressure leads to an increase in renin release and subsequently to an increase in aldosterone production.

In addition to the above mentioned systemic RAAS, several tissues and organs have been found to have their own local RAAS (Tahmasebi, Puddefoot et al. 1999). Such local RAASs have been found to either potentiate the systemic functions or have completely separate actions to adjust the specific local functions of their particular tissues and organs. These effects are normally mediated in a paracrine and autocrine manner (Cooper and Boner 2004).

Angiotensin II (AngII)

AngII has various functions in different target organs that are mediated by distinct mechanisms. On the one hand it stimulates AngII receptors on smooth muscle cells, to induce vasoconstriction mediated by a direct release of intracellular calcium. These actions of AngII are increased by high levels of salt concentration in the body. Furthermore AngII also acts on brain where it activates thirst and the release of specific hormones from the hypophysis, in particular arginine vasopressin (AVP) and adrenocorticotropic hormone (ACTH) (Figure 2) (Chung O 2006). To finally increase renal Na^+ reabsorption and thereby increase the volume of extracellular fluid and blood pressure AngII alters renal hemodynamics in different ways (Figure 2). The hemodynamic effects of AngII on the one hand lead to an increase in the glomerular filtration fraction by increasing the constriction of the efferent but not the afferent arterioles. On the other hand they enhance the Na^+ absorption in the IMCD by decreasing the medullary blood flow and thereby minimizing the medullary washout. Another important task of AngII is to raise the sensitivity of specialized feedback mechanisms in the JGA that trigger the glomerular filtration rate (Boron W F 2005). It also exhibits a direct effect on the Na^+ absorption in the renal tubules by increasing the abundance of Na^+-proton exchangers in the TAL as well as Na^+ channels in the ICT. This effect is then enhanced by the activation of hypertrophy in the renal tubular system. Last but not least AngII activates the synthesis and release of aldosterone in the adrenal glands (Figure 2). As soon as AngII is binding to the AngII receptor AT1 on the plasma membrane of granulosa cells in the adrenal cortex a cascade of different intracellular signals leads to the production and release of the mineralocorticoid hormone aldosterone. This hormone is the major regulator of salt balance and extracellular fluid (ECF) volume in the human body which is a prime determinant of arterial blood pressure (Figure 2) (Boron W F 2005).

Aldosterone

One of the most important regulators of salt and water handling in the distal nephron is the mineralocorticoid hormone aldosterone. It is synthesized from cholesterol in a series of enzymatic reactions in the granulosa cells located in the cortex of the adrenal gland (Williams 2005). Aldosterone production is essentially restricted to these specialized cells, because the last step of the synthesis is done by the enzyme aldosterone synthase which is present in these cells (Boron W F 2005). Around 75% of the circulating aldosterone is inactivated by the liver. Aldosterone inactivation in the kidney leads to a glucuronide conjugate which is used as a diagnostic indicator for aldosterone production measured in the urine (Williams 2005).

Synthesis and release of aldosterone by the adrenal gland is regulated by different factors. K^+ directly activates the aldosterone production via direct action on the glomerulosa cells (Williams 2005) (Figure 2). High K^+ levels depolarize the plasma membrane of these cells which leads to an intracellular signalling cascade and subsequently to the synthesis and release of aldosterone (Boron W F 2005). K^+ is the mediator of a short feedback loop, since aldosterone increases renal excretion of K^+. AngII activates aldosterone release by binding to AT1 receptors on the surface of glomerulosa cells. A signal cascade that involves the $G_{\alpha q}$-mediated pathway to stimulate phospholipase C (PLC) leads to the release of intracellular Ca^{2+}. The rise in Ca^{2+} is primarily responsible for triggering synthesis and secretion of aldosterone. Other regulators of aldosterone secretion are mainly involved in the response to stress, like ACTH, endothelin or serotonin. They generally have minor impact on the release of aldosterone (Boron W F 2005).

Aldosterone has diverse effects in different tissues. It is known, that it acts on epithelial as well as nonepithelial tissues in genomic as well as nongenomic ways mostly to regulate salt homeostasis. In the cardiovascular system aldosterone promotes cardiac hypertrophy, fibrosis and abnormal vascular endothelial function, while in the CNS it impacts on blood pressure control, salt appetite and sympathetic tone (Young and Funder 2000). These latter effects are mediated by the Mineralocorticoid Receptor (MR) and are considered to be genomic. As mentioned above aldosterone was found to trigger also nongenomic rapid effects that appear already after seconds or minutes and that are not sensitive to inhibitors for translation and transcription, like actinomycin and cyclohexamide. These actions are

considered to be independent of direct effects on gene expression (Booth, Johnson et al. 2002). Many of these nongenomic effects are not blocked by MR antagonists implicating, that they are not mediated by the MR but by a nonclassical aldosterone receptor. However a nonclassical receptor for aldosterone was not yet found and it is still unclear whether nongenomic actions can be mediated by the MR (Good 2007). Nevertheless, nongenomic actions of aldosterone have impact on a number of ion transport proteins in the renal tubule that are involved in absorptive and secretory functions. Different studies showed that ion transport proteins like the Na^+ proton exchanger 1 and 3 (NHE1, NHE3), the H^+-ATPase, the Epithelial Na^+ Channel (ENaC) and the Na^+-K^+-ATPase are regulated within minutes by aldosterone, indicating to be a nongenomic effect. It was suggested that these actions of aldosterone are more important for responses mediated by the local aldosterone production (Connell and Davies 2005).

The classic action of aldosterone is the regulation of salt and water reabsorption in the ASDN (Rozansky 2006). The ASDN as well as other aldosterone sensitive epithelia exhibit special characteristics: They are tight epithelia with high resistance tight junctions. Aldosterone is able to increase their permeability to Na^+ by increasing the activity of ENaC and the basolateral Na^+-K^+-ATPase. Furthermore the extrusion of K^+ and protons is augmented. As a consequence water follows the movement of Na^+ across the epithelium, which results in an increase in the extracellular fluid volume, blood volume and blood pressure.

3.2.3 Arginine Vasopressin (AVP)

AVP is a neuropeptide hormone that acts on the collecting duct to increase water reabsorption. The release of AVP can be stimulated by a decrease in arterial blood pressure, an increase in ECF osmolarity as well as by the action of AngII (Boron W F 2005). Water permeability is increased by AVP in all nephron segments beyond the DCT. AVP dramatically increases water permeabilities of the collecting tubules and ducts by causing aquaporin 2 (AQP2) water channels to insert into the apical membrane. Water channels present in the basolateral membrane of these nephron segments are not sensitive to AVP (Boron W F 2005).

3.3 The aldosterone sensitive distal nephron (ASDN)

The ASDN is the most important site of the regulated salt and water reabsorption. It is defined by the coexpression of ENaC, 11-β-hydroxysteroid dehydrogenase type 2 and MR. These features are given for the late part of the DCT (DCT2), the CNT and the collecting ducts. The classic aldosterone target cells are the principal cells of the collecting duct, although intercalated cells are also in some respect sensitive to aldosterone. For example, it was shown that aldosterone has a nongenomic effect on the activity of the proton pump that is expressed in α- intercalated cells but not in principal cells (Winter, Schulz et al. 2004). In the following chapters I am going to focus on the mechanisms and effects of the classical model of aldosterone action in the ASDN.

3.3.1 The principal cells of the ASDN

The Na^+ reabsorption in the ASDN is transcellular and mediated by the majority cell type: the principal cells (Boron W F 2005) (Figure 3). Sodium ions have to cross the apical and the basolateral membrane of principal cells. Specialized Na^+ channels (ENaC) in the apical membrane mediate a central step of the Na^+ absorption over this tight epithelium (Figure 3). ENaC functions under tight control and is the limiting factor of the Na^+ absorption. The regulation of its functional expression in the apical membrane is crucial for the amount of salt and water reabsorbed.

To protect the cells from Na^+ overload, ATP driven Na^+ pumps are located in the basolateral side (Na^+-K^+-ATPase) (Figure 3). These pumps exchange 3 sodium ions for 2 potassium ions by hydrolyzing one ATP. The Na^+-K^+-ATPase is basically expressed in every cell in the body and has mainly the tasks of a housekeeping protein. Nevertheless this pump is crucial for Na^+ reabsorption in the principal cells since it is providing the electrochemical driving force for the apical Na^+ entry (Boron W F 2005). The cell surface expression and function of the Na^+-K^+-ATPase is also regulated by aldosterone (Zecevic, Heitzmann et al. 2004).

Figure 3

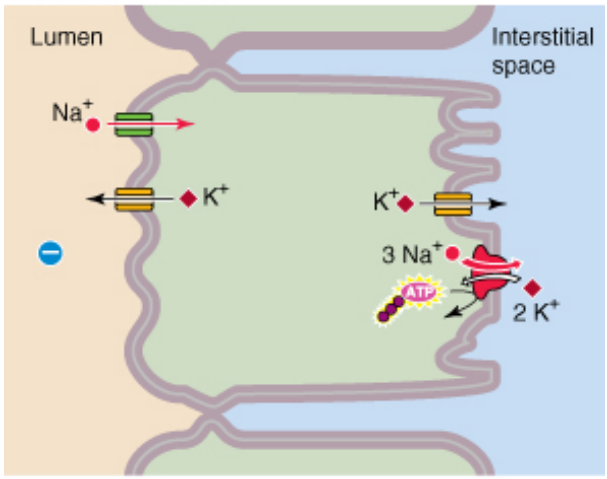

Figure 3: *Scheme of a principal cell in the cortical collecting duct.* On the luminal or apical side Na^+ and K^+ channels are expressed. The basolateral side of this epithelial cell faces the interstitial space and expresses the Na^+-K^+-ATPase and also K^+ channels. This figure was taken from Boron and Boulpaep: Medical Physiology (Boron W F 2005).

Since the Na^+-K^+-ATPase is exchanging K^+ for Na^+ it is necessary for the cell to release K^+. Therefore K^+ channels are expressed in the apical and in the basolateral membrane of principal cells that are in charge of releasing potassium from the cell (Figure 3). The apically expressed potassium channel is additionally in charge to oppose the lumen negative potential generated by the entry of Na^+. The regulation of function and expression of the apical renal outer medullary potassium channels (ROMK) is partly mediated by aldosterone (Fuller and Young 2005).

3.3.2 Classical action of aldosterone in the ASDN

Aldosterone's action is divided into three distinct phases: The rapid nongenomic, the early and the late action (Verrey 1998). Nongenomic effects of aldosterone were described before. The late action of aldosterone is predominantly a chronic effect that occurs after three to six hours and is characterized by an increase in the number of ENaC and Na^+-K^+-ATPase in the membranes of the epithelial cells (Verrey 1998). Subsequently, a long term exposure to aldosterone induces morphological changes in the

target cells for example an increase in the surface of the basolateral membrane (Kaissling and Le Hir 1982).

Early genomic aldosterone effects, mediated by the mineralocorticoid receptor (MR), occur already after 20 minutes. These actions are important for a quick reaction to environmental changes by rapid activation of the Na^+ transport machinery in the ASDN. This challenge is achieved by the activation of a preexisting pool of transport proteins through the increase of trafficking to the membrane or through direct channel or pump activation. The major regulatory site of transepithelial Na^+ transport across tight epithelia is ENaC (Verrey 1998). Early actions of aldosterone are suggested to be mediated by regulatory proteins that are transcriptionally activated via the MR. These regulatory proteins act presumably on the preexisting pool of transport proteins like ENaC (Lu, Pribanic et al. 2007; Harris, Garcia-Caballero et al. 2008) (Figure 4). The aim of my work was to find players of the early aldosterone response that are regulated by the MR and that modulate directly the Na^+ transport machinery in the aldosterone target cells.

Since aldosterone belongs to the class of steroid hormones it is able to enter cells by diffusion through the plasma membrane. It binds to the MR in the cytoplasm and the MR-aldosterone complex subsequently translocates to the nucleus where it functions as a transcription factor (Boron W F 2005). The MR dimerizes and binds to specific steroid response elements (SRE) in the DNA to positively or negatively regulate the expression of responsive genes (Walter F. Boron 2005; Thomas, McEneaney et al. 2007). The MR reflects a high degree of similarity to the glucocorticoid receptor (GR) in terms of DNA and ligand binding domains (Connell and Davies 2005). MRs are mainly expressed in aldosterone target tissues whereas GRs are ubiquitously expressed. Glucocorticoid hormones (like cortisol and corticosterone) and aldosterone bind with approximately the same high affinity to the MR and lower affinities to the GR. Since plasma levels of glucocorticoids are more than 100fold greater than that of aldosterone, glucocorticoids would be likely to occupy the MR under most circumstances.

Figure 4

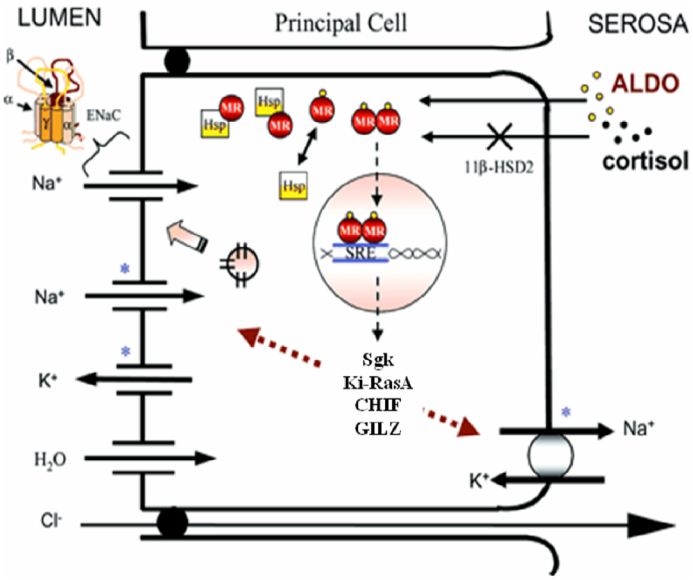

Figure 4: *Model of the classical aldosterone action in a principal cell.* The asterisks assign final effectors of aldosterone that are participating in the transepithelial Na^+ and K^+ transport. The early aldosterone induced proteins (Sgk, Ki-RasA (K-Ras2), CHIF, GILZ) modulate the activity of effector transport proteins. Hsp = Heat shock protein, MR = mineralocorticoid receptor, GR = glucocorticoid receptor, SRE = Steroid response element, 11β-HSD2 = 11-β-hydroxysteroid dehydrogenase type 2. This figure is adapted from Booth, Johnsen et al 2002.

In 1988 a protein was found that prevents MR from binding to glucocorticoids: The enzyme 11-β-hydroxysteroid dehydrogenase type 2 (11β-HSD2). It protects the MR from glucocorticoid occupancy by converting glucocorticoids into inactive metabolites which have little affinity to the MR (Figure 4) (Booth, Johnson et al. 2002). Mutations of the gene encoding 11β-HSD2 results in the syndrome of apparent mineralocorticoid excess which is inherited in an autosomal recessive manner in humans (Connell and Davies 2005).

The early action of aldosterone on ion transport already appears after half an hour. Since transcription, translation, posttranslational modification and trafficking of a substantial portion of the involved transport proteins together takes more than one that it can be expected that for instance ENaC is not regulated directly by transcriptional activation within the early aldosterone response. The common idea is that early effects of

aldosterone on ENaC are due to a reversible activation of preexisting transport proteins (Booth, Johnson et al. 2002). In contrast long term exposure to aldosterone results in a transcriptional induction of the α-subunit of ENaC in the ASDN while γ- and β-subunits are not regulated at that level (Snyder 2005). The activation of a preexisting pool of Na^+ channels is thus mediated by regulatory proteins. In the following section I am going to focus on a number of early aldosterone regulated gene products that where found to be regulators of the transepithelial Na^+ transport (Spindler, Mastroberardino et al. 1997; Naray-Fejes-Toth 1999; Naray-Fejes-Toth, Canessa et al. 1999).

The best studied early aldosterone induced gene product that affect ENaC mediated Na^+ reabsorption is the serum and glucocorticoid activated kinase Sgk1. This is a serine-threonine kinase that phosphorylates the ubiquitin ligase Nedd4-2 (Neural precursor-expressed and developmentally down-regulated protein 4-2). Nedd4-2 was shown to transfer ubiquitin to ENaC and to target it therefore for endocytosis (Kamynina, Debonneville et al. 2001; Kamynina, Debonneville et al. 2001). Since Sgk1 inhibits Nedd4-2 action by phosphorylation surface expression of ENaC increases based on a decrease of its endocytosis (Bhalla, Soundararajan et al. 2006; Rozansky 2006). It was also reported that Sgk1 increases the density of ROMK channels in the plasma membrane (Fuller and Young 2005). Next to ENaC and ROMK also the basolateral surface expression of the Na^+-K^+-ATPase is controlled by Sgk1 (Verrey, Summa et al. 2003; Zecevic, Heitzmann et al. 2004). Since Sgk1 also colocalizes with the Na^+-K^+-ATPase in the kidney it is tempting to propose that Sgk1 is a key player in mediating a coordinated aldosterone response in the ASDN (Verrey, Summa et al. 2003; Zecevic, Heitzmann et al. 2004; Lang, Capasso et al. 2005).

Nevertheless Sgk1 is not the only kinase that has an impact on the Na^+ transport machinery in the ASDN and is regulated by aldosterone on the transcriptional level after a short time. The transcription of a specific isoform of the With No Lysine Kinases (Kindney-specific WNK1, KS-WNK1), that is specifically expressed in the ASDN is also sensitive to aldosterone (Naray-Fejes-Toth, Snyder et al. 2004; O'Reilly, Marshall et al. 2006). KS-WNK1 was also shown to increase transepithelial Na^+ currents in mouse collecting duct cells. Since the KS-WNK1 isoform lacks the kinase domain it is proposed, that this effect is mediated via protein/protein interactions rather then a kinase activity.

KS-WNK1 does not have any effect on ENaC that carries a mutation in the Nedd4-2 binding motif. This leads to the presumption that Nedd4-2 could be a target molecule of that kinase (Naray-Fejes-Toth, Snyder et al. 2004; Subramanya, Yang et al. 2006). However, the exact mechanism of the KS-WNK1 action on transepithelial Na^+ transport is still not fully understood (Subramanya, Yang et al. 2006).

The ubiquitin ligase Nedd4-2 is also a target of the 14-3-3 protein. 14-3-3 proteins are highly conserved regulatory proteins that in general bind to phosphorylated motifs within their target proteins and function as homo- and heterodimers (Aitken 2002; Yaffe 2002; Wilker and Yaffe 2004). 14-3-3 proteins modulate the expression of ENaC probably by blocking the interaction of ENaC with Nedd4-2 and therefore inhibiting ENaC ubiquitylation (Bhalla, Daidie et al. 2005; Ichimura, Yamamura et al. 2005; Liang, Peters et al. 2006). Evidence for this hypothesis was found by Liang et al, showing that specific 14-3-3 isoforms associate selectively with phosphorylated Nedd4-2 in CCD cells (Liang, Peters et al. 2006). The fact that the transcription of 14-3-3 protein isoforms is regulated by aldosterone in mouse CCD epithelia supports the notion that 14-3-3 proteins are key modulators in the regulation of Na^+ transport by aldosterone in the ASDN.

The small G-protein Ki-Ras (K-Ras2A) which is upregulated by aldosterone in amphibian cells increases the function and in the same time decreases surface expression of ENaC in *X. laevis* oocytes (Spindler, Mastroberardino et al. 1997; Mastroberardino, Spindler et al. 1998; Stockand, Spier et al. 1999; Verrey 1999; Rotin 2000; Booth, Johnson et al. 2002). Therefore it was suggested that Ki-Ras plays a role in the mediation of the early effect of aldosterone on Na^+ transport in the ASDN (Spindler, Mastroberardino et al. 1997; Mastroberardino, Spindler et al. 1998; Stockand, Spier et al. 1999; Booth, Johnson et al. 2002; Bhalla, Daidie et al. 2005). Ki-Ras activates ENaC open probability most likely by a GTP-dependent mechanism that is reliant on phosphoinositide 3-OH kinase signaling (Staruschenko, Patel et al. 2004). Conversely, recent in vivo studies displayed that Ki-Ras is upregulated in the rat distal colon but not in the kidney (Brennan and Fuller 2006).

The glucocorticoid-induced leucin zipper protein (GILZ) was also shown to be rapidly induced by aldosterone in mpkCCD_{c14} cells and to increase ENaC mediated Na^+ currents in *X. laevis* oocytes by inhibiting extracellular signal-regulated kinase (ERK) signaling

(Soundararajan, Zhang et al. 2005; Bhalla, Soundararajan et al. 2006). Since ERK signaling is constitutively active, these findings lead to the hypothesis that GILZ plays a role in the early aldosterone mediated regulation of Na^+ transport (Soundararajan, Zhang et al. 2005; Bhalla, Soundararajan et al. 2006).

A further aldosterone-induced protein that modulates the function of the Na^+ transport machinery in the ASDN is the corticosteroid hormone induced factor CHIF (Wald, Goldstein et al. 1996; Wald, Popovtzer et al. 1997). CHIF first identified as an aldosterone-induced protein is an accessory subunit of the Na^+-K^+-ATPase and regulates its function in the colon and in the kidney (Beguin, Crambert et al. 2001). Investigations using a CHIF knock out mouse model support the assumption that it plays a crucial role in maintaining body Na^+ and K^+ homeostasis in aldosterone-responsive tissues (Beguin, Crambert et al. 2001; Goldschimdt, Grahammer et al. 2004).

3.4 The Epithelial Na^+ Channel ENaC

ENaC, the epithelial Na^+ channel, is a Na^+-selective, non-voltage gated non-inactivating ion channel and a member of the ENaC/DEG superfamily. It localizes to the apical membrane of re(absorbing) epithelial cells (Garty and Palmer 1997; Benos and Stanton 1999; Alvarez de la Rosa, Canessa et al. 2000; Kellenberger and Schild 2002; Pochynyuk, Tong et al. 2007). ENaC plays the key role in the movement of electrolytes and water across epithelial barriers in the lung, the kidney, the colon and sweat glands. In concert with the Na^+-K^+-ATPase ENaC allows the directed transepithelial Na^+ transport, since the influx of Na^+ takes place along the electrochemical gradient, which is established by the basolateral Na^+-K^+-ATPase. Several regulatory mechanisms are able to adapt the basolateral efflux and the apical influx of Na^+ (Boron W F 2005).

3.4.1 Structure and function of ENaC

ENaC forms a heteromultimer consistent of three different subunits (α, β, γ), each with two transmembrane spanning domains and a large extracellular domain (~450 amino acids) (Canessa, Horisberger et al. 1993; McNicholas and Canessa 1997; Fyfe and Canessa 1998; Fyfe, Quinn et al. 1998).The comparatively short N- and C-termini (~50-100 amino acids) are located to the cytoplasmic side of the membrane (Canessa, Schild et al. 1994; Renard, Lingueglia et al. 1994; Snyder, McDonald et al. 1994). The three different subunits heteromultimerize to build a pore that is highly selective for sodium ions and sensitive to amiloride at submillimolar concentrations. All three subunits are required for the maximal activity of the channel (Canessa, Horisberger et al. 1993; Canessa, Schild et al. 1994; McNicholas and Canessa 1997; Fyfe and Canessa 1998). The stoichiometry of the heteromultimer is still uncertain. Two different models have been proposed for the stoichiometry of ENaC: The work of Firsov and colleges and Kosari and coworkers suggested ENaC being a heterotetramer with a stoichiometry of α2:β1:γ1(Firsov, Gautschi et al. 1998; Kosari, Sheng et al. 1998). Other investigators showed that the subunits of ENaC are forming a pore each with the same relative ratio: 3α:3β:3γ (Snyder, Cheng et al. 1998; Eskandari, Snyder et al. 1999; Staruschenko,

Medina et al. 2004; Staruschenko, Adams et al. 2005). Recently the structure of the acid sensing ion channel 1 was solved at a resolution of 1.9 Å and showed a heterotrimeric structure (1α:1β:1γ) (Jasti, Furukawa et al. 2007). Since this acid sensing channel is a member of the ENaC/DEG family and closely related to ENaC it is now proposed, that ENaC has a trimeric structure with the stoichiometry 1α:1β:1γ (Canessa 2007). The single channel conductance of ENaC is relatively small, but it is highly selective for Na^+, with a ratio greater than 100:1 over potassium (Canessa 2007). Moreover ENaC exhibits a selectivity for Li^+ over Na^+ by a factor of - 1.3- 1.5:1 (Garty and Palmer 1997) and is to a small extend able to conduct protons (Palmer 1982; Palmer 1987; Garty and Palmer 1997).

ENaC is expressed in many different epithelial tissues where it has the task to absorb and reabsorb Na^+ from the environment or from an extracellular fluid compartment. Its physiological importance is exciting since it was found to be a key player in keeping the balance of Na^+ and K^+ in the body and in extracellular fluids like the mucus in lungs. First Koefoed and Ussing identified a Na^+ conductance at a macroscopic level in the amphibian skin by transepithelial current measurements (Koefoed-Johnsen and Ussing 1958). Later on it was found that these Na^+ currents are mediated by a specific channel (ENaC) that was found to be expressed also in other osmoregulatory organs in amphibians (Koefoed-Johnsen and Ussing 1958; Uchiyama and Konno 2006). Since amphibians occupy a wide variety of ecological habitats they exhibit a great ability to adapt. This is only made possible by the specialization of osmoregulatory epithelial tissues like their skin, kidney or urinary bladder. In each of these organs ENaC was found to be highly expressed and to be involved in osmoregulatory mechanisms (Uchiyama and Konno 2006). In mammals ENaC is expressed in the kidney, the urinary bladder, the colon and in the lungs, as well as in glandular ducts like sweat glands and salivary glands. All of these tissues have a crucial role in fluid transport (Garty and Palmer 1997).

The malfunction of ENaC or its regulation is always linked to diseases. Excessive Na^+ absorption for example results in hypertension whereas diminished Na^+ absorption is linked to hypotension (Gordon 1995; Snyder 2002). Na^+ absorption in the lung is compulsory to convert the lung at the time of birth from a fluid filled to an air filled organ. Afterwards the Na^+ content of the surface liquid in the lungs has to be under tight control which is achieved partly via the regulation of ENaC (Snyder 2002; Snyder 2005).

Excessive Na^+ current in the airways may contribute to the pathogenesis of cystic fibrosis. Two genetic disorders are known that are directly caused by mutations in ENaC: Liddle's syndrome which is an inherited form of hypertension and caused by a dominant gain-of-function mutation (Shimkets, Warnock et al. 1994; Hansson, Nelson-Williams et al. 1995; Snyder 2002) and pseudohypoaldosteronism type 1 that is characterized by hypotension and salt wasting and caused by a loss-of-function mutation of ENaC (Snyder 2002) (Chang, Grunder et al. 1996; Strautnieks, Thompson et al. 1996). Additionally defects in the regulation of ENaC underlie all of the known inherited monogenetic forms of hypertension (Lifton 1996; Snyder 2002).

3.4.2 Regulation of ENaC

Since ENaC has these essential tasks it is evident that its functional surface expression has to be regulated very tightly. Its regulation indeed is critical to maintain a fine balance between Na^+ depletion and excess. Therefore a bunch of mechanisms are involved in the direct regulation of functional expression of ENaC on the cell surface of epithelial cells. Posttranslational modifications and other regulations are very direct and quick; whereas the control of transcription has a slower but therefore also a more durable effect. ENaC exhibits several specific regions within its amino acid sequence that are involved in the mediation of posttranslational control of the functional expression in apical membranes of epithelial cells.

The trafficking of ENaC is controlled by different mechanisms

Defects in ENaC trafficking are responsible for inherited forms of hypertension and hypotension (Snyder 2005). Little is known about the mechanisms that trigger exocytosis of ENaC, but some groups showed that members of the family of N-ethylmaleimide-sensitive attachment receptor (SNARE) proteins can modulate ENaC current (Qi, Peters et al. 1999; Saxena, Quick et al. 1999; Condliffe, Carattino et al. 2003; Berdiev, Jovov et al. 2004; Snyder 2005). Two members of the SNARE family, synthaxin 1A and SNAP23

have been shown to interact with ENaC (Saxena and Kaur 2006) and each of which differentially affects ENaC function (Saxena and Kaur 2006; Saxena, Singh et al. 2006).

Efficient trafficking from the ER to the cell surface requires the assembly of all three ENaC subunits. Under normal circumstances the principal cells in the collecting duct express γ and β subunits to a higher extend than α subunits, therefore trafficking to the cell surface is controlled by the expression level of the α subunit. Since the transcription of α subunits but not the transcription of β and γ subunits is activated by aldosterone in these cells it directly enhances trafficking just by transcriptional regulation of one subunit (Asher, Wald et al. 1996; Escoubet, Coureau et al. 1997; Snyder 2005). This uncoordinated transcription is tissue specific and shows different subunits expressed to a lower or higher extend in different tissues (Snyder 2005).

A sequence conserved at the C-terminus of all three ENaC subunits was identified to impact on its surface expression as mutations in this motifs lead to an increase in the number of channels expressed at the cell surface and are the cause of the inherited disease Liddle's syndrome (Liddle, Island et al. 1963; Shimkets, Warnock et al. 1994; Firsov, Schild et al. 1996; Warnock 1998; Schild 2004; Snyder 2005). It was found that these conserved regions are involved in protein interactions since they show similarities to the known protein interaction motif (PY motif) (Chen and Sudol 1995; Snyder, Price et al. 1995; Sudol, Chen et al. 1995; Schild 1996). The ENaC PY (PPPXYXXL) motifs were then identified to function as a binding site for an ubiquitin ligase namely Neural precursor-expressed and developmentally down-regulated protein 4-2 (Nedd4-2) (Staub, Dho et al. 1996; Kamynina, Debonneville et al. 2001; Kamynina, Debonneville et al. 2001). As discussed later more in detail, Nedd4-2 is able to ligate ubiquitin molecules to ENaC and therefore target it for internalization via endocytosis and subsequently for degradation in the proteasome (Staub, Gautschi et al. 1997; Goulet, Volk et al. 1998; Abriel, Loffing et al. 1999; Snyder 2005). Furthermore the interaction of Nedd4-2 with ENaC is stimulated by its phosphorylation through the extracellular signal-regulated kinase ERK (Shi, Asher et al. 2002). ENaC surface expression is additionally altered by a diversity of other mechanisms that are right now still not fully understood (Snyder 2005).

Protons regulate ENaC activity

Ussing and Zerahn discovered in 1951 on frog skin that intracellular acidification decreases Na^+ permeability of epithelia (Ussing and Zerahn 1951; Palmer 2001). This finding could be confirmed by different groups using different models and techniques (Palmer 1985; Palmer and Frindt 1987; Harvey and Ehrenfeld 1988; Chuard and Durand 1992; Chalfant, Denton et al. 1999). It was discovered that intracellular pH (pH_i) but not extracellular pH (pH_o) has an impact on ENaC activity. Indeed, further investigation showed that pH_i serves also as an important modulator of ROMK (Harvey and Ehrenfeld 1988; Duffey and Devor 1990; Kolb 1990; Wang, Schwab et al. 1990; Wang and Giebisch 1991), and the Na^+-K^+-ATPase (Skou 1982; Eaton, Hamilton et al. 1984; Urbach, Van Kerkhove et al. 1996). The effect of protons on the activity of ENaC is until now not well understood. However, it was observed that the α subunit of ENaC is the one that responds to changes in pH_i (Chalfant, Denton et al. 1999) and that the single channel open probability of apical Na^+ channels in the CCD is affected by pH_i (Palmer and Frindt 1987; Chalfant, Denton et al. 1999). Nevertheless early studies on isolated membrane vesicles from the toad bladder showed no effect on the amiloride sensitive currents at pH 7 to 8 which lead to the suggestion that pH effects would probably be indirect and just appear in intact cells (Garty, Civan et al. 1985; Palmer and Frindt 1987). Since pH_i is altered by aldosterone and ENaC as well as ROMK and the Na^+-K^+-ATPase are important players in the aldosterone regulated Na^+ absorption in the ASDN pH_i could play a role as a second messenger for the rapid effect of aldosterone (Garty and Palmer 1997; Palmer 2001).

Na^+ regulates ENaC activity

The activity of ENaC is regulated also by Na^+ itself in two distinct ways: Na^+ self inhibition and feedback inhibition (Garty and Palmer 1997; Bize and Horisberger 2007). Na^+ self inhibition initially found in experiments done on frog skin (Fuchs, Larsen et al. 1977), is a decrease of inwardly directed Na^+ currents as Na^+ concentration is elevated on the outside (Abriel and Horisberger 1999; Bize and Horisberger 2007). The effect of extracellular Na^+ on ENaC has a rapid time course (~3 s) and is highly temperature

dependent (Chraibi and Horisberger 2002) with the highest efficiency at 37°C (Chraibi and Horisberger 2002). The rapid kinetics of this effect gives rise to the assumption that ENaC is rather directly affected then accessory proteins would be involved (Chraibi and Horisberger 2002). The current opinion is that extracellular Na^+ interacts with a special Na^+ sensing site in the extracellular loop of the Na^+ channel since the effect is prevented through cleavage of the extracellular loop by proteases like furin or trypsin (Chraibi and Horisberger 2002; Bize and Horisberger 2007). However, the exact mechanism of Na^+ self inhibition is still not clear (Bize and Horisberger 2007).

The Na^+ feedback mechanism occurs upon an increase of the intracellular Na^+ concentration and has a slow time course of about 10 – 20 min (Abriel and Horisberger 1999; Bize and Horisberger 2007). The increase in intracellular Na^+ concentration significantly decreases the number of ENaC molecules at the cell surface (Kellenberger, Gautschi et al. 1998). The fact that channels carrying a mutation within the PY motif are not affected by intracellular Na^+ lead to the conclusion that an intact PY motif is required for the Na^+ feedback mechanism (Kellenberger, Gautschi et al. 1998). The Na^+ feedback regulation is considered as an important mechanism to control Na^+ reabsorption and to maintain Na^+ balance (Kellenberger, Gautschi et al. 1998).

Other ions alter ENaC activity

ENaC activity can also be altered by a range of divalent ions. A stimulatory effect of low concentrations of extracellular Ni^{2+} had been observed using the amphibian A6 cell line and *X. laevis* oocytes (Cucu, Simaels et al. 2003). This effect might be due to the inhibition of Na^+ self inhibition (Horisberger and Chraibi 2004). Also Zn^{2+} was found to modulate ENaC by relieving it from Na^+ self inhibition (Sheng, Perry et al. 2004). Both Zn^{2+} and Ni^{2+} have stimulatory effects on the activity of ENaC at low extracellular concentrations. In addition the intracellular Cl^- concentration can modulate ENaC function. Cl^- was shown to have an inhibitory effect on ENaC, when accumulating on the cytosolic side (Kunzelmann, Schreiber et al. 2002; Adam, Ousingsawat et al. 2005).

Regulation of ENaC by proteases

The limited proteolysis of α and γ subunits of ENaC plays a key role in regulating channel gating (Snyder 2005; Kleyman, Myerburg et al. 2006). The proteolysis was found to occur on furin consensus sites in the extracellular loops of the α and γ ENaC subunits near the first membrane spanning domains (Thomas and Itani 2004; Snyder 2005). Furin, a proprotein convertase was suggested to be the responsible enzyme that acts on ENaC within the Trans Golgi Network (Thomas and Itani 2004). The cleavage activates ENaC, converting near silent channels into active channels that are capable of transporting Na^+ ions (Hughey, Bruns et al. 2004; Snyder 2005). On the cell surface, cleaved as well as non-cleaved forms of ENaC are present. The unprocessed population of channels might subsequently be cleaved and activated by serine proteases like trypsin, channel activating protease 1-3 (CAP1-3), TMPRSS3 and neutrophil elastase (Vallet, Chraibi et al. 1997; Chraibi, Vallet et al. 1998; Guipponi, Vuagniaux et al. 2002; Rossier 2004; Caldwell, Boucher et al. 2005; Snyder 2005). Until now it stayed uncertain whether ENaC cleavage is regulated or whether it is a basic step in channel maturation.

CFTR regulates ENaC

The Cystic Fibrosis Transmembrane Conductance Regulator protein CFTR is an ABC transport protein that is expressed in apical membranes of a range of epithelia where it works as a chloride channel and a regulator of other channels (Kunzelmann 1999; Kunzelmann and Schreiber 1999; Gormley, Dong et al. 2003; Adam, Ousingsawat et al. 2005). Several studies showed that ENaC function decreases when CFTR is activated by a cAMP dependent pathway (Stutts, Canessa et al. 1995; Letz and Korbmacher 1997; Ling, Zuckerman et al. 1997; Mall, Bleich et al. 1998; Kunzelmann 1999; Mall, Bleich et al. 1999; Berdiev, Shlyonsky et al. 2000). This phenomenon was shown in kidney, intestine and trachea epithelia (Letz and Korbmacher 1997; Mall, Bleich et al. 1998; Kunzelmann 1999; Mall, Bleich et al. 1999). Evidence was found that the first nucleotide binding fold of CFTR is important for the inhibition of ENaC (Schreiber, Hopf et al. 1999) and that a direct interaction between ENaC and CFTR takes place (Berdiev,

Cormet-Boyaka et al. 2007). These findings suggest that CFTR directly influences ENaC activity in the membrane.

Phophatidylinosites control ENaC activity

Several types of ion channels are directly regulated by phosphatidylinositides and disruption of this mechanism leads in some cases to disease like Bartter's syndrome or Andersen's syndrome (Pochynyuk, Tong et al. 2006). Phosphatidylinositol 4,5-bisphosphate (PIP2) and phosphatidylinositol 3,4,5-triphosphate (PIP3) are phosphatidylinositides that directly interact with these channels. Diverse studies suggest that ENaC is also a target of phosphatidylinositide regulation (Pochynyuk, Tong et al. 2006). Decreasing levels of PIP2 lead to a decrease in ENaC activity and open probability (Ma, Saxena et al. 2002; Yue, Malik et al. 2002; Tong and Stockand 2005; Pochynyuk, Tong et al. 2007) whereas the addition of exogenous PIP3 increases ENaC activity (Pochynyuk, Tong et al. 2007). The identification of a putative PIP3 binding site within the channel supported the hypothesis that direct binding of PIP3 affects ENaC gating (Pochynyuk, Tong et al. 2007).

Hormonal regulation

Aldosterone, AVP and Insulin are the major hormonal regulators of ENaC (Garty and Palmer 1997). These hormones have been shown to increase Na^+ transport by altering ENaC trafficking to and from the cell surface by different pathways (Snyder 2005; Saxena, George et al. 2006; Saxena and Kaur 2006). In the following section I am giving a short summary of hormonal effects on ENaC.

Arginine Vasopressin (AVP) activate ENaC trafficking

The peptide hormone AVP is synthesized in the hypothalamus and released by the posterior pituitary in response to increased plasma osmolality and hypovolemia. Next to its action on the vasculature where it promotes vasoconstriction AVP is the major regulator of water excretion in the kidney (Boron W F 2005). AVP increases intracellular

cAMP levels by activating V2 receptors located in the basolateral membrane of collecting duct cells. The activation of V2 receptors increases ENaC mediated Na^+ transport through a pathway that includes cAMP and PKA. cAMP is known to increase the surface expression of water channels (AQP) as well as ENaC mediated Na^+ currents in target cells. ENaC function is augmented by cAMP via an increase in channel exocytosis and open probability. In contrast to aldosterone AVP increases ENaC activity as rapidly as five minutes after stimulation because it does not depend on *de novo* synthesis of proteins (Snyder 2002; Snyder 2005).

Aldosterone increases ENaC abundance at the apical membrane

The mineralocorticoid hormone aldosterone is important for the regulation of ENaC, to establish Na^+ homeostasis and stabilize blood pressure. The effect of aldosterone can be divided into an early (20 min – 3 h) and a late phase (6 - 24 h). In the early phase the transcription of certain genes is apparently leading to the regulation of ENaC pools at the membrane and in vesicles close to the membrane (Lu, Pribanic et al. 2007; Harris, Garcia-Caballero et al. 2008). Most of the channel proteins are actually located in vesicles close to the apical membrane, a so called silent pool of ENaC (Loffing, Zecevic et al. 2001; Lu, Pribanic et al. 2007). This pool ensures that the epithelial cell is able to respond very quickly to changes in the environment, and mobilize a lot of channels very quickly. To mobilize and/or stabilize this pool the cell needs to be able to regulate the endo- and exocytosis of these vesicles. Aldosterone is in charge to regulate the transcription of specific genes that encode regulatory proteins acting on the activation and trafficking of ENaC (Spindler, Mastroberardino et al. 1997; Ichimura, Yamamura et al. 2005; Bhalla, Soundararajan et al. 2006; Liang, Peters et al. 2006; Rozansky 2006). Known proteins that are transcriptionally regulated by aldosterone and influence the Na^+ transport in aldosterone target cells were mentioned and described above. In the late phase the transcription of α ENaC is induced by aldosterone in collecting duct cells. This triggers the assembly and trafficking of the whole channel complex (Asher, Wald et al. 1996; Escoubet, Coureau et al. 1997; Loffing, Zecevic et al. 2001; Snyder 2005).

Insulin influences ENaC trafficking

Transepithelial Na^+ transport in principal cells of the CCD is also regulated by insulin and/or Insulin-like growth factor 1 (IGF-1), which is thought to induce a rapid increase in the number of Na^+ channels in the luminal membrane (Record, Johnson et al. 1996; Gonzalez-Rodriguez, Gaeggeler et al. 2007). This hypothesis is supported by the fact that insulin also increases the density of Na^+ channels expressed in the apical membrane in a toad kidney cell line (A6 cell line) (Erlij, De Smet et al. 1994). The increase of Na^+ transport in these cells mediated by insulin treatment is synergistic to the effect of aldosterone which can be explained by the fact that insulin activates Sgk1 by phosphorylation while aldosterone increases Sgk1 expression (Record, Johnson et al. 1996; Wang, Barbry et al. 2001; Faletti, Perrotti et al. 2002; Lee, Ma et al. 2007; Tiwari, Nordquist et al. 2007). These findings suggest that insulin influences ENaC trafficking. Furthermore insulin has been suggested to induce the direct phosphorylation of ENaC which is linked to an increase in channel activity (Shimkets, Lifton et al. 1998; Zhang, Alvarez de la Rosa et al. 2005).

3.5 Ubiquitylation / Deubiquitylation

Ubiquitylation is not only involved in the regulation of ENaC as mentioned earlier but rather a general mechanism for triggering many different cellular mechanisms. Ubiquitin a small 7.6 kDa protein which is ubiquitously expressed in eukaryotic cells plays an important role in mechanisms regarding a variety of cellular functions (Stryer 1999; Haglund and Dikic 2005; Staub and Rotin 2006). It is highly conserved through the evolution and can be covalently bound to ε amino goups of lysine residues of specific target proteins. The ubiquitylation of proteins shows similarities to the phosphorylation of proteins: it is inducible, reversible and specific (Haglund and Dikic 2005). The attachment of ubiquitin to proteins regulates gene transcription, DNA repair and replication, intracellular trafficking as well as virus budding (Haglund and Dikic 2005). Proteins are beforehand targeted for ubiquitylation, which can be genetically programmed or acquired by phosphorylation or by binding to an adapter protein as well as by protein damage (Wilkinson 2000). The covalent binding to target proteins is performed in a process with three distinct steps involving ubiquitin-activating (E1), ubiquitin-conjugating (E2) and ubiquitin-ligating (E3) enzymes (Haglund and Dikic 2005). The E1 enzyme is in charge to activate ubiquitin. The terminal carboxyl group of ubiquitin is bound by a thiolesther bond to a sulfhydryl group of the E1 enzyme. This reaction reminds the ATP driven activation of fatty acids or amino acids. The activated ubiquitin is then transferred to a sulfhydryl group of the E2 Enzyme. The ubiquitin ligase E3 finally catalyses the transfer of ubiquitin from E2 enzymes to target proteins (Stryer 1999) and is responsible for substrate recognition (Staub and Rotin 2006). Two major types of E3 enzymes are existing: HECT (homologous to E6-AP COOH terminal) E3s and RING (really interesting new gene) finger E3s. RING finger E3 enzymes have a cluster containing cystein and histidin residues which are coordinated by zinc ions. RING finger E3 enzymes work in concert with the E2 enzyme to ubiquitylate the target. Target proteins are directly ubiquitylated by HECT E3 enzymes after ubiquitin was transferred to a conserved cystein within the HECT domain of the E3 enzyme. HECT domain E3 enzymes include the family of Nedd4/Nedd4-like ubiquitin protein ligases (Staub and Rotin 2006).

Figure 5

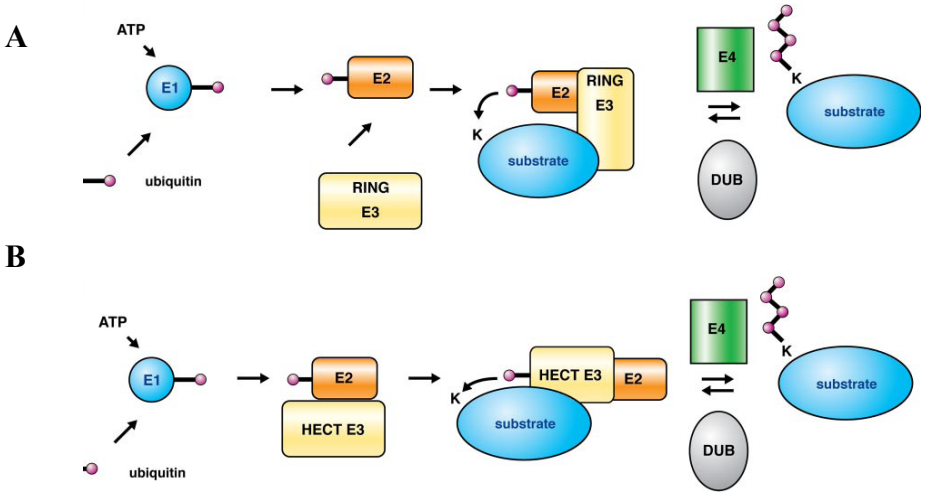

Figure 5: *Ubiquitylation of substrates through two different E3 enzymes.* An ubiquitin-activating enzyme, E1, activates ubiquitin in an ATP-dependent manner, whereby a transfer of ubiquitin to the active site cysteine of an ubiquitin-conjugating enzyme, E2 is accomplished. A) E3 is an ubiquitin-protein ligase that facilitates the transfer of ubiquitin from the E2 onto a lysine residue of a target protein (substrate). B) HECT domain containing E3 ligases carry out isopeptide formation between ubiquitin and the substrate. E4 enzymes promote the construction of polyubiquitin chains and deubiquitylating enzymes (DUBs) are in charge to reverse the ubiquitylation reaction. This figure was adapted from Staub and Rotin 2006.

Ubiquitylation occurs in different flavours: Monubiquitylation, diubiquitylation, multiubiquitylation and polyubiquitylation. Monoubiquitylation occurs if one ubiquitin is linked to a lysine residue of the targed protein, while diubiquitylation is the attachement of one diubiquitin on one lysine residue. Are several lysine residues tagged with a single ubiquitin molecule the target is multiubiquitylated. In contrast, polyubiquitylation is defined by the binding of ubiquitin chains to the target protein. Cytosolic proteins that are designated for proteosomal degradation are in general polyubiquitylated while membrane proteins and proteins of the trafficking machinery are usually monoubiquitylated or diubiquitylated (Staub and Rotin 2006).

3.5.1 The ubiquitylation of ENaC

Each of the ENaC subunits contains a PY motif at its cytoplasmic C-terminus that was identified as a binding site for members of the Nedd4/Nedd4-like ubiquitin protein ligase family (Schild, Lu et al. 1996; Staub, Dho et al. 1996; Abriel and Staub 2005; Staub and Rotin 2006). One member of the Nedd4 family, Nedd4-2 was identified to regulate ENaC activity by controlling its cell surface stability (Staub, Dho et al. 1996; Staub, Gautschi et al. 1997; Rotin, Staub et al. 2000). Mutations in the PY motifs of ENaC lead to the inherited disease Liddle's syndrome since ENaC ubiquitylation is impaired and channel internalization is reduced (Abriel and Staub 2005; Staub and Rotin 2006). Nedd4-2 exhibits three consensus phosphorylation sites for Sgk1 and protein kinase A (PKA) which are mediators of the aldosterone and the AVP pathways respectively (Debonneville, Flores et al. 2001; Snyder, Olson et al. 2002; Snyder, Olson et al. 2004; Snyder 2005). ENaC is ubiquitylated at lysine residues of the α, β and γ subunit. Subsequently its surface expression and the Na^+ transport are decreased (Adam, Fakitsas et al 2007; Snyder 2005). Sgk1 is decreasing the internalization of ENaC by phosphorylating and blocking Nedd4-2. It was shown that indeed Nedd4-2 phosphorylation blocks the interaction with ENaC (Staub, Dho et al. 1996; Staub, Gautschi et al. 1997; Staub, Yeger et al. 1997; Abriel and Staub 2005; Butterworth, Edinger et al. 2007). Further involved in the ubiquitylation of ENaC is the aldosterone induced protein 14-3-3, a member of a family of highly conserved regulatory molecules (Yaffe 2002; Liang, Peters et al. 2006). The functionally important Sgk1 target motif within Nedd4-2 conforms to the 14-3-3 consensus motif. It could be shown that Nedd4-2 is a substrate of 14-3-3 protein binding in response to Sgk1 phosphorylation (Bhalla, Daidie et al. 2005; Liang, Peters et al. 2006). It is suggested that binding of 14-3-3 physically obstructs the interaction between ENaC and Nedd4-2 and that the concerted action of 14-3-3 and Sgk1 inhibit ENaC ubiquitylation by Nedd4-2 (Bhalla, Daidie et al. 2005; Liang, Peters et al. 2006).

Figure 6

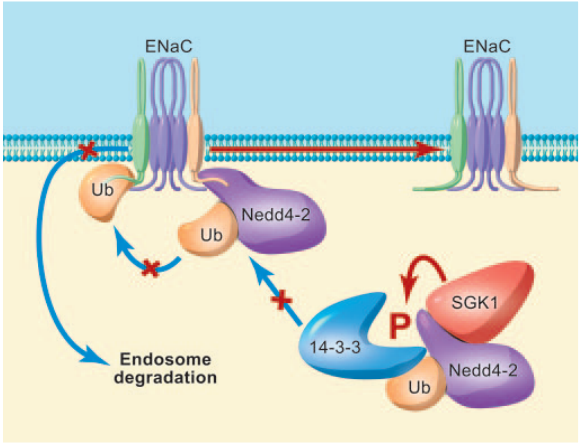

Figure 6. *Schematic representation of the effect of serum and glucocorticoid induced kinase 1 (Sgk1) and Nedd4-2 on the regulation of ENaC.* Sgk1 that is transcriptionally induced by aldosterone interacts with Nedd4-2 to phosphorylate it. Interaction of Nedd4-2 with ENaC is inhibited by 14-3-3 that binds to the amino acid residue in Nedd4-2 that was beforehand phosphorylated by Sgk1. Subsequently, ENaC ubiquitylation, internalization, and degradation in the lysosomal pathways is blocked which leads to an increase in the amount of intact Na^+ channels at the cell surface. (Illustration by Josh Gramling - Gramling Medical Illustration. Figure was taken from Staub and Verrey 2005.

3.6 Voltage gated ion channels

The main types of stimuli known to activate ion channels are changes in membrane voltage, mechanical stress and ligand binding. The focus of this section is on the activation of ion channels by voltage changes and the structure and function of voltage gated ion channels. I have included this section since we identified a voltage gated proton channel as one of the early aldosterone induced gene products in mouse ASDN.

Many physiological processes are mediated by members of the voltage gated ion channel superfamily which comprises more than 140 members. Seven groups of ion channel families are included in this superfamily. General convergences between all subgroups are that they are all transmembrane proteins and triggered by voltage differences over the plasma membrane (Yu, Yarov-Yarovoy et al. 2005). Voltage gated ion channels are the basis of diverse physiological key functions in the body like nerve impuls conduction, muscular contraction and synaptic transmission. The different voltage gated ion channels exhibit different ion selectivities for cations like Na^+, K^+ or Ca^{2+} (Terlau and Stuhmer 1998; Elinder, Nilsson et al. 2007). The best studied voltage gated ion channels are voltage gated potassium channels (K_v-channels) which exhibit a secondary structure that is typical for the whole voltage gated ion channel protein family (Figure 7). K_v channels are a construction of four homologous subunits each of which exhibits six transmembrane helices (S1-S6). Corresponding to its functions voltage gated ion channel subunits contain two different but functionally coupled domains: The pore domain and the voltage sensor domain (VSD). The pore domain, responsible for the selective ion conductance, is constructed by two transmembrane segments (S5-S6) and a membrane reentrant loop from each subunit which form a cavity that is filled with permeant ions (Figure 7). This ion conducting pore contains a selectivity filter that is formed by a characteristic amino acid sequence (Sands, Grottesi et al. 2005; Yu, Yarov-Yarovoy et al. 2005; Tombola, Pathak et al. 2006). Since the K_v channels are homotetramers the pore is built by the arrangement of four S6/S5 domains surrounded by the four VSDs (Tombola, Pathak et al. 2006) (Figure 7).

Figure 7

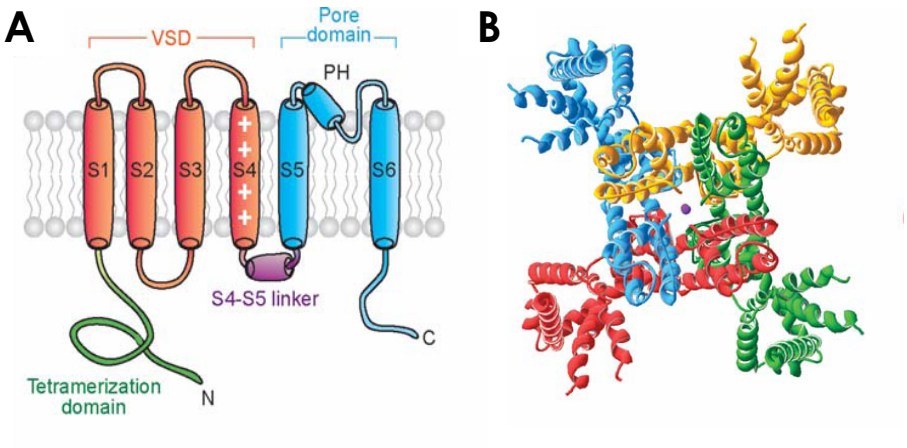

Figure 7: *Topology model of a K_v channel* (A) The transmembrane topology of a K_v channel subunit, showing the voltage sensor domain (VSD) in red, the pore domain in blue, the S4-S5 linker in purple, and the tetramerization domain in green. The intact channel is made up of four such subunits. (B) The $K_v1.2$ tetramer is shown in a top view (extracellular side) whereby each subunit is revealed in a different color. Potassium ions are colored purple. This figure was adapted from Tombola, Pathak et al. 2006.

Since voltage gated channels need to sense the electrical field over the plasma membrane, they contain a so called "voltage sensor". The VSD, responsible for the voltage sensing and gating reacts to changes in the electrical field by a conformational change within the protein which is driven by the movement of electrical charges (Sands, Grottesi et al. 2005; Yu, Yarov-Yarovoy et al. 2005). The charge movement within the molecule is called gating current and causes the pore structure to open and to conduct ions. During channel activation an outward translocation of positive charges takes place. The S4 transmembrane helix is responsible for the ability of the VSD to act as a molecular voltmeter. It contains repeated motifs of one positively charged amino acid surrounded by hydrophobic residues (Catterall 1986; Yu, Yarov-Yarovoy et al. 2005) (Figure 7). It is believed that these positively charged amino acid residues are forcing the VSD to move within the lipid bilayer dependent on the transmembrane voltage (Miller 2006). Different models of voltage sensor movement are currently discussed within the field. However, it is known that the four VSD of a typical K_v channel are working independently but that the opening of the pore only happens after allosteric interaction between all four subunits (Okamura 2007).

3.6.1 Voltage sensor domain proteins (VSP)

Until recently the VSD was considered to be a structure that only regulates the gating of voltage gated ion channels, but proteins were discovered that have the structure of a VSD and do not include a pore domain. These types of proteins were named voltage sensor proteins (VSP) (Okamura 2007). It was found that these proteins exhibit diverse voltage regulated functions like enzymatic activity or proton conductance (Murata, Iwasaki et al. 2005; Ramsey, Moran et al. 2006; Sasaki, Takagi et al. 2006). One of these proteins is composed of a VSD with four transmembrane segments and a phosphatase domain that is similar to the well characterized phosphatase PTEN (phosphatase and tensin homologue deleted on chromosome 10) (Maehama, Taylor et al. 2001; Murata, Iwasaki et al. 2005). Since gating currents in response to changes in membrane voltage could be observed in oocytes expressing this voltage sensor containing phosphatase (Murata, Iwasaki et al. 2005) it is assumed that the VSD is a functional unit by itself. Furthermore, it is the first phosphatase characterized which is directly regulated by voltage changes over the membrane (Murata and Okamura 2007). However, the stoichiometry and the mechanism of voltage dependent regulation within the voltage sensor containing phosphatase is still uncertain and remains to be explored in detail (Okamura 2007). Next to the VSD containing phosphatase also a Na^+-H^+-exchanger, an adenylate cyclase and a proton channel was found within the VSPs (Okamura 2007).

Figure 9

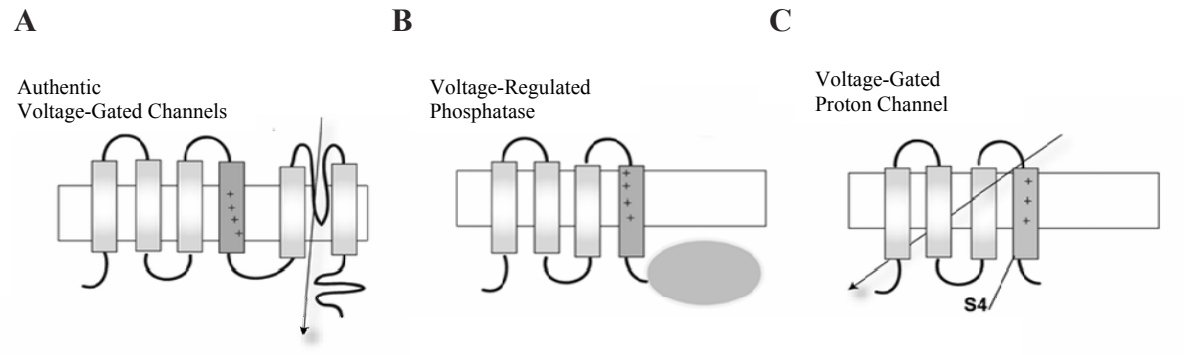

Figure 9: *Membrane topology model of a voltage gated ion channel and two voltage sensor domain proteins: A voltage-regulated phosphatase and a voltage gated proton channel.* (A) Voltage-gated ion channel, (B) voltage-regulated phosphatase, (C) voltage-gated proton channel. The voltage sensing TM domain is depicted in dark gray and shows a number of positive charges. Arrows are showing the ion flow though the protein. This figure was taken from Okamura 2007.

3.6.2 Voltage gated proton channels

In 2006 a VSP was identified that showes a voltage and pH dependent proton conductance in heterologous expression systems (Ramsey, Moran et al. 2006; Sasaki, Takagi et al. 2006). Two independent research groups investigated the human (H_v1) and the mouse (mVSOP) ortholog, respectively. Similar to other VSP these voltage gated proton channels are composed of four transmembrane helices (S1-S4) whereupon the S4 transmembrane helix comprises three positively charged arginine residues bordered by each two hydrophobic residues. Voltage gated proton channels (H_v channels) were first described 1982 by Thomas et al in snail neurons and subsequently found in rat alveolar epithelial cells, mammalian eosinophils, macrophages, microglia, and in a wide variety of other cell types (Thomas and Meech 1982; Decoursey 2003; Morgan and DeCoursey 2003). H_v channels exhibit several properties that distinguish them from other ion channel or proton transporters. Their characteristic feature is the unique pH dependence of gating, in which the voltage activation relationship depends strongly on the intracellular (pH_i) and extracellular pH (pH_o) (Decoursey 2003; Sasaki, Takagi et al. 2006). These channels were until recently only characterized by electrophysiology and it was proposed that the newly identified VSPs (H_v1 and mVSOP) which exhibit a voltage dependent proton

conductance could be the molecular basis of electrophysiologically well characterized H_v channels (Decoursey 2003; Okamura 2007).

H_v channels were found to be highly selective for protons, while other ion permeabilities could not be detected. External Zn^{2+}, Cd^{2+} and other polyvalent metal ions are potent inhibitors for H_v channels. Noteworthy is that the conductance and gating kinetics of H_v channels are remarkably temperature dependent (Decoursey 2003). Even though all H_v channels exhibit voltage and pH dependent gating many different types of H_v channels exist which are mainly distinguished by their differences in gating kinetics (Decoursey 2003).

4 Material and Methods

4.1 Constructs for in vitro cRNA synthesis, retroviral transfection and site-directed mutagenesis

Mouse kidney, spleen or muscle RNA was isolated with RNeasy Mini Kit according to the manufacturer's protocol (Qiagen, Hombrechtikon, Switzerland) and reverse transcribed (oligoDT primers) using the TaqMan Reverse Transcription Kit (Applied Biosystem, Foster City, USA). cDNAs were amplified by PCR using 2.5 U of a proofreading polymerase (Pfu) (Promega, Madison, USA), 1x Pfu-reaction buffer (Promega), 2 mM dNTPs, 0.5 µM 5'-Primer, 0.5 µM 3'-Primer for 40 cycles (30 sec 95°C, 1 min 50-68°C, 1-7 min 68°C). Primers for PCR were designed to include restriction sites for cloning and were synthesized by Microsynth (Balgach, Switzerland) (Table 2). PCR products were separated from the template by agarose gel electrophoresis and purified with Quiagen Gel extraction kit. The amplified PCR fragments were cloned in oocyte and cell expression vectors (Table 2). PCR products and target vectors were cut with the corresponding restriction enzymes (Fermentas, Harrington, Canada; New England Biolabs Inc., Ipswich, USA) and ligated using T4 ligase (Fermentas). The constructs were used to transform supercompetent *E. coli* bacteria (DH5 alpha, Invitrogen, Basel, Switzerland). Correct cloning was checked by DNA sequencing (Microsynth, Balgach, Switzerland).

For changing cysteine 67 of Usp2-45 to alanine the QuickChange® site directed mutagenesis kit (Stratagene, La Jolla, USA) was used with following primer pair:

5'-AACCTTGGGAACACGGCTTTCATGAACTCAATT-3';

5'-AATTGAGTTCATGAAAGCCGTGTTCCCAAGGTT-3'.

Oocyte expression vectors containing *X. laevis* ENaC (αβγ*X*ENaC) (Puoti, May et al. 1997), rat ENaC (αβγrENaC) (Canessa, Schild et al. 1994), *X. laevis* Sgk1 (*X*Sgk)

(Mastroberardino, Spindler et al. 1998; Firsov, Schild et al. 1996; Puoti, May et al. 1995), rat ROMK2 (Chen, Bhargava et al. 1999), flounder Napi-IIb (Forster, Wagner et al. 1997), rat αNa$^+$-K$^+$-ATPase (αrNa$^+$-K$^+$-ATPase) (Shull, Greeb et al. 1986), *X. laevis* βNa$^+$-K$^+$-ATPase (β*X*Na$^+$-K$^+$-ATPase) (Pfeiffer, Beron et al. 1999) cDNAs were also used for cRNA synthesis and microinjection in several experiments (Adam, Fakitsas et al. 2007).

Table 2

cDNA	**Primer Sequences**	**Vector**	**Linearizing enzyme**
mUsp2-45:	5'-AAAACTCGAGCCGCGTTGGGTTTGGGGCATAG-3', 5'-AAAAAAGCTTGGGGCCACCACAGGGAAGAG-3'	pSDeasy pLPCX	BglI
mUsp15:	5'-AAAACTCGAGGCTAGTGGAAGAAGATGGCGGAAG-3' 5'-AAAAAAGCTTGGGATTTATTTGGGATTTCCT-3'.	pSDeasy	PvuI
mUsp53fl:	5'-AAAACTCGAGGTTGTCCACTGGTCACATTACAGAT-3' 5'-AAAACCCGGGTAAAGGTCTTTGTTCAGAAGGACAG-3'	KSM pCDNA3	NotI
mUsp53t:	5'-AAAACTCGAGCTTTGCCTGTCACGACGTT-3' 5'-AAAACCCGGGTGTTCAGAAGGACAGTTGACG-3'	KSM pLNCX	XbaI
mUsp2-69	5'-AAAACTCGAGCCCATGAGGCTCCCAGTACC-3' 5'-AAAAAAGCTTGGCCACCACAGGGAAGAGGGAAG-3'	pSDeasy pLPCX	PvuI
mVSOP (mH_v1)	5'-AAAACTCGAGATGACTTCCCATGACCCAAA-3' 5'-AAAAAAGCTTAGGCAGAGATGGAGACTGGA-3'	pCDNA3	StuI or SmaI

4.2 cRNA synthesis

For cRNA synthesis, plasmids were linearized with distinct restriction enzymes (Table 2), purified by using PCR purification kit (Quiagen) and used as template for RNA synthesis with T7, T3 or SP6 mMESSAGE mMACHINE™ kit (Ambion, Applied Biosystems) dependent on the vector. The procedures were done following the instructions of the manufactorers. cRNA was purified with the RNeasy mini kit (Quiagen) and the integrity was checked by agarose gel electrophoresis. Quantification was done by using the NanoDrop ND-1000 spectrophotometer (Agilent Technologies, Santa Clara, USA) (Adam, Fakitsas et al. 2007).

4.3 *Xenopus laevis* oocytes

Stage V and VI oocytes were treated for 25-35 minutes at room temperature with 2mg/ml collagenase type 1A in Ca^{2+}-free buffer (82.5 mM NaCl, 2 mM KCl, 1 mM $MgCl_2$, 10 mM HEPES pH7.4) containing 0.2 mg/ml trypsin inhibitor (Sigma-Aldrich Chemie GmbH, Buchs, Schwitzerland) to detach from the ovarium and to remove follicular cells. The oocytes were then kept at 16°C in Barth's solution (88 mM NaCl, 1 mM KCl, 0.82 mM $MgSO_4$, 0.41 mM $CaCl_2$, 0.33 mM $Ca(NO_3)_2$, 2.4 mM $NaHCO_3$, 5 mM HEPES, pH 7.4). After cRNA injection oocytes were incubated at 16°C in ND96 (96 mM NaCl, 2 mM KCl, 1 mM $MgCl_2$, 1.8 mM $CaCl_2$, HEPES pH 7.4) or ND10 (10 mM NaCl, 2 mM KCl, 1.8 mM $CaCl_2$, 1 mM $MgCl_2$, 86 mM NMDG, 5 mM HEPES, pH 7.4) dependent on the cRNA injected and the following experimental procedure. All solutions for oocyte incubation were supplemented with antibiotics (10 mg/l gentamycin/doxycycline (Fluka, Buchs, Switzerland)).

4.4 Two-electrode voltage-clamp (TEVC)

The two-electrode voltage clamp technique was used for the recording of whole-cell currents from *X. laevis* oocytes at room temperature 40-48 h after injection of αβγENaC, Sgk, Usp15, Usp2-69, Usp2-45, Usp53t/fl, H_v1 and 3 days after injection of αrNa^+-K^+-ATPase, β*X*Na^+-K^+-ATPase, NaPi-IIb cRNA using a commercial two electrode voltage-clamp (Oocytes Clamp OC725C, Warner Instrument Corp. Hamden, USA) connected to a data acquisition hardware (Digidata 11322A, Axon Instrument Foster. City, USA). A computer running pClamp8 software (Axon Instruments) was used to control the clamp, the valves switching the solutions, and to record currents, as previously described (Forster, Wagner et al. 1997). Microelectrodes (resistance $\leq$ 7 MΩ) were filled with 3 M KCl. Two basic protocols were used for generating steady-state recordings: (1) Continuous current recordings. *X. laevis* oocytes were tested at a membrane holding potential of -50 mV, recorded data was low pass filtered at 10 Hz and digitized at 20 Hz. (2) Current-Voltage (I-V) recordings. Oocytes were clamped at -50 mV and step changes in membrane holding potential were applied (Range and increments varied dependent on the experiment). At each membrane potential four pulses were averaged. Current records were low-pass filtered at 500 Hz and digitized at 20 µsec/point. Calculations and graphs were made using GraphPad Prism™ Version 4.0 (GraphPad Inc., San Diego, USA) and significance was tested using the Student's t-test, Kruskal-Wallis or Mann-Whitney test (Adam, Fakitsas et al. 2007).

4.4.1 Electrophysiological measurements of I_{amil} carried by ENaC

ENaC expressing oocytes as well as the corresponding control oocytes were kept in ND10 solution for 40-48 hour after cRNA injection (0.05 ng/SU/oocyte ENaC). Recordings were made in ND10 and ND96 solutions; 10 µM amiloride (Sigma) was added to the ND96 solution to measure the amiloride-sensitive part of the current (I_{amil}). Applied voltage steps were ranging from -140 mV to +20 mV or from -100 to +100 mV in 20 mV increments of 80 ms duration. cRNAs of Usp2-45 (10-36 ng cRNA injected), Usp2-

45mut (10 ng cRNA/oocyte), Usp53t (15 ng cRNA/oocyte), Usp53fl (15 ng cRNA/oocyte), H_v1 (1-20 ng cRNA/oocyte) or Usp2-69 (10 ng cRNA/oocyte) were coinjected. All measurements were done at similar conditions (Adam, Fakitsas et al. 2007).

4.4.2 TEVC measurements in H_v1 expressing oocytes

Oocytes expressing H_v1 were kept for 2-3 days in ND96 or Barth's solution at 16°C prior the experiment. Applied voltage steps were ranging from -100 mV to +180 mV in 20 mV increments of 80-1000 ms duration. Recordings were performed in ND96 solution with varying pH (pH 6, pH 7.4, pH 8) or supplemented with 1 µM $ZnCl_2$. pH was adjusted by using Tris base. For the examination of Zn^{2+} sensitivity, a specific voltage step protocol was used (Figure 24 A). After clamping the voltage to 100 mV for 150 ms, voltage steps ranging from 20 mV to -100 mV in 20 mV increments were applied for 150-300 ms. The basic membrane potential was clamped to -50 mV, at each membrane potential four pulses were averaged.

4.4.3 Measurements of ROMK2 mediated K^+ current

Oocytes expressing ROMK2 (2 ng cRNA per oocyte injected) and coexpressing ROMK2 with H_v1 (20 ng cRNA injected) were kept for 40-48 h in ND96 solution. ROMK2-mediated current was defined as Ba^{2+}-sensitive current. The current recorded at a membrane potential of -50 mV was inhibited by substitution of 1.8 mM Ca^{2+} with Ba^{2+} in the ND96 solution (Chen, Bhargava et al. 1999).

4.4.4 Napi-IIb mediated currents

10 ng flounder Napi-IIb cRNA was injected 3-4 days before the TEVC measurements. Phosphate currents carried by type IIb Na^+/P_i cotransporter (NaPi-IIb) (Forster, Wagner et al. 1997) were obtained by addition of 1 µg/ml phosphate (P_i) (K_2HPO_4 and KH_2PO_4 stocks that were mixed to give pH 7.4) to ND96. Currents were recorded at a stable membrane potential of -50 mV. Napi-IIb mediated currents were calculated by subtracting the values of basal currents from currents obtained after P_i addition.

4.4.5 Pump current measurements

The activity of the exogenous and endogenous Na^+-K^+-ATPase was determined as the outward current activated by addition of K^+ in the presence of K^+ channel blocker such as TEA and $BaCl_2$ (Horisberger, Jaunin et al. 1991). After injection with cRNA for α and β subunits of the pump, oocytes were kept in ND10 solution for 2-4 days. Pump current measurements were done in two different ways. (1) Coexpression of ENaC for controlled Na^+ loading (2) Na^+ loading without ENaC expressed.

(1) To control Na^+ loading of oocytes I used oocytes coexpressing ENaC. Oocytes were kept in Na-free solution (50 mM NMDG-Cl, 40 mM KCl, 1 mM $CaCl_2$, 1 mM $MgCl_2$, 10 mM NMDG-HEPES pH 7.4) over night before measurements. For Na^+ loading, oocytes were first clamped at -50 to -100 mV and washed with K^+-free Na^+-solution (100 mM Na-gluconate, 1 mM $MgCl_2$, 1 mM $CaCl_2$, 10 mM Na-HEPES pH 7.4) until the membrane potential reached a stable baseline. The absence of extracellular K^+ prevents the pump from functioning as it needs both the intracellular Na^+ and the extracellular K^+ as substrates for its ATPase activity. The intracellular Na^+ concentration was determined by applying Na-measurement solution with and without 10 µM amiloride (5 mM Na-gluconate, 0.5 mM $MgCl_2$, 2.5 $BaCl_2$, 95 mM NMDG-Cl, 10 mM NMDG-HEPES pH 7.4) (Crambert, Hasler et al. 2000). IV curves performed in voltage steps of 20 mV from -100 mV to +80 mV of the duration of 80 msec were applied in the Na^+-measurement solution with or without 10 µM amiloride to identify the Na^+ current carried via ENaC.

The crossing point of two subsequent current to voltage relationship curves (IV) indicates on the voltage axis the reversal potential for Na^+ (E_{rev}) from which the intracellular concentration for Na^+ can be calculated using the Nernst equation. The IV curves were performed until the crossing point fell into the range between 0 and +15 mV (equivalent to an intracellular Na^+ concentration of ~70 mM), ensuring that the starting condition of intracellular Na^+ concentration was similar for all oocytes. After the determination of the intracellular Na^+ concentration pump current measurements were performed at a stable membrane potential of -50 mV using the pump-current-measurement solution (120 mM sucrose, 0.82 mM $MgCl_2$, 0.41 mM $CaCl_2$, 10 mM NMDG-HEPES, 5 mM $BaCl_2$, 10 mM TEA-Cl, 10 mM KCl, 10 µM amiloride) (Zecevic, Heitzmann et al. 2004). The current carried by the pumps containing the endogenous *X. laevis* α-subunit is sensitive to 50 µM strophantidin and the subsequent addition of 3 mM ouabain blocks the current that corresponds to the hybrid pumps (exogenous) containing the ouabain-resistant rat α-subunit. A typical pump current recording is shown in figure 10.

(2) Oocytes were first loaded with Na^+ by a 2-3 h exposure to a K^+ free solution (100 mM Na-gluconate, 1 mM $MgCl_2$, 0.5 mM $CaCl_2$, 10 mM HEPES pH 7.4). Whole cell currents were measured at membrane potential clamped to -50 mV. The pump was activated by application of external K^+ upon exposure to K^+-containing solution (80 mM Na-gluconate, 10 mM KCl, 0.8 mM $MgCl_2$, 0.4 mM $CaCl_2$, 5 mM $BaCl_2$, 10 mM TEA-Cl, 10 mM Hepes-NMDG pH 7.4). Outward current is recorded and its sensitivity to strophantidin (50 µM) or ouabain (3 mM) (Sigma) dissolved in the same solution is measured (Jaisser, Horisberger et al. 1992).

Figure 10

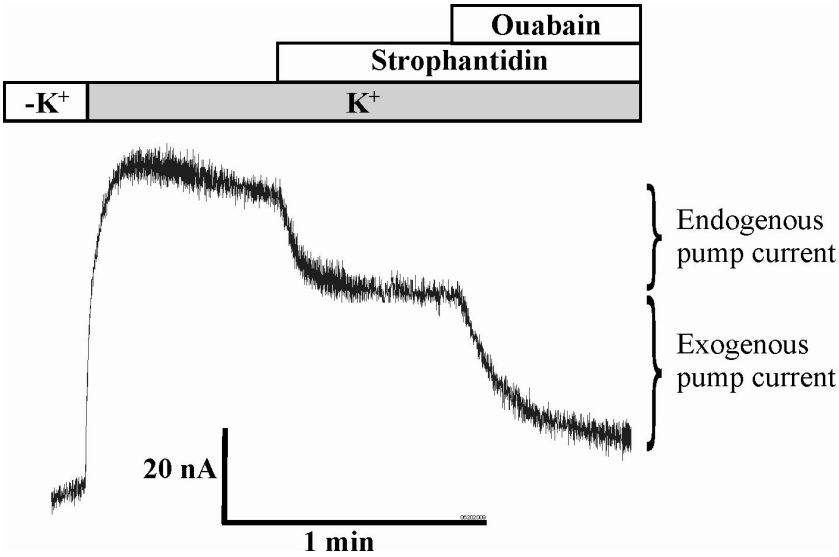

Figure 10: *Typical recording of Na^+-K^+ATPase mediated current.* As the Na^+-K^+-ATPase pumps three sodium ions out of the cell in exchange for two potassium-ions that enter, the resulting net positive charge flux is visible as outward current. Oocytes clamped at -50 mV were perfused with the K^+ containing solution to activate the pump. The endogenous pump current is inhibited by strophantidin in a µM range, while the exogenous rat α Na^+-K^+-ATPase is almost resistant to this blocker at this concentration. To identify the portion of current carried by the rat isoform, 3 mM ouabain is applied in the same solution and further decrease of K^+ stimulated current is observed (exogenous pump current).

4.5 Culture and retroviral transduction of mpkCCD$_{c14}$ cells

The mouse kidney cell line mpkCCD$_{cl4}$ and its culture were originally described by Bens et al. (Bens, Vallet et al. 1999). mpkCCD$_{cl4}$ cells were seeded respectively on 12 mm diameter snapwell filters or 24 mm diameter 24-well plastic plates (Corning Costar) in standard medium (DMEM:Ham's F12, 1:1 vol/vol; 60 nM Na^+-selenate, 5 mg/ml transferrin, 2 mM glutamine, 50 nM dexamethasone, 1 nM triiodothyronine, 10 ng/ml epidermal growth factor, 5 mg/ml insulin, 20 mM D-glucose, 2% fetal calf serum (FCS), and 20 mM Hepes, pH 7.4) and incubated at 37°C in 5% CO_2/95% air. For electrophysiological measurements, real-time PCR or Western blot analysis, cells were grown for 5–7 days in standard medium of culture and for electrophysiology an additional 2-7 days in filter medium (standard medium without serum, Apo-transferrine and EGF)

cells were transferred into serum- and hormone-deprived medium 12 – 20 h prior to the experiments. To obtain maximal effects that are mediated *via* the glucocorticoid receptor, aldosterone was used at 10^{-6} M (Bens, Vallet et al. 1999).

Stable populations of mpkCCD$_{c14}$ cells expressing Usp2-45, and Usp-2-45mut were obtained according to the protocol provided on the website http://www.stanford.edu/group/nolan/ with slight modifications (Summa, Camargo et al. 2004; Adam, Fakitsas et al. 2007). Briefly, ecotropic pseudoretroviral producer cells (Phoenix, Nolan Lab, Stanford, USA) were plated 24 h prior to transfection at 50% density on 60 mm plates. The next day, 5 µg of the retroviral construct encoding Usp2-45 or Usp2-45mut were applied using FuGENE6 (Roche, Basel, Switzerland) according to the manufacturers recommendation. The medium was replaced after 24 h and the cells subsequently kept at 32°C. The pseudo-retrovirus-containing supernatant was harvested after 24 h and filtered through a 45 µm sterile filter. After addition of Polybrene (Sigma) at a final concentration of 4 µM, the entire supernatant (3 ml) was given to 5% confluent mpkCCD$_{cl4}$ cells plated the day before on 6-well plates (35 mm diameter). The cells were centrifuged at 130 g and 32°C for 30 min and then kept for 6 h at 32°C (5% CO_2) before the supernatant was replaced by usual medium. The procedure was repeated the next day using fresh retroviral supernatant harvested from the same Phoenix cells. A transduction efficiency of 70–100% was achieved when using EGFP (enhanced green fluorescent protein) as a marker. This protocol was repeated 2 times to achieve maximal expression. The resulting multiclonal cell populations were then kept under selective pressure with 1 µg ml^{-1} puromycin (Adam, Fakitsas et al. 2007).

4.6 Western blotting and lysis of mpkCCD$_{c14}$ cells and *X. laevis* oocytes

An antibody selective for the mUsp2-45 isoform of mUsp2 was raised against a NH_2-terminal epitope (MRTSYTVTLPEEPAAC) (Pineda Antibody Services, Berlin, Germany) and affinity purified on antigen peptide using the SulfoLink® Kit (Pierce/Perbio, Bonn, Germany) according to the manufacturer's protocol (Adam, Fakitsas et al. 2007). An antibody selective for the mUsp53 was raised against the epitope CGLPFHVDESSVAGK in rabbit and the serum was directly used for detection of proteins on Western blot. The antibody specific for mouse H_v1 was raised against an epitope (CSEKEQEIERLNKL) as described before (Ramsey, Moran et al. 2006). The antibody against both, Usp2-45 and Usp2-69 (pan Usp2) was ordered from Abgent (Cat.Nr.:AP2131c). Anti-myc-HRP monoclonal antibody was ordered at Invitrogen (Cat.Nr.:46-0709) and the monoclonal anti-HA antibody was purchased from Sigma (Cat.Nr.: H9658).

mpkCCD$_{c14}$ cells were harvested from plastic cultures and lysed in RIPA buffer (150 mM NaCl, 1% IPGAL, 0.5% DOC, 0.1% SDS, 50 mM Tris, pH 7.5) by passing them 10 times through a 25 G needle and *X. laevis* oocytes were lysed in buffer containing 250 mM sucrose, 0.5 mM EDTA, 5 mM Tris-HCl, pH 6.9, 1 mM PMSF, and 1 mg/ml of leupept also by passing them 10 times through a 25 G needle. Oocyte debris were pelleted by two consecutive centrifugations at 100 g for 10 min at 4°C. Equal amounts of proteins derived from mpkCCD$_{c14}$ cells and a smaller amount from oocyte expressing Usp2-45, Usp2-69, Usp53t, Usp53fl, H_v1 and/or ENaC (protein amount per lane equivalent to 1 oocyte) were loaded on a 10% or 12% SDS PAGE and subsequently transferred electrophoretically to a PVDF-membrane (Immobilon-P, Millipore, USA). After blocking with 3-5% milk in Tris-buffered saline / 0.1% Triton X-100 (Sigma) overnight at 4°C or 1 h at room temperature, the blots were incubated with primary antibody (10 µg/ml anti-Usp2-45 affinity purified or anti-Usp53 rabbit serum 1:1000) in 2.5% milk for 2 h at room temperature or over night at 4°C. After washing and subsequent blocking for 1 h at room temperature, blots were incubated with goat anti-rabbit secondary antibody conjugated with horseradish peroxidase (1:10,000; BD Transduction Laboratories, Franklin Lakes,

USA) for 1 h at room temperature. Antibody binding was detected with the Super-Signal1 West Pico Substrate (Pierce). Chemiluminescence was detected with a DIANA III camera (Raytest, Straubenhardt, Germany) after different exposure times (Adam, Fakitsas et al. 2007).

4.7 Aldosterone treatment and total RNA extraction from mpkCCD$_{c14}$ cells

1 µM aldosterone was added to the minimal culture medium of mpkCCD$_{c14}$ cells grown on 100 mm plastic dishes. At 5 different time points cells were harvested and the RNA was extracted. Cells were lysed by scratching them from the plate using RLT buffer supplemented with β-mercaptoethanol (10 µl/ml) and passing them at least five times through a 20 G needle. For RNA extraction Quiagene RNA extraction Kit was used and the procedures were done following the manufacturers instructions. The quantification of the total RNA extracted from a 100 mm dish was perfomed using NanoDrop ND-1000 spectrophotometer (Agilent Technologies). For real-time RT PCR 10-100 ng of RNA per reaction was used.

4.8 Real-Time RT-PCR

Samples of 3 µl RNA (out of 60 µl) were used as templates for reverse transcription using TaqMan® Reverse Transcription Kit (Applied Biosystems) in the presence of 2.5 µM random hexamer primers (Applied Biosystems). Real-time PCR was performed using 3.5 µl of the cDNA as template using the TaqMan® Universal PCR master mix (Applied Biosystems). Primers and probes were designed using Primer Express 2.0 software (Applied Biosystems) to result in amplicons of 70-100 bp that span intron-exon boundaries. Each primer pair was first tested on mouse kidney cDNA and resulted in a single product of the expected size (data not shown). Probes were labelled with reporter dye FAM at the 5' end and the quencher dye TAMRA at the 3' end (Microsynth).

Reactions were run in 96-well optical reaction plates using a Prism 7700 cycler (Applied Biosystems). Thermal cycles were set at 95°C (10 minutes) and the 40 cycles at 95°C (15 seconds) and 60°C (1 minute) with auto ramp time. To analyze the data, the threshold was set to 0.06 (value in the linear range of amplification curves). All reactions were run in triplicates and the abundance of the target mRNAs was calculated relative to a reference mRNA coding for hypoxanthine guanine phosphoribosyl transferase (HPRT). Assuming an efficiency value of 2 (fold-increase in input mRNA required to decrease the cycle number by 1), relative expression ratios were calculated as $R = 2^{(Ct(HRPT) - Ct(test))}$, where Ct is the cycle number at the threshold and test stands for the tested mRNAs (Adam, Fakitsas et al. 2007). The real-time PCR primers and probes used were the following:

HPRT:

Forward primer: 5'-TATCAGACTGAAGAGCTACTGTAATGACC-3'

Reverse primer: 5'- TTACCAGTGTCAATTATATCTTCAACAACAATC-3'

Probe : 5'-TGAGAGATCATCTCCACCAATAACTTTTATGTCCC-3'

Usp53:

Forward primer : 5'-TTGTGTGACTCATCAGAAGTTTGC-3'

Reverse primer: 5'-AAAGGGCAGAGGCTCTGAGG-3'

Probe: 5'-ACACGTGAAGGAGATGGGAACCAGATG-3'

H_v1:

Forward primer: 5'-CACCAAGATCCAGCATCTGGA-3'

Reverse primer: 5'-CAGCTTGTTGAGCCGCTCA-3'

Probe: 5'-TTCAGCTGCTCCGAGAAGGAACAAGAA-3'

4.9 Transepithelial electrophysiological measurements

The resistance across intact monolayers of mpkCCD$_{c14}$ cells was measured with a Millicell (Millipore) device. A transepithelial resistance of 2 kOhm x cm^2 was considered as prerequisite for using the filter cultures for further electrophysiological measurements. Filters were mounted in a multichannel voltage current clamp device (Model VCC MC6 Revision B, Physiological Instruments) and monolayers maintained under current clamp conditions at a DC clamp level of 0 µA. Bipolar pulses of 5 µA were given for 620 ms every 60 sec. After 90 min, aldosterone (300 nM) was added to the medium. The medium was kept at 35-38°C and pH was continuously adjusted by CO_2 supply. The ENaC-mediated Na^+ current was specifically blocked by 10 µM amiloride after another 150 min and calculated as the difference in short circuit current before and 15 min after amiloride addition (Beron, Mastroberardino et al. 1995; Summa, Mordasini et al. 2001; Adam, Fakitsas et al. 2007).

Figure 11

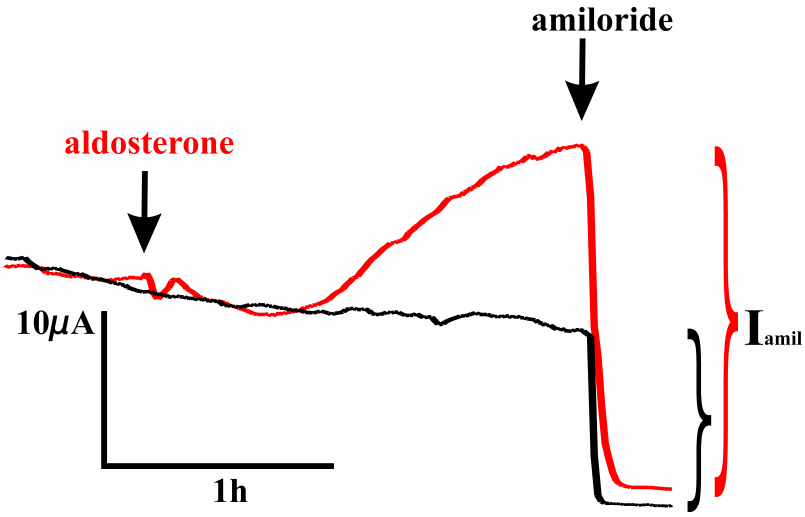

Figure 11 : *Original transepithelial current recording using an Ussing chamber system.* mpkCCD$_{c14}$ monolayers were treated with aldosterone (300 µM) (red) and after 150 min amiloride was applied to visualize the ENaC mediated current. In parallel mpkCCD$_{c14}$ cells were mounted and treated with the vehicle as a control (black). I_{amil} is significantly higher in aldosterone treated cells.

4.10 Kidney fixation

Male mice were anesthetized with ketamine (90 mg/kg body weight, Narketan 10, Vétoquinol, Lure, France) and xylazine (10 mg/kg body weight, Streuli, Uznach, Switzerland) intraperitoneally and perfused through the left cardiac ventricle with phosphate-buffered saline (PBS, 0.9% NaCl in 10 mM phosphate buffer, pH 7.4) followed by a buffered paraformaldehyde solution (4%, pH 7). The thoracic and abdominal cages were opened to allow access to the heart and to the vena cava distally to the kidneys. The vena cava was sectioned and the whole body perfused through the left heart ventricle, with 50 ml of PBS, followed by 50 ml a paraformaldehyde-lysine periodate (PLP, 4% paraformaldehyde, 7 mM NaH_2PO_4, 30.5 mM Na_2HPO_4, 10.5 mM Na^+ periodate, 58 mM L-Lysine, 146 mM sucrose), as previously described (Paunescu et al Jul 2004). Kidneys were removed, incubated overnight in PLP, washed several times with PBS and stored in PBS-0.02% Na^+ azide at 4°C (Paunescu, Da Silva et al. 2004). Kidney was then mounted with Kryostat OCT (Medite, Nunningen, Switzerland), frozen in liquid propane and stored at – 80°C.

4.11 Immunofluorescence

Kidney sections of 5 µm were cut on a Leica CM1850 cryostat (Leica, Wetzlar, Germany), applied to polylysine-coated slides (Kindler, Freiburg, Germany) and stored at -20°C. Sections were hydrated 15 min in PBS, washed three times with PBS, and then incubated with the primary antibodies diluted in PBS-0.04% Triton X-100 for 1 h at room temperature. The primary antibody rabbit anti-mH_v1 was diluted 1:50 (Pineda, Berlin, Deutschland) and the polyclonal goat anti human AQP2 antibody 1:500 (Santa Cruz Biotechnology, Inc, Santa Cruz, USA) and the rabbit anti m-pendrin (kind gift of C. Wagner; (Schulz, Dave et al. 2007)). Sections were then washed three times and incubated with the secondary antibody diluted in PBS-0.04% Triton X-100 for 1 h at room temperature. The secondary antibodies Alexa Fluor 488 donkey anti-goat IgG, 594 goat anti-mouse IgG (Molecular Probes, Invitrogen, Carlsbad, USA), Cy2 donkey anti-

guinea pig (Jackson ImmunoResearch Laboratories Inc. Newmarket Suffolk, UK) were diluted (1:500 - 1:1000). After being washed three times, the sections were mounted with Glycergel medium (DakoCytomation, Glostrup, Denmark). Digital images were viewed by using a Nikon Eclipse TE300 epifluorescence microscope (Nikon Instruments Inc., Melville, USA) equipped with a DS-5M Standard CCD camera (Nikon) and acquired with NIS-Elements (Nikon). Images were further processed using Photoshop 7 (Adobe, San Jose, USA) (Romeo, Dave et al. 2006).

4.12 Statistics

Data were expressed as means ± SEM. Calculations and graphs were made using GraphPad Prism™ Version 4.0 (GraphPad Inc.) and significance was tested using the Student's t-test, Kruskal-Wallis or Mann-Whitney test.

5 Results

Using an Affymetrix gene-screen, we identified a list of mouse connecting and collecting duct genes that are regulated by aldosterone in a short term manner (Adam, Fakitsas et al. 2007). The gene screen was done by Panos Fakitsas. My work focused on three significantly up-regulated gene products: the ubiquitin-specific proteases Usp2 and Usp53 and the voltage gated proton channel mVSOP (H_v1). Their impact on channels and transporters involved in Na^+ absorption in the collecting duct was investigated using mainly exogenous co-expression in the *X. laevis* oocyte system. Further experiments were performed in mpkCCD$_{c14}$ cells. The retroviral transduction of mpkCCD$_{c14}$ cells was done by Dr. Simone M. R. Carmargo and mouse kidney fixation was elegantly performed by Dustin Singer.

5.1 Original research article

This section contains an original research article published in January 2007 in the Journal of the American Society of Nephrology. It gives new insights in the short term regulation of ENaC by aldosterone *via* ubiquitylation/deubiquitylation. The article provides informations about a gene screen performed on mRNA obtained from microselected mouse distal nephron. One of new aldosterone regulated gene products, Usp2-45 was shown to regulate ENaC function by deubiquitylation.

Panos Fakitsas performed the gene screen analysis and members of the laboratory of Prof. O. Staub contributed to the article performing experiments in Hek293 cells. My contribution to the research article was showing ENaC activation by Usp2-45 in oocytes and mpkCCD$_{c14}$ cells. A more detailed description of the results that I provided to this article is to be found in section 5.2 of this thesis. Panos Fakitsas who did the gene screen analysis shared with me the first authorship.

Early Aldosterone-Induced Gene Product Regulates the Epithelial Sodium Channel by Deubiquitylation

Panagiotis Fakitsas,* Gabriele Adam,* Dorothée Daidié,† Miguel X. van Bemmelen,† Fatemeh Fouladkou,† Andrea Patrignani,‡ Ulrich Wagner,‡ Richard Warth,* Simone M.R. Camargo,* Olivier Staub,† and François Verrey*

**Institute of Physiology and Centre for Integrative Human Physiology, University of Zurich, ‡Functional Genomics Centre, Eidgenössische Technische Hochschule & University of Zurich, Zurich, and †Institute of Pharmacology and Toxicology, University of Lausanne, Lausanne, Switzerland*

The mineralocorticoid hormone aldosterone controls sodium reabsorption and BP largely by regulating the cell-surface expression and function of the epithelial sodium channel (ENaC) in target kidney tubules. Part of the stimulatory effect of aldosterone on ENaC is mediated by the induction of serum- and glucocorticoid-regulated kinase 1 (Sgk1), a kinase that interferes with the ubiquitylation of ENaC by ubiquitin-protein ligase Nedd4-2. *In vivo* early aldosterone-regulated mRNA now has been identified in microselected mouse distal nephron by microarray. From 22 mRNA that displayed a two-fold or more change, 13 were downregulated and nine were upregulated. Besides Sgk1, the induced mRNA include Grem2 (protein related to DAN and cerebrus [PRDC]), activating transcription factor 3, cAMP responsive element modulator, and the ubiquitin-specific protease Usp2-45. The induction of this last enzyme isoform was verified in mouse distal nephron tubule at the protein level. With the use of Hek293 cells, *Xenopus* oocytes, and mpkCCD$_{c14}$ cells as expression systems, it was shown that Usp2-45 deubiquitylates ENaC and stimulates ENaC-mediated sodium transport, an effect that is not additive to that of Sgk1. A deubiquitylating enzyme that targets ENaC *in vitro* and thus may play a role in sodium transport regulation was identified within a series of new *in vivo* early aldosterone-regulated gene products.

J Am Soc Nephrol 18: 1084–1092, 2007. doi: 10.1681/ASN.2006080902

The stimulatory action of the mineralocorticoid hormone aldosterone on Na^+ reabsorption and K^+ secretion can be arbitrarily divided in an early regulatory and a late anabolic phase (1). Early changes in salt transport can be observed within 30 min after initiation of a hormonal treatment and correspond to short-term regulatory effects that occur during circadian fluctuations and at the onset of more drastic regulatory changes as elicited by restricted salt uptake or loss of extracellular volume (2,3). These early actions are thought to be mediated mostly by the induction/repression of proteins that belong to the regulatory pathways that control the function of preexisting transport effectors such as the epithelial sodium channel (ENaC) and the Na^+,K^+-ATPase and K^+ channels. As yet, only a few aldosterone-induced regulatory proteins have been identified and experimentally shown to have an impact on ENaC function. These are K-Ras2, identified in amphibian cells, GILZ, identified in mammalian kidney cells, and the serum and glucocorticoid-regulated kinase serum- and glucocorticoid-regulated kinase 1 (Sgk1) that was also shown to be regulated in mammalian kidney (4–8). Furthermore, the kidney-specific short form of Wnk1 that stimulates Na^+ reabsorption *via* the Na^+-Cl^- co-transporter (NCC) was shown to be regulated by aldosterone in cultured kidney cells (9).

An important mechanism by which Sgk1 stimulates ENaC cell-surface expression and function is by phosphorylating the ubiquitin-protein ligase Nedd4-2 and thereby interfering with its function. Ubiquitylation (*i.e.*, the labeling of target proteins with ubiquitin polypeptides) of membrane proteins has been recognized in recent years as an important mechanism for controlling the cell-surface expression and endosomal/lysosomal degradation of this type of protein (10,11). When Nedd4-2 is not phosphorylated, it can bind to the PY motif in the COOH-termini of ENaC subunits and ubiquitylate ENaC on lysine residues that are situated in the NH_2 termini, thereby inducing channel downregulation at the plasma membrane (12–16). It is interesting that the lack of PY motif in β- or γ-ENaC that is characteristic of Liddle syndrome, an inherited form of salt-sensitive hypertension (17–19), leads to an increase in cell-surface ENaC expression and possibly also to an augmentation in its open probability (P_o), causing Na^+ retention, low K^+, and hypertension (7,20–22). The short signaling cascade that leads from Sgk1 induction *via* inhibition of Nedd4-2 to the activation of ENaC represents the first direct link between the aldosterone-regulated transcriptional activity of the mineralocorticoid receptor and the function of ENaC that has been demonstrated (13).

Received August 25, 2006. Accepted January 22, 2007.

Published online ahead of print. Publication date available at www.jasn.org.

P.F. and G.A. contributed equally to this work. R.W.'s current affiliation is Institute of Physiology, University of Regensburg, Regensburg, Germany.

Address correspondence to: Dr. François Verrey, Institute of Physiology, University of Zurich, Winterthurerstrasse 190, CH-8057 Zurich, Switzerland. Phone: +41-44-635-5044/46; Fax: +41-44-635-6814; E-mail: verrey@access.unizh.ch

ISSN: 1046-6673/1804-1084

The Sgk1–Nedd4-2 pathway, however, cannot be the only link between aldosterone and ENaC function. This has been indicated by the results of experiments that were performed with mpkCCD$_{cl4}$ cells that expressed Liddle-type ENaC channels or with mice that expressed an ENaC-β subunit with Liddle mutation, thus displaying impaired ENaC/Nedd4-2 interaction (23,24). In these systems, aldosterone was still able to stimulate transepithelial sodium transport. Hence, the pathways that link the transcriptional activity of activated mineralocorticoid receptor to ENaC function independent of ENaC PY motif and thus presumably independent of Nedd4-2–mediated ubiquitylation still need to be clarified. In that respect, it is interesting to mention two observations that support the possibility of an additional aldosterone-induced regulatory mechanism that has an impact on ENaC function/surface expression, namely the demonstration of an unsuspected regulatory role of γ-ENaC in collecting duct cells and of a stimulation of ENaC by Sgk1 that is mediated by the phosphorylation of the α subunit (25,26). It therefore is anticipated that other gene products are rapidly regulated by aldosterone in target cells that participate to the control of Na^+ reabsorption and K^+ secretion.

In this study, we describe the comparison by microarray of RNA that were extracted from epithelial cells of the aldosterone-sensitive distal nephron (ASDN) of control and aldosterone-treated mice. We thereby identified 22 significantly and more than two-fold regulated RNA. We anticipate that some of them encode proteins that participate in early regulatory effects of aldosterone that are independent of ENaC ubiquitylation. However, in this study, we focused on the induced deubiquitylating enzyme Usp2-45 and demonstrated in expression systems that it deubiquitylates ENaC and increases its function.

Materials and Methods

Animal studies were in accordance with the Guide for Care and Use of Laboratory Animals (Institute of Laboratory Animal Resources, National Academy of Science, Bethesda, MD).

Mouse Treatment, Kidney Dissection, and Tubule Microcollection

Female C57BL/6JOlaHsd mice (Harlan, Horst, The Netherlands), approximately 8 wk of age, received drinking water that contained 0.3% NaCl for at least 5 d before the treatment. All mice were housed in a temperature- and humidity-controlled room with an automatic 12-h light/dark cycle (6 a.m./6 p.m.). Aldosterone (Acrôs Organics, Pittsburgh, PA; 10 μg/kg body wt in 0.33% ethanol and 0.9% NaCl) or canrenoate (Sigma, Sternheim, Germany; 10 mg/kg in 0.9% NaCl) was injected intraperitoneally, or mice were left untreated. Forty-two minutes later, mice were anesthetized with ketamine (Vétoquinol AG, Uznach, Switzerland) and xylazine (Streuli AG, Uznach, Switzerland; intraperitoneally 100 and 0.5 μg/g, respectively). They were then perfused through the left ventricle with Ringer solution that contained collagenase and protease (5 and 1 mg in 15 ml, respectively; Sigma) while the lower vena cava was opened. Kidneys were removed and cut transversally in 2-mm slices that were incubated for 10 min at 38°C in a collagenase solution (1 mg/ml Ringer solution). These tubule preparations were then transferred to ice-cold Ringer (1 h after aldosterone injection), washed, and resuspended three times. Segments (75 to 85) of cortical collecting duct/connecting tubule (CCD/CNT; approximately 1.1 mm of total length) were identified under a binocular microscope (SMZ1000; Nikon AG, Egg, Switzerland) at 4°C and transferred directly into RLT lysis buffer of the Qiagen RNeasy Micro Kit (Qiagen AG, Hombrechtikon, Switzerland) that contained 1% β-mercaptoethanol (Sigma-Aldrich, Buchs, Switzerland) using a pair of sharp forceps (F.S.T. GmbH, Heidelberg, Germany). For plasma aldosterone and corticosterone measurements, mice were anesthetized as described, and blood was collected by puncture of the vena cava. Plasma aldosterone and corticosterone levels were measured using an ELISA and a ^{125}I-RIA kit from Immuno-Biologic Laboratories (Hamburg, Germany), respectively.

RNA Purification and Quality Control, Microarray Target cRNA Preparation, Target cRNA Hybridization and GeneChip Scanning, Real-Time Reverse Transcriptase–PCR, Quality Control of Microarrays, and Statistical Analyses

Please refer to online supplementary materials for detailed methods.

Prediction of Mineralocorticoid Hormone Response Elements in the Promoter Region of the Mouse Usp2-45 Gene and Western Blotting of Usp2-45 in Microcollected Mouse Kidney CNT and CCD

Please refer to online supplementary materials for detailed methods.

Cloning of Mouse Usp2-45, Usp2-69, and Usp15; Site-Directed Mutagenesis and cRNA Preparation; and Coexpression of mUsp2-45, Usp2-69, mUsp15, $\alpha\beta\gamma$XENaC, and XSgk in Xenopus laevis *Oocytes*

Please refer to online supplementary materials for detailed methods.

Two-Electrode Voltage Clamp on Xenopus *Oocytes, Ubiquitylation of ENaC in Hek293 Cells, and Culture and Retroviral Transduction of mpkCCD Cells*

Please refer to online supplementary materials for detailed methods.

Western Blotting and Real-Time PCR of Usp2-45 in mpkCCD$_{c14}$ Cells and Transepithelial Electrophysiologic Measurements

Please refer to online supplementary materials for detailed methods.

Results

Microarray to Identify Early Aldosterone-Regulated mRNA in Mouse ASDN

To identify other early aldosterone-regulated gene products in kidney target cells *in vivo*, we first established a short-term aldosterone treatment scheme in mice. Female C57BL/6J mice that received 0.3% NaCl in their water to repress partially their endogenous aldosterone production were administered an injection at 10:00 a.m. (4 h after beginning of daytime) with aldosterone (10 μg/kg body wt; Figure 1, A and B) or were left untreated. The aldosterone injection led to a transient increase in plasma aldosterone that 15 min after injection was at a level of approximately 10 nM, a value within the range expected for mice on a low-salt diet (27). The plasma aldosterone concentration was nearly back to the initial value of approximately 0.5 nM after 60 min.

To obtain kidney aldosterone-target tissue RNA 1 h after hormone injection, mice were anesthetized 42 min after aldosterone injection and rapidly perfused with collagenase solution. Kidneys were removed, sliced, and further digested in

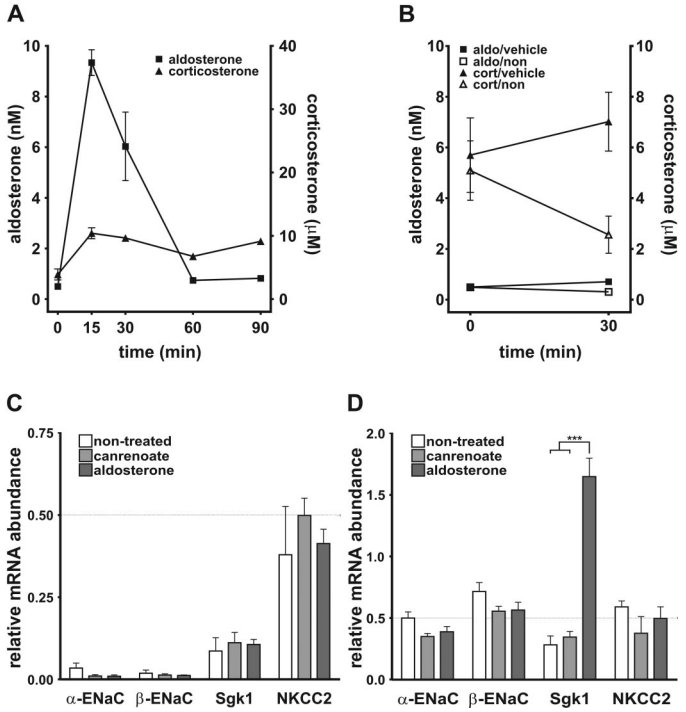

Figure 1. Conditions of short-term aldosterone stimulation. (A) Time course of plasma aldosterone and corticosterone levels after intraperitoneal aldosterone injection (10 μg/ kg body wt) at 10 a.m. (means ± SEM, $n = 3$ mice per time point). (B) Comparison of plasma aldosterone (aldo) and corticosterone (cort) at 10 a.m. and at 10:30 a.m. with or without injection of vehicle at 10 a.m. (means ± SEM, $n = 3$ to 6 mice per point). (C and D) Test for enrichment and aldosterone stimulation of RNA prepared from microselected connecting tubule/cortical collecting duct (CNT/CCD). Mice were administered an injection of aldosterone as in A or canrenoate or were left untreated, and RNA was prepared from tubules that were obtained after 1 h. The abundance of α and β epithelial sodium channel (ENaC), Sgk1 and Na^+,K^+,Cl^- co-transporter 2 (NKCC2) mRNA was measured by real-time reverse transcriptase–PCR (RT-PCR) in RNA that was prepared from total kidney (C) and from microselected tubule segments (D). Given are means relative to β-actin ± SEM; $n = 6$ mice. ***$P < 0.0001$ by one-way ANOVA.

collagenase solution at 38°C for the rest of the hour (in the absence of aldosterone). The tubule preparation was then transferred to 4°C, and segments of CNT/CCD were microselected.

The RNA samples that were prepared from single mice were tested in terms of quantity, integrity, enrichment, contamination, and response to aldosterone (Figure 1, C and D). These measurements revealed that in microisolated CNT/CCD segments, ENaC mRNA was enriched 15- to 40-fold over total kidney, whereas thick ascending limb–specific triple co-transporter Na^+,K^+,Cl^- co-transporter 2 (NKCC2) mRNA was not increased. Sgk1 mRNA was enriched three- to four-fold over the total kidney preparation and specifically further increased five- to six-fold by aldosterone. It is interesting that the mere manipulation of the mice increased plasma corticosterone slightly (Figure 1, A and B) but did not have an impact on Sgk1 expression (Figure 1, C and D). More than two thirds of the prepared RNA samples fulfilled the selection criteria of quantity, integrity, enrichment, lack of contamination, and Sgk1 induction and could be used as template for cDNA amplification and labeled target RNA synthesis. Target cRNA made from six control and from six aldosterone-injected mice were separately hybridized to mouse full genome GeneChip microarrays (MOE 430 v2; Affymetrix, Santa Clara, CA). Raw array data were processed using the GCRMA and the MAS5 algorithms (Microarray data are available at Array Express with the accession number E-TABM-229.) The data were filtered using a t test with a cutoff $P \leq 0.05$ and using a fold-change limit of 2.0. The cumulative list of genes that fulfilled these criteria after processing with one of the algorithms comprised 90 genes (73 genes with GCRMA and 39 with MAS5). As detailed in Table 1, 22 genes fulfilled these criteria with both algorithms, nine that are upregulated and 13 that are downregulated. A scatter plot and the hierarchical clustering of the results that were calculated by the GCRMA method are shown in Supplementary Figure 1B. We retested the differential expression level of eight mRNA that were identified in the microarray screen by real-time RT-PCR (see primers and probes sequences in the online supplementary material) on RNA from three other mice per condition. As shown in Table 1, the regulation was verified in six cases.

Aldosterone-Induced Usp2-45 Deubiquitylates ENaC

Ubiquitylation of ENaC had previously been shown to play an important role in the control of Na^+ reabsorption (12) and our screening had confirmed that Sgk1, a kinase that is known to inhibit the action of the ubiquitin-protein ligase Nedd4-2 on ENaC, was rapidly induced by aldosterone. We focused now on Usp2, a ubiquitin-specific protease that was also induced and belongs to a large protein family that is involved in reversing the ubiquitylation of target proteins (28–30). We specifically investigated the potential role of the isoform Usp2-45 that we detected in kidney by reverse transcriptase–PCR (RT-PCR), unlike the other isoform Usp2-69 that is expressed only at low levels in the kidney (31) (P.F. and F.V., unpublished observation) and in mpkCCD$_{c14}$ cell (10-fold difference; discussed further). The analysis of the promoter region around the TATA box of the Usp2-45 isoform identified at least four potential hormone response elements that support the possibility of a direct regulation by aldosterone (see Supplementary Figure 2). An induction by aldosterone of the shorter Usp2-45 isoform but not of the Usp2-69 isoform was also detected in mpkCCD cells (discussed further).

To test whether the aldosterone-induced Usp2-45 mRNA induction translates *in vivo* into an increase in Usp2-45 protein, we performed Western blotting of proteins that were prepared from microselected segments of CNT/CCD that were obtained from mice that were subjected to the same hormone treatment as previously performed for the mRNA studies. As shown in Figure 2, the polyclonal rabbit anti-mouse Usp2-45 antibody recognized a 45-kD band that was blocked by competing immunizing peptide. This band was selectively increased 1 h after an aldosterone injection by a factor of approximately 2, as

Table 1. Kidney CNT/CCD RNA that changed two-fold or more by 1 h of aldosterone[a]

RNA[b]	Affymetrix GeneChip				Real-Time RT-PCR	
	Genebank Accession No.	Fold Change[c]	Range	*P*	Fold Change[d]	*P*
Upregulated genes						
protein related to DAN and cerberus	NM_011825	7.2	2.1 to 17.7	0.045	5.6	0.029
serum/glucocorticoid regulated kinase	NM_011361	4.0	3.0 to 5.1	<0.0001	8.1	0.001
activating transcription factor 3	BC019946	3.5	2.5 to 4.9	0.001	8.6	0.018
cAMP responsive element modulator	NM_013498	3.0	1.3 to 4.5	0.004	1.1	0.651
mus musculus transcribed sequences	AI098139	2.9	1.7 to 3.6	<0.001		
RIKEN cDNA clone 6430570G24	BG069663	2.8	1.7 to 4.4	0.004		
ubiquitin specific protease 2	AI553394	2.2	1.2 to 3.8	0.019	1.6	0.001
growth arrest and DNA-damage-inducible 45 gamma	AK007410	2.2	1.5 to 3.2	0.001		
RIKEN cDNA clone 6430570G24	BG069663	2.2	1.5 to 2.9	<0.0001		
Downregulated genes						
RIKEN cDNA 4833417L20 gene	AK017914	0.5	0.3 to 0.9	0.014		
imilarity to pir:A45973 (H.sapiens)	AI597080	0.5	0.3 to 0.6	0.009		
argininosuccinate synthetase 1	BM213298	0.4	0.3 to 0.5	0.007		
RIKEN cDNA clone:D630044A17	BB498095	0.4	0.2 to 0.6	0.006		
partial mRNA for hypothetical prot.	BG817292	0.4	0.3 to 0.6	0.006		
fatty acid binding protein 1, liver	NM_017399	0.4	0.2 to 0.8	0.006		
transcribed sequences	BE991175	0.4	0.2 to 0.6	0.006		
RIKEN cDNA clone:C230084M03	BM123508	0.4	0.2 to 0.8	0.005		
RIKEN cDNA 4833417L20 gene	BM217861	0.4	0.3 to 0.4	0.004		
H+/K+-ATPase alpha, nongastric	NM_138652	0.4	0.1 to 0.8	0.004	1.0	0.946
Slc22a8 (Oat3)	AV330315	0.3	0.1 to 0.6	0.004	0.1	0.024
G0/G1 switch gene 2	NM_008059	0.3	0.2 to 0.6	0.003	0.2	0.015
RIKEN cDNA clone E030031K24	BB533736	0.3	0.2 to 0.5	0.003		

[a]RNA in italics were also tested by real-time reverse transcriptase–PCR.
[b]RNA with fold-change ≥2 and *t* test $P \leq 0.05$ using GCRMA and MAS5 algorithms.
[c]Values were obtained using GCRMA.
[d]Real-time PCR data were obtained with specific intron spanning primer/probe sets, $n = 3$ mice.

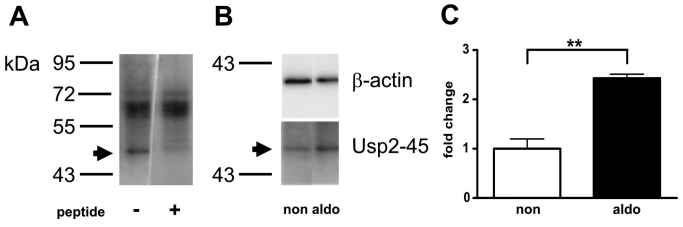

Figure 2. Usp2-45 detected by Western blot in CNT/CCD. Aldosterone treatment and tubule microselection were as described for mRNA preparations. (A) Western blot with rabbit anti-mouse Usp2-45 antibody with or without immunizing peptide identifies a 45-kD band that is competed by immunizing peptide. (B) Representative pair of Western blots from a control and an aldosterone-treated mouse. The top panels show the actin band, and the bottom panels show the Usp2-45 band visualized on the same blots. (C) The Usp2-45 signals were normalized to the actin signal of the same mouse ($n = 3$ for each condition), and the means are shown. $^{**}P < 0.01$.

previously shown for the mRNA. That the Usp2-45 mRNA indeed encodes an active ubiquitin-specific protease was confirmed by the fact that its core domain that is produced in *Escherichia coli* very efficiently cleaves ubiquitin off from a test substrate *in vitro* (B. Oberfeld *et al.*, unpublished observations) (32).

To test the possible impact of Usp2-45 on ENaC function, we coexpressed it with ENaC in *Xenopus laevis* oocytes and compared the effect of Usp2-45 with that of Sgk1, the kinase that inhibits endogenous Nedd4-2. Coexpression of Usp2-45 with ENaC increased the level of amiloride-sensitive Na^+ current nearly four-fold, an effect similar to that of Sgk1 (Figure 3A and Supplementary Figure 3, A and B). It is interesting that coexpression of Sgk1 with Usp2-45 did not further increase ENaC function, suggesting that these two enzymes have an impact on the same regulatory mechanism (Figure 3A and Supplementary Figure 3B).

To test whether the effect of Usp2-45 was mediated by its protease activity, we mutated its cysteine 67 that corresponds to one of the catalytically active amino acids of its cysteine protease motif (31,33). Consistent with a requirement for an enzymatically active Usp2-45, this mutant did not affect ENaC activity at the membrane (Figure 3B and Supplementary Figure 3C). To control whether this effect of Usp2-45 was specific for this ubiquitin-specific protease, we carried out the same experiment with another randomly chosen ubiquitin-specific protease, Usp15. The results indicated that the effect of Usp2-45 is specific, because coexpression of Usp15 in contrast rather decreased ENaC function (Figure 3C and Supplementary Figure 3D). It is probable that this latter effect is due to the deubiquitylation of other proteins that interfere with the expression of ENaC. In addition, we coexpressed the longer Usp2-69 isoform that turned out not to have an impact on ENaC function (Figure

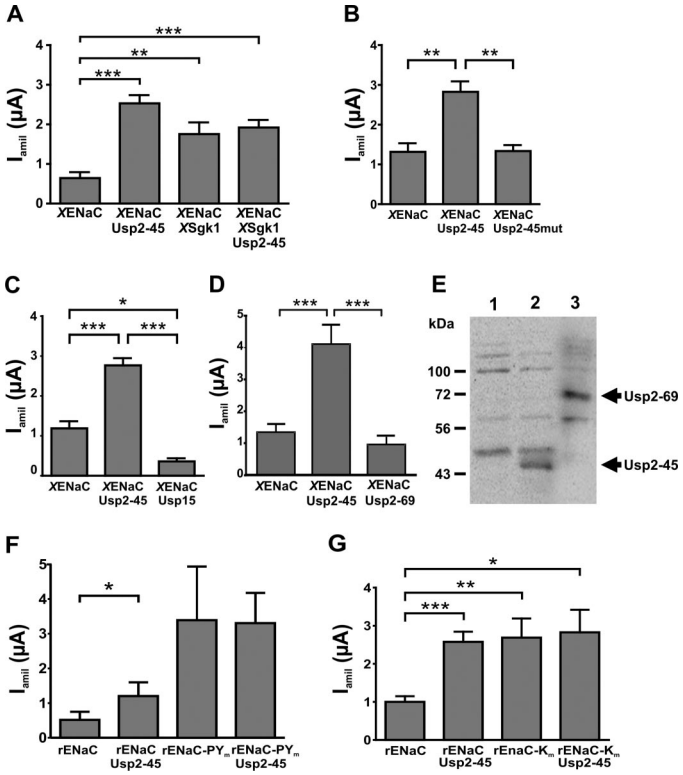

Figure 3. Usp2-45 increases amiloride-sensitive Na^+ current (I_{amil}) carried by coexpressed $\alpha\beta\gamma$-ENaC. Original tracings are shown in Supplementary Figure 3. (A) Summary of amiloride-sensitive whole-cell currents at a holding potential of −100 mV. Coexpression of Usp2-45 or of XSgk1 increased the ENaC-mediated amiloride-sensitive I_{amil} to a similar extent. These effects were not additive. Data are means ± SEM; $n = 23$ to 27. $^{**}P < 0.01$; $^{***}P < 0.001$. (B through D) Characterization of Usp2-45 stimulatory effect on I_{amil} in *Xenopus* oocytes. (B) Cys67Ala protease-dead Usp2-45 mutant (Usp2-45mut) does not stimulate XENaC current I_{amil} at −100 mV. Data are means ± SEM; $n = 12$ to 15. $^{**}P < 0.01$. (C) Another Usp (Usp15) does not stimulate XENaC-mediated I_{amil} at −100 mV. Data are means ± SEM; $n = 20$ to 24. $^{*}P < 0.05$; $^{***}P < 0.001$. (D) The Usp2-45 isoform does not stimulate XENaC-mediated I_{amil} at −100 mV. Data are means ± SEM; $n = 20$ to 22. $^{***}P < 0.001$. (E) Western blot made with lysate of control and Usp2-45– and Usp2-69–expressing *Xenopus* oocytes and incubated with a pan-Usp2 antibody shows specific bands that correspond to each isoform, confirming that both were similarly expressed and that the lack of ENaC stimulation by Usp2-69 was not due to a lack of expression of this isoform. (F) Effect of Usp2-45 on ENaC-mediated I_{amil} is prevented by mutation of rENaC PY motif (rENaC-PY$_m$). I_{amil} at −100 mV is shown. Data are means ± SEM; $n = 4$ independent experiments with a total of 20 oocytes. $^{*}P < 0.05$ using paired t test. (G) Effect of Usp2-45 on ENaC-mediated I_{amil} is prevented by mutation of rENaC ubiquitylation site (lysine-mutant rENaC-K$_m$). I_{amil} at −100 mV is shown. Data are means ± SEM; $n = 4$ to 5 independent experiments with a total of 20 and 25 oocytes, respectively. $^{*}P < 0.05$; $^{**}P < 0.01$; $^{***}P < 0.001$.

3D). In this case, we also verified by Western blotting that this ubiquitin-specific protease isoform was indeed expressed as expected (Figure 3E).

We then asked whether Usp2-45 interferes with Nedd4-2–dependent regulation of ENaC, a mechanism that involves the interaction of Nedd4-2 with PY motifs that are present on the C-termini of the ENaC subunits and is defective in Liddle syndrome (14). ENaC that was devoid of PY motifs (α Y673A, β Y618H, γ Y628A) is resistant to Nedd4-2 and thus displayed a higher level of amiloride-sensitive Na^+ current than did wild-type ENaC. This current was indeed resistant to the stimulatory action of Usp2-45 (Figure 3F). This observation supports the hypothesis that Usp2-45 cleaves off ubiquitin moieties that Nedd4-2 ligates onto ENaC. The involvement of direct ENaC ubiquitylation was then verified by coexpressing Usp2-45 with ENaC that was devoid of potential ubiquitylation sites (lysine residues of the intracellular NH_2-terminal domains of all three subunits mutated to arginine) in *Xenopus* oocytes. As expected for the case that Usp2-45 deubiquitylates ENaC directly, this mutant channel was not activated in the presence of Usp2-45 (Figure 3G).

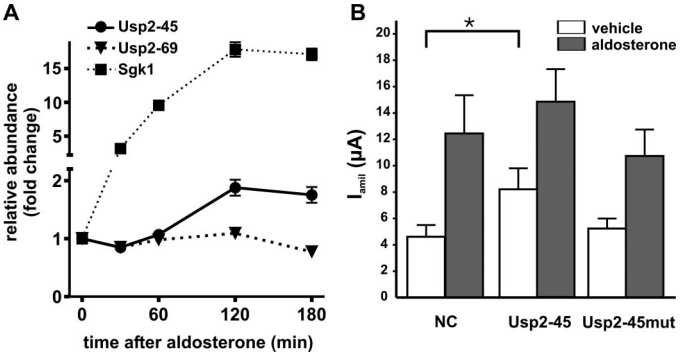

Figure 4. Expression of endogenous and exogenous Usp2-45 in mpkCCD$_{cl4}$ cells. (A) Regulation of endogenous Usp2-45, Usp2-69, and Sgk1 mRNA by aldosterone (10^{-6} M; see Materials and Methods in online supplementary material and reference [35]) in mpkCCD$_{cl4}$ cells. Usp2-45 upregulation is slightly more delayed than that of Sgk1. Unlike its isoform Usp2-45, Usp2-69 is not induced by aldosterone. Baseline mRNA abundance of Usp2-45 was 10-fold higher than that of Usp2-69. Fold changes of normalized means relative to β-actin ± SEM are given ($n = 3$). The isoform-specific real-time RT-PCR primers and probes are shown in online supplementary material. (B) Baseline transepithelial I_{amil} across mpkCCD$_{cl4}$ cell monolayers that were cultured on permeable supports is significantly increased in cells that overexpressed Usp2-45 compared with vector-transduced negative control cells (NC) and cells that were transduced with protease-dead Usp2-45mut (□). $^{*}P < 0.05$; $n = 9$ to 12. Aldosterone (300 nM) given for 3 h increased I_{amil} similarly in the monolayers that were made of the different mpkCCD$_{cl4}$ cell populations (■).

To verify that the effect of Usp2-45 on ENaC function was not an artifact that was due to the coexpression of two proteins in *Xenopus* oocytes but also takes place with endogenous ENaC in CCD cells, we addressed this question using the mouse CCD cell line mpkCCD$_{cl4}$ (34). We actually first verified whether Usp2-45 is expressed and regulated by aldosterone in these cells. The relative expression of the two isoforms in mpkCCD$_{cl4}$ cells was similar to the observation made in microdissected CNT/CCD with a 10-fold higher expression of the Usp2-45

mRNA. The time course of the regulation by aldosterone revealed that only the Usp2-45 isoform was regulated (Figure 4A). To investigate the effect of Usp2-45 on the transepithelial Na^+ transport function, we expressed exogenous Usp2-45 as well as mutant protease-dead Usp2-45 in mpkCCD cells by retroviral transduction and verified by Western blot that the expression levels were equal (Supplementary Figure 4). As expected, when ENaC expression and activity were limited by its ubiquitylation, expression of functional Usp2-45 increased the baseline transepithelial amiloride-sensitive Na^+ transport (Figure 4B). In contrast, the expression of the protease-dead mutant had no effect. The increase in Na^+ transport that was induced by aldosterone (300 μM; see Materials and Methods in the online supplementary material and reference [35]) that was given for 3 h was not modified significantly by the expression of wild-type and mutant Usp2-45, as expected considering that short-term aldosterone prevents the Nedd4-2–mediated ubiquitylation of ENaC by inducing Sgk1. These results that were obtained in CCD cells confirm that Usp2-45, a ubiquitin-specific protease that was identified because of its *in vivo* regulation by aldosterone, also acts on endogenous ENaC in kidney tubule cells.

To test directly the hypothesis that Usp2-45 counteracts the effect of Nedd4-2 by deubiquitylating ENaC, we used Hek293 cells as an expression system. Coexpression of Nedd4-2 with ENaC in Hek293 cells massively increased the ubiquitylated form of the channel that was visualized with anti-ubiquitin antibody on immunoprecipitates of α- and γ-ENaC, thereby confirming that ENaC was itself ubiquitylated (Figure 5A). The impact of ubiquitylation on the total amount of ENaC was demonstrated by the decreased amount of ENaC that was visualized in the same samples with anti-ENaC antibody. Importantly, Usp2-45 coexpression decreased the amount of ubiquitylated ENaC and increased total ENaC, demonstrating that Usp2-45 antagonizes the effect of Nedd4-2 by directly deubiquitylating ENaC. The low level of ubiquitylated ENaC and the substantial level of total ENaC that was observed with Usp2-45 coexpression were similar to those that were observed with Nedd4-2cs, a catalytically inactive Nedd4-2 (Figure 5A).

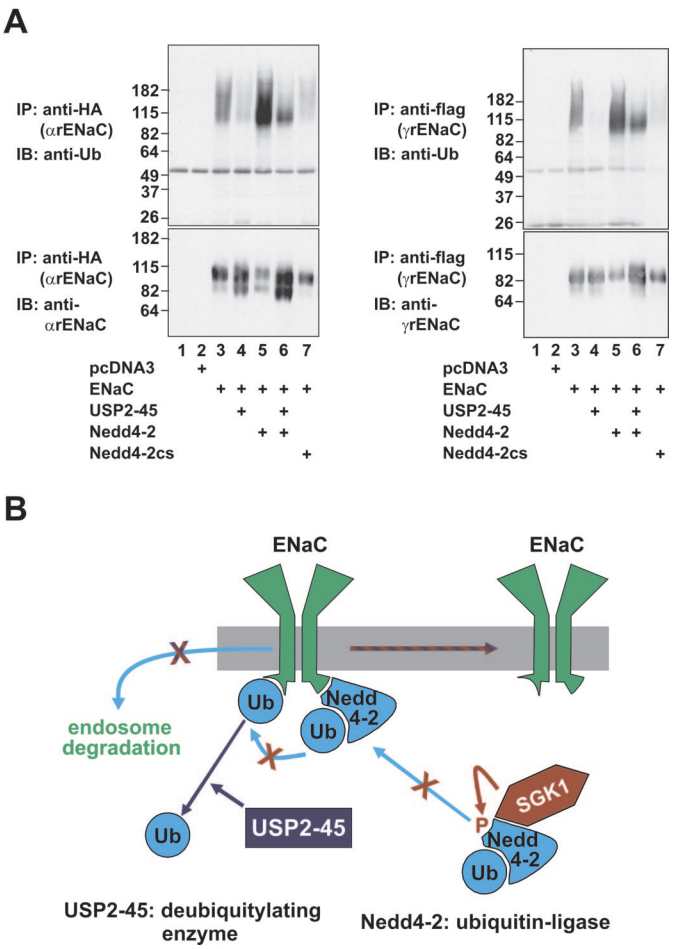

Figure 5. Inverse regulation of ENaC ubiquitylation and ENaC amount. (A) The ubiquitylated and the total amount of ENaC expressed in Hek293 cells are visualized by Western blotting (IB) of immunoprecipitated (IP) HA- and Flag-tagged α- and γ-rENaC subunits, respectively. The molecular weight of marker proteins is indicated in kD. Coexpression of Nedd4-2 and not of ligase-inactive Nedd4-2 (Nedd4-2cs) increases the ubiquitylation of both tested ENaC subunits, whereas it decreases their total amount. In the presence of Usp2-45, ENaC ubiquitylation is decreased and the total subunit amount is increased. (B) Schematic representation of the convergent effect of Sgk1 and Usp2-45 that both decrease the amount of ubiquitylated ENaC and thus increase the amount of intact channel. The subcellular localization of these ubiquitylation/deubiquitylation reactions has not yet been identified.

Discussion

Early Aldosterone-Regulated Gene Products

The number of mRNA the level of which was changed twofold or more in mouse ASDN within 1 h after an aldosterone injection is relatively low (22 mRNA). It is noteworthy that the signal intensity of these regulated mRNA on control mice arrays differs by more than two orders of magnitude, indicating large differences in their absolute baseline expression levels (see Supplementary Figure 1A). Not unexpected, the gene product with the highest absolute expression level and the second highest relative level of induction is Sgk1, the only early aldosterone-regulated gene product of mammalian kidney that has been identified earlier and shown to activate ENaC.

The gene product with the highest fractional increase (7.2-fold in Affymetrix screen, 5.6-fold by real-time RT-PCR) is Grem2 (protein related to DAN and cerebrus [PRDC]), an antagonist of bone morphogenic proteins 2, 4, 6, and 7 (36). The second upregulated gene product on the list is the already mentioned Sgk1 that is followed by two members of the cAMP response element binding (CREB) family of transcription factors, activating transcription factor 3 and cAMP responsive element modulator.

Our list of early aldosterone-regulated mRNA also included 13 mRNA that are downregulated (Table 1). The known mRNA with the highest fractional decrease (0.3-fold in Affymetrix screen, 0.2-fold by real-time RT-PCR) encodes G0s2, a putative G0/G1 switch gene the downregulation of which might prevent proliferation and thus favor differentiation. It is interesting

that there are also two transport proteins among the downregulated gene products, namely the polyspecific organic anion transporter 3 (Slc22a8) and the colonic H^+,K^+-ATPase.

Role of Deubiquitylation in Aldosterone Action

The regulation of the gene products discussed in the previous section seems to favor a decrease in proliferation of aldosterone target cells and to foster their differentiation. In addition, our screen identified with Sgk1 and Usp2-45 two aldosterone-induced gene products that interfere with protein ubiquitylation. As mentioned at the beginning of this article, Sgk1 was identified earlier as aldosterone-induced mRNA and protein, and its effect on ENaC function has been shown to be mediated to a large extent by its inhibitory action on the ubiquitylating enzyme Nedd4-2.

We have now indeed shown that the newly identified aldosterone-induced Usp2-45 directly deubiquitylates ENaC in the Hek273 cell expression system (Figure 5A). As expected, if the ubiquitylation of ENaC would lead to ENaC degradation, then the presence of Usp2-45 not only decreases the amount of ubiquitylated ENaC but also increases the total amount of ENaC. This biochemical evidence of ENaC deubiquitylation by Usp2-45 is supported by functional experiments made in *Xenopus* oocytes that show an increase in ENaC function that specifically is mediated by Usp2-45 and that depends on the integrity of its protease motif. Furthermore, we show both that the disruption of ENaC PY motifs and the disruption of ENaC lysine residues that potentially are targeted by Usp2-45 prevent the action of Usp2-45 on ENaC function. These results also strongly support the hypothesis that Usp2-45 acts on ubiquitin moieties that are ligated onto ENaC by the ubiquitin ligase Nedd4-2 (Figure 5B).

That a deubiquitylating enzyme that acts on ENaC is induced by aldosterone strengthens the notion that ubiquitylation plays a central role in the short-term regulation of ENaC. Although deubiquitylation of target proteins has been described since the early days of the ubiquitin system discovery (37), it has only recently gained considerable interest as a regulatory mechanism (for a review on deubiquitylation, see reference [29]). The mouse as the human genome encodes approximately 100 putative deubiquitylating enzymes, the function of most of which is not known. The Affymetrix screen that was presented in this article revealed that approximately 26 of these Usp are expressed in the aldosterone target cells of the mouse kidney tubule (present calls), but only Usp2-45 appeared in the list of regulated RNA (Table 1). On the basis of our results, the deubiquitylation of ENaC by Usp2-45 seems to be specific for Usp2-45, because none of the four other Usp that we tested in expression systems activated and/or deubiquitylated this channel (Figure 3, C and D; unpublished results). As yet, actually only a few examples of plasma membrane protein deubiquitylation have been published. One such example is the deubiquitylation of yeast membrane permeases that leads to their targeting to the vacuole (equivalent to the mammalian lysosome) by the ubiquitin-specific protease Doa4 (38). Another is the deubiquitylation and stabilization of the EGF receptor by the endosomal ubiquitin isopeptidases AMSH (associated molecule with the SHB domain of STAM) and UBPY (ubiquitin-specific protease Y) (39,40).

The identification of ENaC as a target of Usp2-45 represents the first report of a hormonally controlled channel-deubiquitylating mechanism. It is noteworthy to mention that this effect is not selective for kidney tubule, because Usp2-45 is also expressed and regulated in distal colon, yet another target epithelium of aldosterone (P.F. and F.V., unpublished observations). Previously published data on Usp2 suggest that its isoform Usp2-69 is regulated by androgens in liver and prostate, where it deubiquitylates and stabilizes fatty acid synthase (33). Furthermore, Usp2 was shown to be regulated in bone by parathyroid hormone (41), indicating that the *Usp2* gene products mediate various important hormonally regulated functions.

That the stimulatory action of Usp2-45 on ENaC depends on previous ENaC ubiquitylation indicates, however, that Usp2-45 induction cannot explain the effect of aldosterone on Liddle-type mutant ENaC (see the beginning of this article) (23,24). Therefore, it is expected that still other aldosterone-induced gene products, possibly also identified in our screen, act *via* different pathways on ENaC expression and function.

Conclusion

Our list of early aldosterone-regulated gene products contains two induced elements that interfere with the ubiquitylation of ENaC. Besides Sgk1, we identified Usp2-45 that we show to deubiquitylate ENaC in expression systems and thus represents a first example of a deubiquitylating enzyme acting on a channel.

Acknowledgments

The laboratory of F.V. was supported by Swiss National Science Foundation grants 31-59141 and 31-108021/1 and that of O.S. by Swiss National Science Foundation grant 31-103779. P.F. and G.A. received support from the Hartmann-Müller-Foundation, the EMDO-Foundation, the Zurich University Research Priority Program "Integrative Human Physiology," and the Functional Genomics Centre Zurich. We are grateful to Hubert Rehrauer for technical assistance.

Disclosures

None.

References

1. Verrey F, Hummler E, Schild L, Rossier BC: Control of Na^+ transport by aldosterone. In: *The Kidney, Physiology and Pathophysiology*, 3rd ed., edited by Seldin DW, Giebiesch G, Philadelphia, Lippincott Williams & Wilkins, 2000, pp 1441–1471
2. Horisberger JD, Diezi J: Effects of mineralocorticoids on Na+ and K+ excretion in the adrenalectomized rat. *Am J Physiol* 245: F89–F99, 1983
3. Wang Q, Horisberger JD, Maillard M, Brunner HR, Rossier BC, Burnier M: Salt- and angiotensin II-dependent variations in amiloride-sensitive rectal potential difference in mice. *Clin Exp Pharmacol Physiol* 27: 60–66, 2000
4. Spindler B, Mastroberardino L, Custer M, Verrey F: Characterization of early aldosterone-induced RNAs

identified in A6 kidney epithelia. *Pflugers Arch* 434: 323–331, 1997
5. Chen SY, Bhargava A, Mastroberardino L, Meijer OC, Wang J, Buse P, Firestone GL, Verrey F, Pearce D: Epithelial sodium channel regulated by aldosterone-induced protein sgk. *Proc Natl Acad Sci U S A* 96: 2514–2519, 1999
6. Naray-Fejes-Toth A, Canessa C, Cleaveland ES, Aldrich G, Fejes-Toth G: Sgk is an aldosterone-induced kinase in the renal collecting duct: Effects on epithelial Na+ channels. *J Biol Chem* 274: 16973–16978, 1999
7. Loffing J, Zecevic M, Feraille E, Kaissling B, Asher C, Rossier BC, Firestone GL, Pearce D, Verrey F: Aldosterone induces rapid apical translocation of ENaC in early portion of renal collecting system: Possible role of Sgk. *Am J Physiol Renal Physiol* 280: F675–F682, 2001
8. Soundararajan R, Zhang TT, Wang J, Vandewalle A, Pearce D: A novel role for glucocorticoid-induced leucine zipper protein in epithelial sodium channel-mediated sodium transport. *J Biol Chem* 280: 39970–39981, 2005
9. Naray-Fejes-Toth A, Snyder PM, Fejes-Toth G: The kidney-specific WNK1 isoform is induced by aldosterone and stimulates epithelial sodium channel-mediated Na+ transport. *Proc Natl Acad Sci U S A* 101: 17434–17439, 2004
10. Rotin D, Staub O, Haguenauer-Tsapis R: Ubiquitination and endocytosis of plasma membrane proteins: Role of Nedd4/Rsp5p family of ubiquitin-protein ligases. *J Membr Biol* 176: 1–17, 2000
11. Hicke L, Dunn R: Regulation of membrane protein transport by ubiquitin and ubiquitin-binding proteins. *Annu Rev Cell Dev Biol* 19: 141–172, 2003
12. Debonneville C, Flores SY, Kamynina E, Plant PJ, Tauxe C, Thomas MA, Munster C, Chraibi A, Pratt JH, Horisberger JD, Pearce D, Loffing J, Staub O: Phosphorylation of Nedd4-2 by Sgk1 regulates epithelial Na+ channel cell surface expression. *EMBO J* 20: 7052–7059, 2001
13. Staub O, Verrey F: Impact of Nedd4 proteins and serum and glucocorticoid-induced kinases on epithelial Na+ transport in the distal nephron. *J Am Soc Nephrol* 16: 3167–3174, 2005
14. Abriel H, Loffing J, Rebhun JF, Pratt JH, Schild L, Horisberger JD, Rotin D, Staub O: Defective regulation of the epithelial Na+ channel by Nedd4 in Liddle's syndrome. *J Clin Invest* 103: 667–673, 1999
15. Snyder PM, Olson DR, Thomas BC: Serum and glucocorticoid-regulated kinase modulates Nedd4-2-mediated inhibition of the epithelial Na+ channel. *J Biol Chem* 277: 5–8, 2002
16. Flores SY, Loffing-Cueni D, Kamynina E, Daidie D, Gerbex C, Chabanel S, Dudler J, Loffing J, Staub O: Aldosterone-induced serum and glucocorticoid-induced kinase 1 expression is accompanied by Nedd4-2 phosphorylation and increased Na+ transport in cortical collecting duct cells. *J Am Soc Nephrol* 16: 2279–2287, 2005
17. Liddle GW, Bledsoe T, Coppage WS: A familial renal disorder simulating primary aldosteronism but with negligible aldosterone secretion. *Trans Assoc Am Physicians* 76: 199–213, 1963
18. Shimkets RA, Warnock DG, Bositis CM, Nelson-Williams C, Hansson JH, Schambelan M, Gill JR, Ulick S, Milora RV, Findling JW, *et al.*: Liddle's syndrome: Heritable human hypertension caused by mutations in the beta subunit of the epithelial sodium channel. *Cell* 79: 407–414, 1994
19. Hansson JH, Nelson-Williams C, Suzuki H, Schild L, Shimkets R, Lu Y, Canessa C, Iwasaki T, Rossier B, Lifton RP: Hypertension caused by a truncated epithelial sodium channel gamma subunit: Genetic heterogeneity of Liddle syndrome. *Nat Genet* 11: 76–82, 1995
20. Bonny O, Hummler E: Dysfunction of epithelial sodium transport: From human to mouse. *Kidney Int* 57: 1313–1318, 2000
21. Firsov D, Schild L, Gautschi I, Merillat AM, Schneeberger E, Rossier BC: Cell surface expression of the epithelial Na channel and a mutant causing Liddle syndrome: A quantitative approach. *Proc Natl Acad Sci U S A* 93: 15370–15375, 1996
22. Alvarez de la Rosa D, Zhang P, Naray-Fejes-Toth A, Fejes-Toth G, Canessa CM: The serum and glucocorticoid kinase sgk increases the abundance of epithelial sodium channels in the plasma membrane of Xenopus oocytes. *J Biol Chem* 274: 37834–37839, 1999
23. Dahlmann A, Pradervand S, Hummler E, Rossier BC, Frindt G, Palmer LG: Mineralocorticoid regulation of epithelial Na+ channels is maintained in a mouse model of Liddle's syndrome. *Am J Physiol Renal Physiol* 285: F310–F318, 2003
24. Auberson M, Hoffmann-Pochon N, Vandewalle A, Kellenberger S, Schild L: Epithelial Na+ channel mutants causing Liddle's syndrome retain ability to respond to aldosterone and vasopressin. *Am J Physiol Renal Physiol* 285: F459–F471, 2003
25. Volk KA, Husted RF, Sigmund RD, Stokes JB: Overexpression of the epithelial Na+ channel gamma subunit in collecting duct cells: Interactions of Liddle's mutations and steroids on expression and function. *J Biol Chem* 280: 18348–18354, 2005
26. Diakov A, Korbmacher C: A novel pathway of epithelial sodium channel activation involves a serum- and glucocorticoid-inducible kinase consensus motif in the C terminus of the channel's alpha-subunit. *J Biol Chem* 279: 38134–38142, 2004
27. Pacha J, Frindt G, Antonian L, Silver RB, Palmer LG: Regulation of Na channels of the rat cortical collecting tubule by aldosterone. *J Gen Physiol* 102: 25–42, 1993
28. Lin H, Keriel A, Morales CR, Bedard N, Zhao Q, Hingamp P, Lefrancois S, Combaret L, Wing SS: Divergent N-terminal sequences target an inducible testis deubiquitinating enzyme to distinct subcellular structures. *Mol Cell Biol* 20: 6568–6578, 2000
29. Amerik AY, Hochstrasser M: Mechanism and function of deubiquitinating enzymes. *Biochim Biophys Acta* 1695: 189–207, 2004
30. Wilkinson KD: Ubiquitination and deubiquitination: Targeting of proteins for degradation by the proteasome. *Semin Cell Dev Biol* 11: 141–148, 2000
31. Gousseva N, Baker RT: Gene structure, alternate splicing, tissue distribution, cellular localization, and developmental expression pattern of mouse deubiquitinating enzyme isoforms Usp2-45 and Usp2-69. *Gene Expr* 11: 163–179, 2003
32. Renatus M, Parrado SG, D'Arcy A, Eidhoff U, Gerhartz B, Hassiepen U, Pierrat B, Riedl R, Vinzenz D, Worpenberg S, Kroemer M: Structural basis of ubiquitin recognition by the

deubiquitinating protease USP2. *Structure* 14: 1293–1302, 2006
33. Graner E, Tang D, Rossi S, Baron A, Migita T, Weinstein LJ, Lechpammer M, Huesken D, Zimmermann J, Signoretti S, Loda M: The isopeptidase USP2a regulates the stability of fatty acid synthase in prostate cancer. *Cancer Cell* 5: 253–261, 2004
34. Bens M, Vallet V, Cluzeaud F, Pascual-Letallec L, Kahn A, Rafestin-Oblin ME, Rossier BC, Vandewalle A: Corticosteroid-dependent sodium transport in a novel immortalized mouse collecting duct principal cell line. *J Am Soc Nephrol* 10: 923–934, 1999
35. Summa V, Mordasini D, Roger F, Bens M, Martin PY, Vandewalle A, Verrey F, Feraille E: Short term effect of aldosterone on Na,K-ATPase cell surface expression in kidney collecting duct cells. *J Biol Chem* 276: 47087–47093, 2001
36. Sudo S, Avsian-Kretchmer O, Wang LS, Hsueh AJ: Protein related to DAN and cerberus is a bone morphogenetic protein antagonist that participates in ovarian paracrine regulation. *J Biol Chem* 279: 23134–23141, 2004
37. Hershko A, Ciechanover A, Heller H, Haas AL, Rose IA: Proposed role of ATP in protein breakdown: Conjugation of protein with multiple chains of the polypeptide of ATP-dependent proteolysis. *Proc Natl Acad Sci U S A* 77: 1783–1786, 1980
38. Dupre S, Haguenauer-Tsapis R: Deubiquitination step in the endocytic pathway of yeast plasma membrane proteins: Crucial role of Doa4p ubiquitin isopeptidase. *Mol Cell Biol* 21: 4482–4494, 2001
39. McCullough J, Clague MJ, Urbe S: AMSH is an endosome-associated ubiquitin isopeptidase. *J Cell Biol* 166: 487–492, 2004
40. Mizuno E, Iura T, Mukai A, Yoshimori T, Kitamura N, Komada M: Regulation of epidermal growth factor receptor down-regulation by UBPY-mediated deubiquitination at endosomes. *Mol Biol Cell* 16: 5163–5174, 2005
41. Miles RR, Sluka JP, Halladay DL, Santerre RF, Hale LV, Bloem L, Patanjali SR, Galvin RJ, Ma L, Hock JM, Onyia JE: Parathyroid hormone (hPTH 1-38) stimulates the expression of UBP41, an ubiquitin-specific protease, in bone. *J Cell Biochem* 85: 229–242, 2002

Supplemental information for this article is available online at http://www.jasn.org/.

5.2 Usp2

The results concerning Usp2 shown in this section were part of a research article published in January 2007 in JASN.

The ubiquitylation of ENaC had previously been shown to play an important role for the regulation of transepithelial Na^+ transport (Rotin, Staub et al. 2000; Debonneville, Flores et al. 2001). Our screening identified in addition to Sgk1 (a 4-fold upregulated kinase known to decrease ENaC ubiquitylation) Usp2, a deubiquitylating enzyme that was significantly up-regulated 2.2 fold. Usp2 belongs to a large protein family involved in reversing the ubiquitylation of target proteins (Loffing, Loffing-Cueni et al. 2000; Wilkinson 2000; Amerik and Hochstrasser 2004). Since Nedd4-2, an ubiquitin ligase, suppresses ENaC activity at the plasma membrane by ubiquitylation, we asked whether Usp2 counteracts the Nedd4-2 effect by deubiquitylating ENaC.

5.2.1 Usp2-45 but not Usp2-69 affects ENaC function in *X. laevis* oocytes

To investigate the function of Usp2 I initially co-expressed the two known isoforms of Usp2 (Usp2-45, Usp2-69) (Gousseva and Baker 2003) with αβγ*X*ENaC in *X. laevis* oocytes and recorded the amiloride sensitive Na^+ currents (I_{amil}) by two electrode voltage clamp (TEVC) electrophysiology. cRNA injected *X. laevis* oocytes were incubated for two days in a low Na^+ solution (ND10) before testing. Inward Na^+ currents can be observed when clamped oocytes are switched from a low to a high Na^+ solution (ND96) (Figure 12 A). ENaC mediated currents are specifically blocked by amiloride (10 μM). The I_{amil} represents ENaC activity on the cell surface (Figure 12 A). The TEVC recording showed that co-expression of Usp2-45 increases I_{amil} significantly, while Usp2-69 does not affect the I_{amil} (Figure 12 A, B, C). The current voltage (I-V) plot in figure 10 B shows that this is true over a range of given voltages (-140 to 20 mV). To exclude that the stimulation of ENaC by Usp2-45 was due to a difference in Usp2 protein expression in the oocytes, Western blots were performed using oocyte lysates. The specific bands of Usp2-45 and Usp2-69 that were detected by a pan-Usp2 antibody show that similar levels of Usp2-45 and Usp2-69 protein are expressed (Figure 12 D).

Figure 12

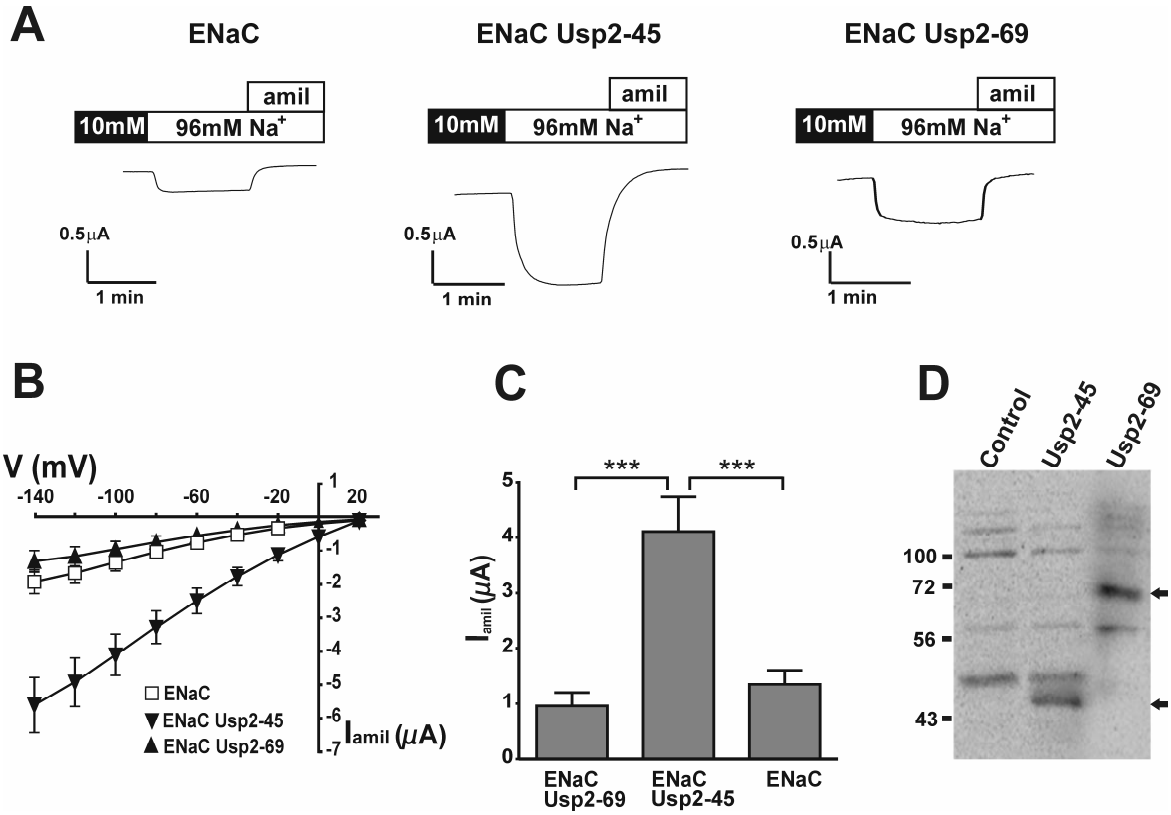

Figure 12: *Usp2-45 but not Usp2-69 increases I_{amil}.* (A) Typical recordings of TEVC measurements done in *X. laevis* oocytes. Bath Na^+ concentrations and the presence of 10 μM amiloride are indicated. The measurements were done at a stable membrane potential of -50 mV. Switching from 10 to 96 mM Na^+ increased the positive inward current that was blocked with 10 μM amiloride. I_{amil} is increased by co-expression of Usp2-45 but not of Usp2-69. (B) Current-voltage (I-V) relations of I_{amil}; Data are means ± SEM, n = 20-22. I_{amil} is shown for a range of given voltages (-140 mV- 20 mV). (C) Means ± SEM of the I_{amil} at -100 mV; n = 20 to 22. ***P <0.001. (D) Western blot performed with lysates of control, Usp2-45- or Usp2-69- expressing *X. laevis* oocytes. Specific bands, detected with a pan-Usp2 antibody appear at ~45 kDa (Usp2-45) and at ~69 kDa (Usp2-69) indicated by arrows on the right.

To control whether the effect of Usp2-45 on ENaC function is specific, further experiments were performed with another arbitrarily chosen ubiquitin-protease, Usp15 that is ubiquitously expressed (Angelats, Wang et al. 2003). Usp15 co-expression decreases ENaC mediated I_{amil} while Usp2-45 increases it (Figure 13 A). The I-V plot shown in figure 13 B indicates that these effects are consistent over a wide range of

membrane voltages. These results point out that the effect is Usp2-45 specific, since co-expression of Usp15 does not increase ENaC function (Figure 13). The fact that co-expression of Usp15 decreases I_{amil} may be due to the deubiquitylation of other proteins that interfere with the expression of ENaC in *X. laevis* oocytes.

Figure 13

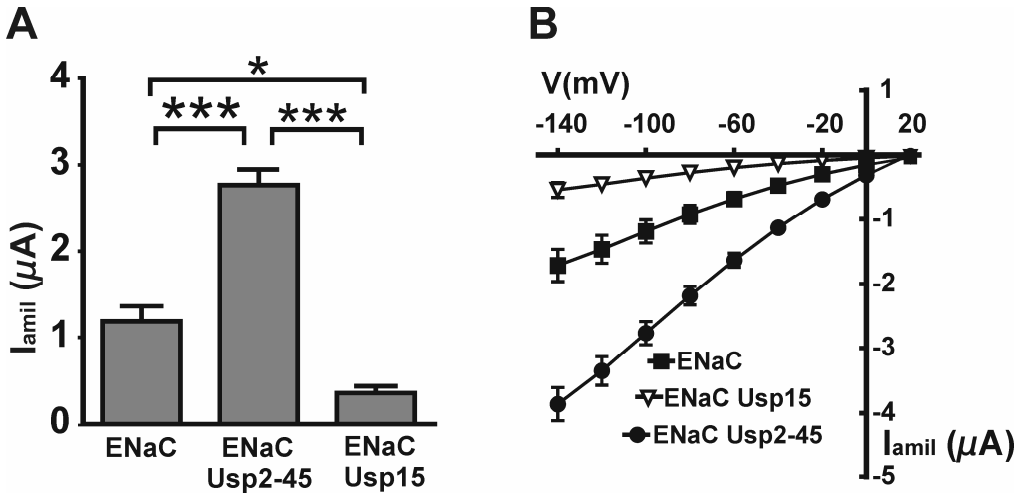

Figure 13: *Usp15 does not increase I_{amil} in X. laevis oocytes.* (A) Summary of I_{amil} means ± SEM at -100 mV holding potential; n = 20 - 24. **P* < 0.05; ****P* < 0.001. (B) Current-voltage relationship of I_{amil} measured at a range of given voltages (-140 to 20 mV). Data are means ± SEM, n = 20-24

5.2.2 Co-expression of Usp2-45 with Sgk1 does not further increase I_{amil}

Sgk1 increases ENaC currents by inhibiting its ubiquitylation *via* phosphorylation of Nedd4-2. Since both Sgk1 and Usp2-45 act on the ubiquitylation / deubiquitylation of ENaC, Usp2-45 was co-expressed with Sgk1 to test whether the effects of Usp2-45 and Sgk1 on I_{amil} influence each other. Control experiments showed that Sgk1 increases I_{amil} in *X. laevis* oocytes co-expressed with ENaC as expected (Chen, Bhargava et al. 1999) (Figure 14). The stimulation of I_{amil} by Sgk1 was not enhanced by Usp2-45 and vice versa (Figure 14). These results demonstrate that effects of Sgk1 and Usp2-45 are not additive

and are consistent with the hypothesis that Sgk1 and Usp2-45 act on the same regulatory pathway, namely the ubiquitylation of ENaC.

Figure 14

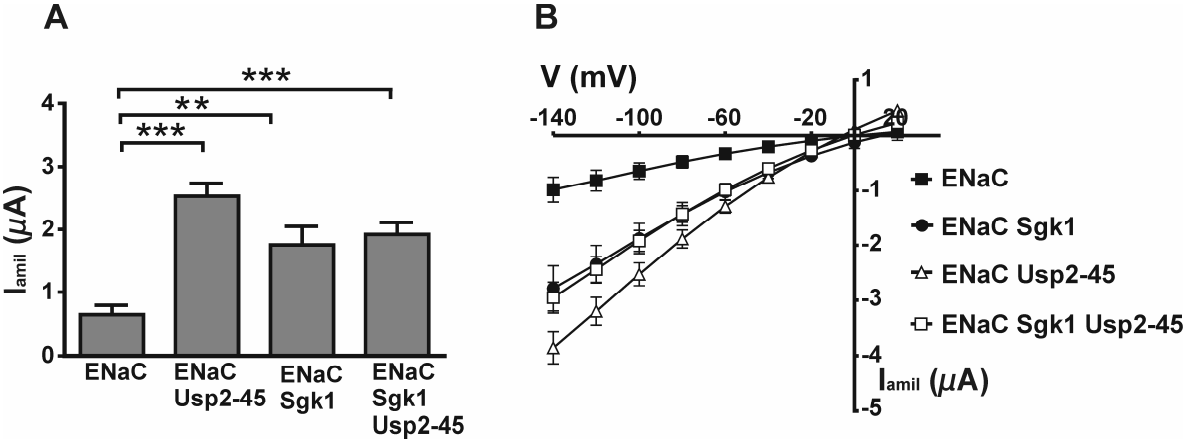

Figure 14: *Usp2-45 increases I_{amil} of co-expressed ENaC.* (A) Summary of I_{amil} at a holding potential of -100 mV. Co-expression of Usp2-45 or Sgk1 increased the ENaC-mediated I_{amil} to a similar extent. Data are means ± SEM; n = 23 to 27. **<*P* 0.01; ****P* < 0.001. (B) Current-voltage (I-V) relationships of the I_{amil}; Data are means ± SEM, n = 23 - 27.

5.2.3 The protease dead Usp2-45 mutant does not increase I_{amil} in *X. laevis* oocytes

Since protein ubiquitylation and deubiquitylation regulate many cellular functions we asked whether the effect of Usp2-45 on ENaC was specific to its protease activity. The protease dead Usp2-45 mutant was constructed by substitution of cysteine 67, which corresponds to one of the catalytically active amino acids of its cysteine protease motif, with alanine (Gousseva and Baker 2003). I_{amil} measured by TEVC in *X. laevis* oocytes co-expressing the protease dead Usp2-45 mutant (Usp2-45mut) with ENaC was similar to that in oocytes expressing ENaC alone. The control experiment with wild type Usp2-45 showed an increase in ENaC mediated I_{amil} (Figure 15 A). The I-V curves demonstrate that these effects are consistent over a broad range of membrane potentials (Figure 15 B).

Further it was shown -by Benjamin Oberfeld- that the core domain of Usp2-45 produced in *E. coli* very efficiently cleaves ubiquitin off from a test substrate *in vitro* (Oberfeld, Verrey and Pos, unpublished results). Taken together, these results confirm that Usp2-45 is an active ubiquitin protease acting on ENaC.

Figure 15

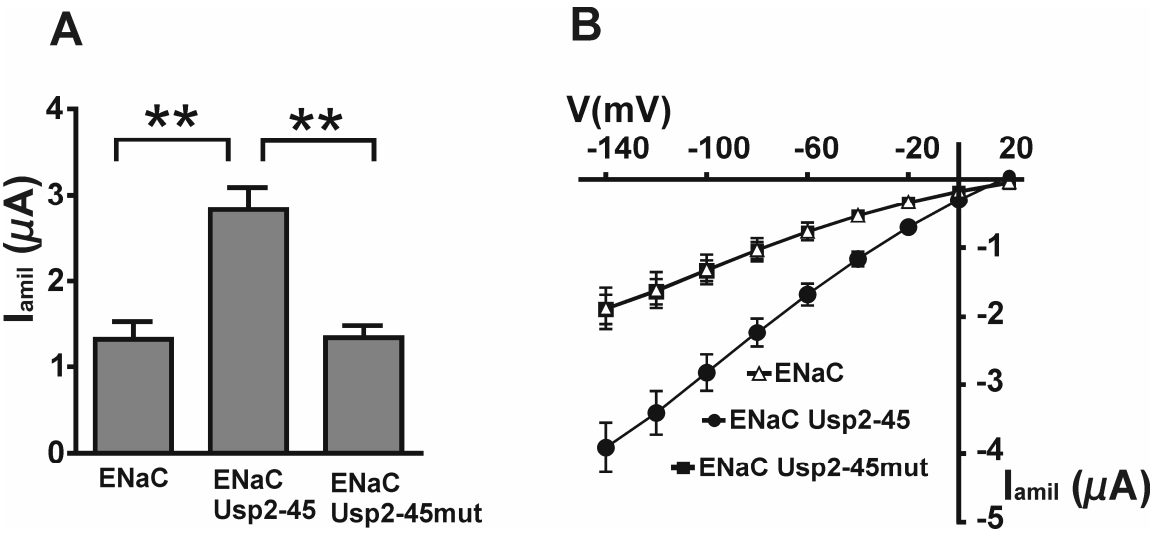

Figure 15: *Cys67Ala protease-dead Usp2-45 mutant (Usp2-45mut) does not stimulate ENaC current.* (A) Summary of I_{amil} at -100 mV, data are means ± SEM; n =12 -15. ***P* < 0.01. (B) Corresponding current-voltage (I-V) relationship over a range of given voltages from -140 to +20 mV; Data are means ± SEM, n = 12-15.

5.2.4 Usp2-45 increases transepithelial I_{amil} in mouse CCD cells

To test whether Usp2-45 effects on ENaC function also occur with endogenous ENaC in CCD cells, I performed measurements of the transepithelial I_{amil} in mpkCCD$_{c14}$ cells (Bens, Vallet et al. 1999; Summa, Mordasini et al. 2001). Usp2-45, as well as Usp2-45mut was expressed in mpkCCD$_{c14}$ cells using retroviral transduction. Western blot analysis confirmed that Usp2-45 and Usp2-45mut proteins are expressed at similar levels (Figure 16). Transepithelial I_{amil} was measured in mpkCCD$_{c14}$ monolayers that were

cultured on permeable supports using an Ussing chamber setup (Materials and Methods, (Ussing and Zerahn 1951)). The expression of functional Usp2-45 increased the baseline transepithelial I_{amil} (Figure 16). Expression of the protease-dead mutant Usp2-45mut had no effect, consistent with the hypothesis that the activity of endogenous ENaC was limited by its ubiquitylation in polarized mouse collecting duct cells. The increase in Na^+ transport induced by aldosterone within 2.5 hours is not affected by the over-expression of wild type and mutant Usp2-45. This result was expected considering that the induction of endogenous Sgk1 by aldosterone prevents the Nedd4-2-mediated ubiquitylation of ENaC in CCD cells.

Figure 16

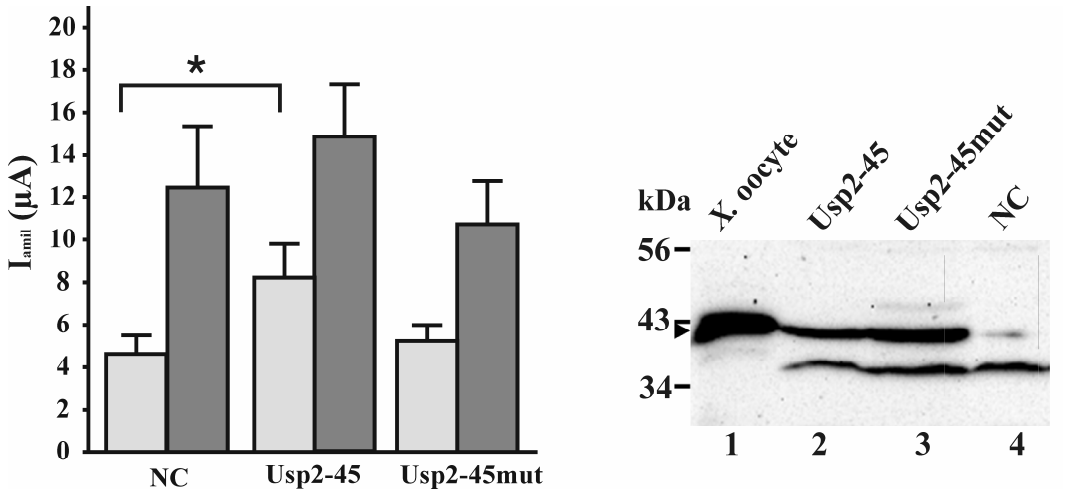

Figure 16: *Usp2-45 increases transepithelial Na^+ current.* (A) Transepithelial I_{amil} across $mpkCCD_{cl4}$ cell monolayers. The baseline I_{amil} is depicted by light grey bars and the aldosterone induced I_{amil} by dark grey bars. Baseline I_{amil} is significantly increased in cells over-expressing Usp2-45 compared with vector-transduced negative control cells (NC) and cells that were transduced with Usp2-45mut. I_{amil} increased 2.5 h after application of 300nM aldosterone to the same level in all three tested $mpkCCD_{cl4}$ cell populations $*P \leq 0.05$; n = 9 - 12. (B) Western blotting of Usp2-45 in $mpkCCD_{c14}$ cells. In transduced $mpkCCD_{c14}$ cells, Usp2-45 wild type (lane 2) and protease dead mutant (lane 3) appear as ~41 kDa bands (arrow head) of similar intensity. Endogenous Usp2-45 is not clearly visible in wild type and vector-transduced $mpkCCD_{cl4}$ cells (lane 4). Lane 1 shows Usp2-45 expressed in *X. laevis* oocytes. The band at ~36 kDa in lane 2 - 4 ($mpkCCD_{c14}$ lysate) is unspecific.

5.2.5 Summary concerning Usp2 regulation

It could indeed be shown that the newly identified aldosterone-induced Usp2-45 activates ENaC in the *X. laevis* oocyte and mpkCCD$_{c14}$ cell expression systems. The biochemical evidence of ENaC deubiquitylation by Usp2-45 done in Hek 273 cells was published together with the latter section of my thesis in the Journal of the American Society of Nephrology in january 2007 and supports the functional experiments made in *X. laevis* oocytes. Additional tests done in Prof. Olivier Staubs laboratory showed that the disruption of ENaC PY motifs and the disruption of ENaC lysine residues that potentially are targeted by Usp2-45 prevent the action of Usp2-45 on ENaC function. Taken together, these results strongly support the hypothesis that Usp2-45 removes ubiquitin molecules that are ligated onto ENaC by the ubiquitin ligase Nedd4-2 (Adam, Fakitsas et al. 2007).

5.3 Usp53

Usp53 is a member of a large protein family involved in reversing the ubiquitylation of target proteins (Loffing, Loffing-Cueni et al. 2000; Wilkinson 2000; Amerik and Hochstrasser 2004). Little is known about the function of Usp53. Since it lacks a highly conserved residue near the Usp protease catalytic site (Hu, Li et al. 2002), Usp53 is considered a non-protease homologue of the Usp family (Quesada, Diaz-Perales et al. 2004). Nevertheless, we found Usp53 mRNA significantly upregulated by aldosterone in microselected CNT/CCD tubules in the gene chip analysis performed in our laboratory.

5.3.1 Usp53 exists in two different isoforms

Two splice variants of Usp53 exist: the full-length (Usp53fl) and the truncated isoform (Usp53t). Usp53t lacks the entire N-terminal domain comprising the complete catalytic site (Figure 17 A). cRNA from both Usp53 isoforms was injected in *X. laevis* oocytes. Using our pan mouse Usp53 antibody, the expression of both Usp53 isoforms in *X. laevis* oocytes was shown by Western blot 3 days after cRNA injection (Figure 17 B). The specific bands are visible at ~120 kDa (Usp53fl) and ~80 kDa (Usp53t) (Figure 17 B).

Figure 17

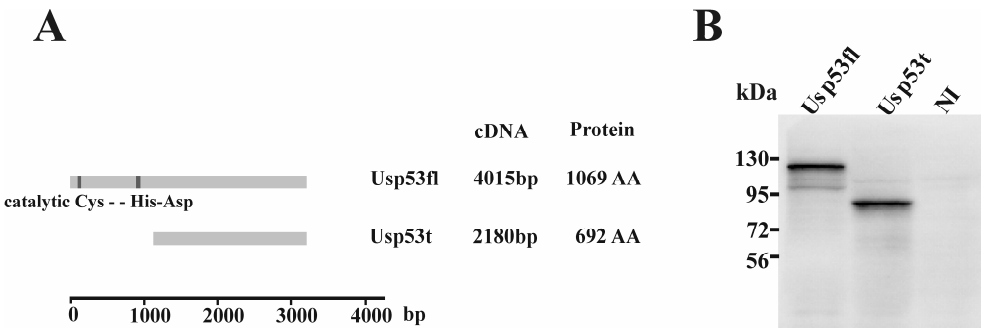

Figure 17: *Two different isoforms of Usp53 are expressed in X. laevis oocytes*. (A) Simplified sketch showing the truncated (Usp53t) and the full length form of Usp53 (Usp53fl). Usp53t is lacking the catalytic site which comprises a cystein (Cys) and a histidin-asparagine (His-Asp) box. (B) Western blot analysis showing the expression of both Usp53t and Usp53fl detected in lysates of injected *X. laevis* oocytes.

5.3.2 Usp53 does not modulated ENaC mediated I_{amil} in *X. laevis* oocytes

To see whether Usp53 has an impact on the function of individual members (i.e. ENaC, Na^+-K^+-ATPase, K^+-channels) of the Na^+ transport machinery of the ASDN, I carried out TEVC measurements of I_{amil} on *X. laevis* oocytes expressing Usp53. Oocytes injected with Usp53t and Usp53fl respectively and ENaC cRNA were incubated for 2 days. I_{amil} recordings revealed that Usp53t, as well as Usp53fl do not impact on the ENaC mediated I_{amil} (Figure 18).

Figure 18

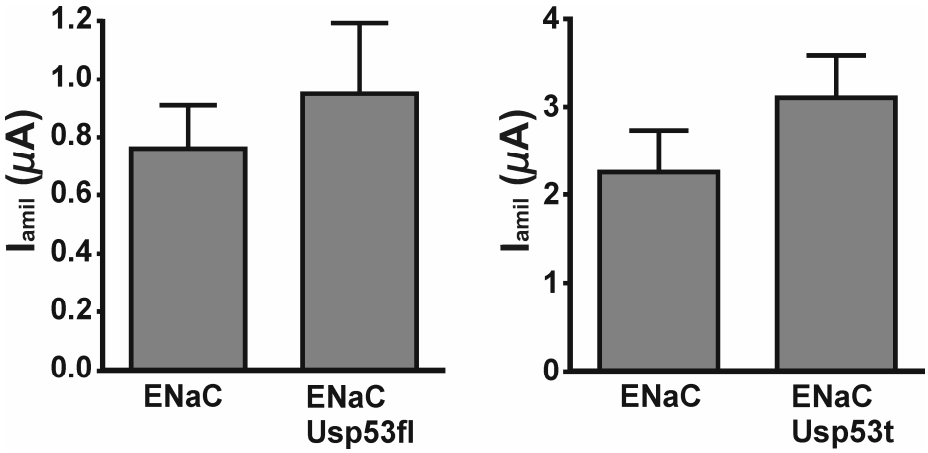

Figure 18: *Usp53 does not affect ENaC mediated currents in oocytes.* I_{amil} was measured at a holding potential of -50 mV. The left panel compares I_{amil} in oocytes expressing ENaC or ENaC and Usp53t ; data are means ± SEM; n = 15. The right panel shows the I_{amil} of oocytes coexpressing Usp53fl with ENaC or expressing ENaC alone. Data are means ± SEM; n = 12 - 15.

5.3.3 In *X. laevis* oocytes Usp53t increases exogenously expressed Na^+-K^+-ATPase function

The Na^+-K^+-ATPase, a member of the Na^+ transport machinery of the ASDN, is a possible target for the deubiquitylating enzyme Usp53 as it had been shown to be ubiquitylated (Dada, Welch et al. 2007). To test this hypothesis the Na^+-K^+-ATPase was

co-expressed in *X. laevis* oocytes with the different Usp53 isoforms and TEVC recordings were performed. Since oocytes express endogenous Na^+-K^+-ATPase a special protocol was used to distinguish between endogenous and exogenous pump currents (see materials and methods) (Jaisser, Horisberger et al. 1992). Three days after cRNA injection whole cell currents were recorded. The coexpression of Usp53fl does not influence currents carried by the endogenous or exogenous Na^+-K^+-ATPase (Figure 19 A). Interestingly coexpression of Usp53t tends to increase the function of the exogenous Na^+-K^+-ATPase, but does not affect the endogenous one (Figure 19 B). However, co-expression of Usp2-45 did not affect endogenous or exogenous Na^+-pump currents (Figure 19 C).

Figure 19

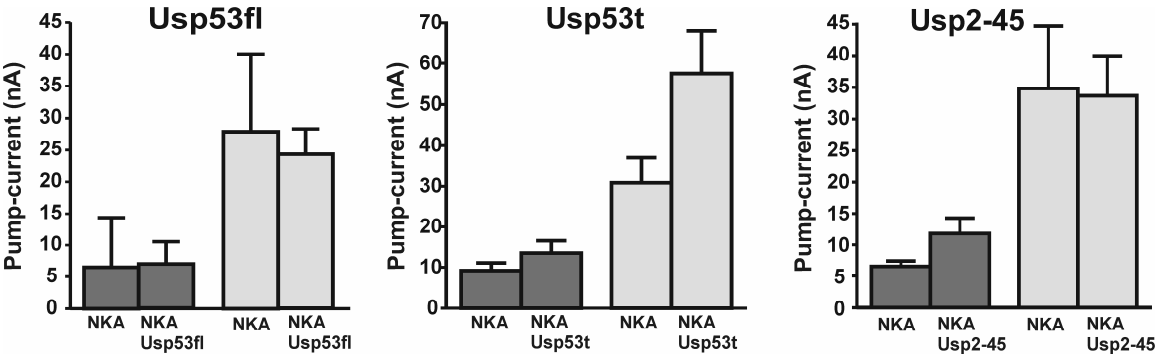

Figure 19: *Endogenous pump currents were not affected by Usp53t or Usp53fl.* Exogenous pump currents: light gray bars; endogenous pump currents: dark gray bars. The middle panel shows that Usp53t has the tendency to increase currents of the exogenously expressed Na^+-K^+-ATPase but has no effect on the endogenous one (means ± SEM; n = 16 - 21; $P = 0.062$). Usp2-45 as well as Usp53fl exhibit no significant effect on either of the pump currents measured (means ± SEM, n = 5-9).

5.3.4 Usp53 expression in mpkCCD$_{c14}$ cells

The endogenous mRNA expression of Usp53 in wild type mpkCCD$_{c14}$ cells (derived from principal cells of the collecting duct) was determined by quantitative RT real-time PCR. The primers used for RT-real-time PCR detect the two isoforms of Usp53, since they recognize a common region in the C-terminal part of both (Figure 17). The bargraph in figure 18 shows that the Usp53 mRNA level did not change significantly after aldosterone treatment relative to the level of non treated cells (Figure 20).

Figure 20

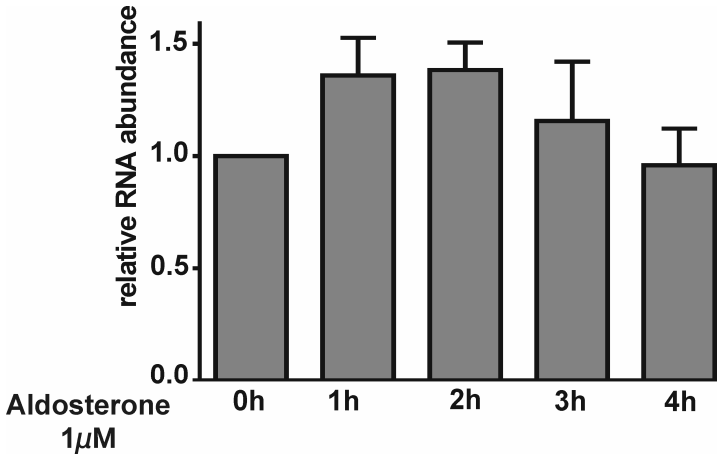

Figure 20: *Usp53 mRNA abundance in mpkCCD$_{c14}$ cells.* Quantitative RT real-time PCR was performed on total RNA extracted from cultured and aldosterone treated mpkCCD$_{c14}$ cells. CT values are relative to the housekeeping gene HPRT and normalized to the value at time point zero (n = 4).

5.4 The voltage gated proton channel H_v1/mVSOP

It was shown by electrophysiology that almost every cell type, from cultured cancer cells to native tissue, expresses voltage gated proton channels (DeCoursey and Cherny 1998; Decoursey 2003; Okamura 2007). However, until 2006 they were not identified at a molecular level and not much is known about their role in the regulation of cellular functions. A putative voltage gated proton channel was recently identified by two groups in parallel. Sasaki and colleges and Ramsey and co-workers investigated the function of two orthologs (mouse: mVSOP (Sasaki, Takagi et al. 2006), human: H_v1(Ramsey, Moran et al. 2006)) of a voltage sensor domain protein. Both described that it functions as a voltage gated proton channel. We observed in the gene screen performed in our lab that this voltage gated proton channel is significantly upregulated by aldosterone in microselected CNT/CCD of mouse kidney. I started to investigate the possible action of the mouse ortholog of this channel, H_v1 (or mVSOP) in the context of aldosterone regulated Na^+ transport.

5.4.1 H_v1 is suggested to localize at the apical side of principle cells in the ASDN

Using an affinity purified rabbit antibody raised against the H_v1 peptide CSEKEQEIERLNKL according to Ramsey, Moran et al 2006, the localization of the H_v1 protein was examined in mouse kidney by immunofluorescence. Double stainings were performed using a commercially available aquaporin 2 (AQP2) antibody that is a marker for principal cells in the distal nephron (Loffing, Loffing-Cueni et al. 2000). Several experiments showed labeling suggesting that the channel is mainly localized in the apical side of principal cells in the collecting duct, since AQP2 staining could by observed in the same cells (Figure 21 A, B). In some cases AQP2 positive cells were not labeled by the H_v1 antibody, but instead staining of intercalated cells (AQP2-negative) could be detected. Since pendrin is a marker for β-intercalated cells co-staining with a polyclonal

pendrin antibody (Schulz, Dave et al. 2007) revealed that H_v1 antibody labeled the apical pole of β-intercalated cells (Figure 21 B, C). No H_v1 labelling could be detected in α-intercallated cells (data not shown). Based on the practical experience of Prof. J. Loffing this staining was however rejected as probably artifactual. Taken together, these results suggest that H_v1 is localized on the apical pole of principle cells in the collecting duct.

Figure 21

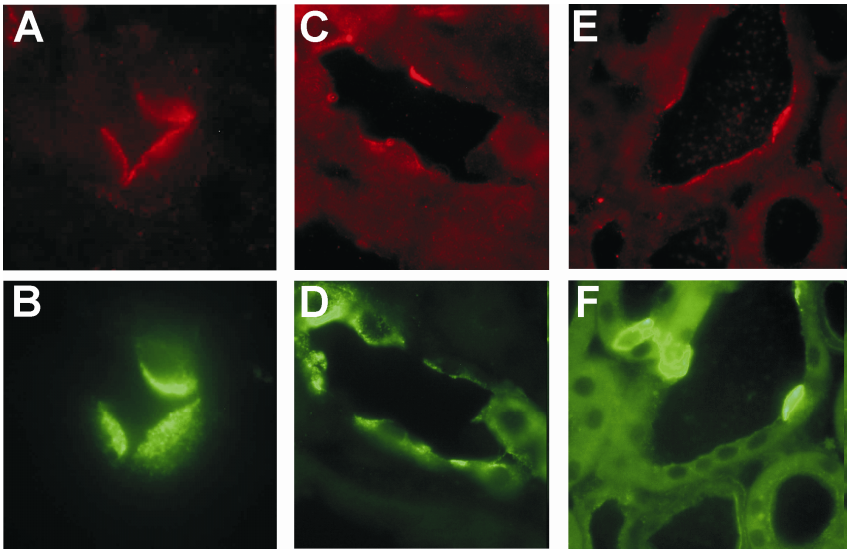

Figure 21: *Expression of H_v1 in the mouse kidney.* Staining of mouse kidney cryosection with H_v1 antibody showed a localization of H_v1 in the collecting duct. (A) A labeling of the apical pole of principal cells using the H_v1 antibody is visualized in red. (B) AQP2 antibody stains principal cells (green). (C) Labeling of the apical pole of an intercalated cell in the CD with the $H_v1$antibody. (D) Staining with AQP2 antibody shows labeling of principal cells in the same tubule. (E, F) H_v1 was detected in the same cell (red fluorescence, E) like Pendrin, a specific marker for β-intercalated cells (green labeling, F).

5.4.2 H_v1 is endogenously expressed in the mpkCCD$_{c14}$ cell line

The endogenous expression of H_v1 was tested in cultured mpkCCD$_{c14}$ cells (Bens, Vallet et al. 1999) using real-time RT PCR performing four independent experiments. After aldosterone application at a pharmacological level that stimulates also the glucocorticoid receptor (1 µM) cell populations grown on plastic dishes were harvested and total mRNA

was extracted every hour. This experiment was repeated four times. A comparison of non-treated and aldosterone treated cell populations shows that H_v1 mRNA level was apparently increased ~2 fold after aldosterone treatment but without reaching a level of significance. It could further be observed that the variation between the tested cell populations is very high (Figure 22). The reason for the differences between the single experiments could be the fact that the cells were probably in different stages of differentiation which affects the mRNA expression pattern.

Figure 22

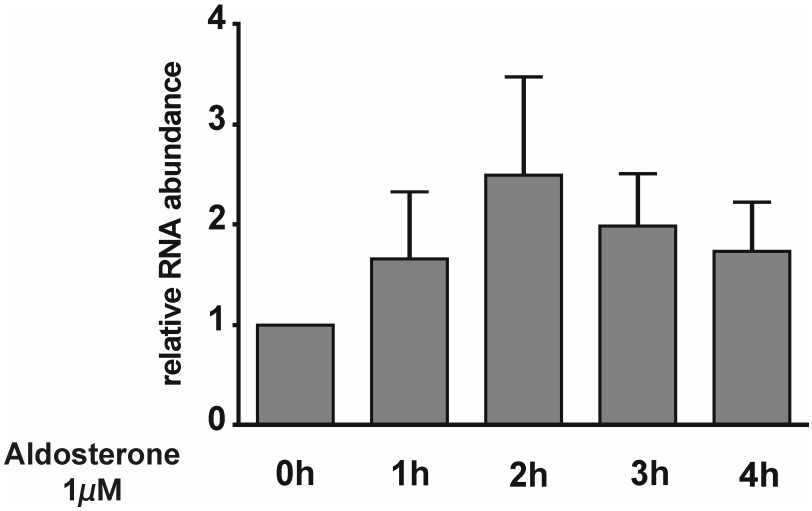

Figure 22: *H_v1 mRNA abundance in $mpkCCD_{c14}$ cells.* Quantitative RT real-time PCR was performed on total RNA extracted from cultured aldosterone treated $mpkCCD_{c14}$ cell populations. CT values were normalized to the housekeeping gene HPRT. The graph shows H_v1 mRNA levels after aldosterone application (1µM) relative to the level of nontreated cells (n = 4).

5.4.3 Functional expression of H_v1 in *X. laevis* oocytes

Since H_v1 is upregulated by aldosterone in the ASDN and is probably localized in the apical pole of principal cells in the collecting duct we planned to investigate its potential functional role in the modulation of salt reabsorption in the kidney. A common and well

established tool to explore the function of ion channels is the *X. laevis* oocyte expression system. The action of H_v1 was initially tested in *X. laevis* oocytes heterologously expressing H_v1. The cRNA of H_v1 was injected into *X. laevis* oocytes 2-3 days before functional tests were performed. The expression of myc-tagged H_v1 could be detected in lysed oocytes by Western blot using a commercial anti-myc antibody (Figure 23 A). A specific band for H_v1 appears at the apparent molecular weight of 35 kDa as it was reported before (Ramsey, Moran et al. 2006). As a negative control non-injected (NI) or ENaC injected (ENaC) oocytes were used.

Since this first series of experiments suggested that exogenous H_v1 is functionally expressed at the surface membrane of oocytes, further experiments to characterize its function were undertaken. The following describes results that could however not confirm the functional surface expression of H_v1.

The possible activity of exogenous H_v1 in the plasma membrane of oocytes was examined by eletrophysiology. The analysis of pre-steady-state currents evoked by voltage steps uncovered in some experiments, but not in all a distinct behavior of H_v1 expressing oocytes compared to non-injected ones. During repolarisation slow inward tail currents are observed in H_v1 expressing cells which are not seen in non-injected ones (Figure 23 A). Tail currents are thought to result from charge movements over the membrane mediated by H_v1 molecules. A characteristic feature of voltage gated proton channels is their unique pH dependence of gating, in which the voltage activation relationship depends strongly on both the intracellular (pH_i) and extracellular pH (pH_o) (Sasaki, Takagi et al. 2006). To examine whether H_v1 exhibits this feature in *X. laevis* oocytes, we applied bath solutions with different pHs and tested the function of H_v1 by TEVC. I-V relations were measured from the same cell at 2 different extracellular pHs (pH 6, pH 8). Considering that pH_i is ~ 7.3-7.5 (Broer 2003) the ratio pH_o/pH_i is < 1 applying pH 6 in the extracellular solution and pH_o/pH_i is > 1 when pH_o = 8. I-V relations measured in noninjected oocytes did not change in conditions with different pH ratios. Oocytes expressing H_v1 showed a decrease in outward currents at depolarizing voltages when pH_o/pH_i is > 1 (pH_o = 8) but not when pH_o/pH_i < 1 (pH_o = 6) (Figure 23 C). Sasaki and coworkers showed that the I-V curve in H_v1 expressing Hek293 cells shifted about 50 mV in the positive direction at pH_o/pH_i is < 1 and to the same extend towards the negative direction at pH_o/pH_i is > 1. This observation could not be confirmed in the oocyte system

since no shift of the I-V curves (or E_{rev}) could be observed (Figure 23 C). Under conditions with pH_o/pH_i is > 1 we did not see any differences in the I-V relation compared to the control group (Figure 23 C). The reason for these discrepancies could be endogenous oocyte specific ion conductances that are switched on at strong membrane depolarization and that could cover the effects mediated by H_v1.

Figure 23

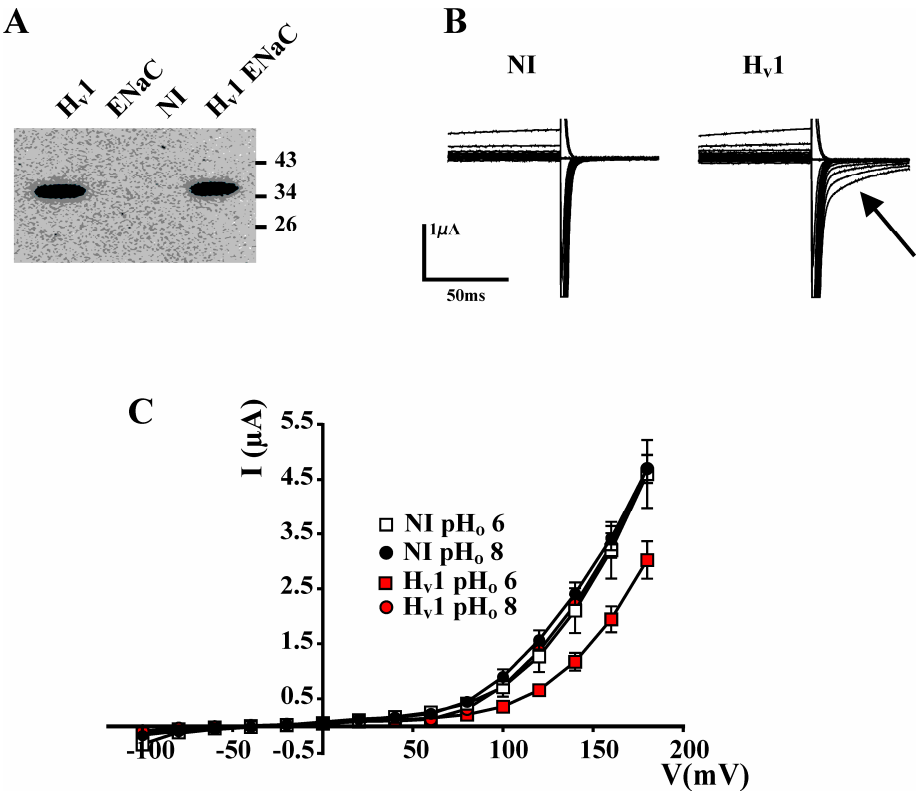

Figure 23: *H_v1 was functionally expressed in X. laevis oocytes.* (A) Expression of myc-tagged H_v1 in *X. laevis* oocytes is shown by Western blot using lysates from oocytes co-/expressing H_v1 with and without co-expression of ENaC (H_v1, H_v1 ENaC). (B) Single TEVC recordings showing slow inward tail currents (arrow) in H_v1 (H_v1) expressing oocytes in comparison to noninjected (NI) oocytes. (C) I-V relations evoked by a series of voltage steps in 20 mV increments (-100 to 180 mV) under pH_o = 8 (cycles) or 6 (squares). NI = Non-injected oocytes, H_v1 = H_v1-injected oocytes.

As described earlier, zinc a specific blocker for proton channels, blocks proton currents mediated by H_v1(Ramsey, Moran et al. 2006; Sasaki, Takagi et al. 2006). Tail currents during repolarisation to various potentials were elicited after depolarizing prepulses to observe the effect of zinc on H_v1 expressing and control oocytes. Oocytes were clamped at -50 mV before +100 mV was applied to depolarize the cell. The following voltage steps reach from -100 mV to +20 mV before the oocyte is clamped again at -50 mV (Figure 22 A). The reversal potential (E_{rev}, intersection of the I-V curve with the x-axis) shifted strongly towards the negative direction in H_v1 expressing oocytes as 1 µM $ZnCl_2$ was added to the bath solution (Figure 25 B). Furthermore a flattening of the I-V curve could be observed after $ZnCl_2$ treatment in oocytes expressing H_v1. I-V relations of the noninjected oocytes tested did not change after $ZnCl_2$ application. So far, these results are compatible with the possibility that H_v1 is functionally expressed on the surface of *X. laevis* oocytes and is affected by zinc. Indeed, that the I-V relation flattens after the addition of $ZnCl_2$ is in line with the results obtained in the Hek cell expression system by Sasaki and coworkers. Application of extracellular zinc in a µM range could be shown to inhibit proton channels (Byerly and Suen 1989; Cherny and DeCoursey 1999; Ramsey, Moran et al. 2006; Sasaki, Takagi et al. 2006). In contrast, the shift in E_{rev} in the oocytes was unexpected and can not be explained by the inhibition of a proton conductance. We therefore have to consider the possibility that the expression of H_v1 in *X. laevis* oocytes does not itself lead to the zinc-inhibitable conductance but that it influences endogenous ion conductance that could be affected by the addition of zinc.

Figure 24

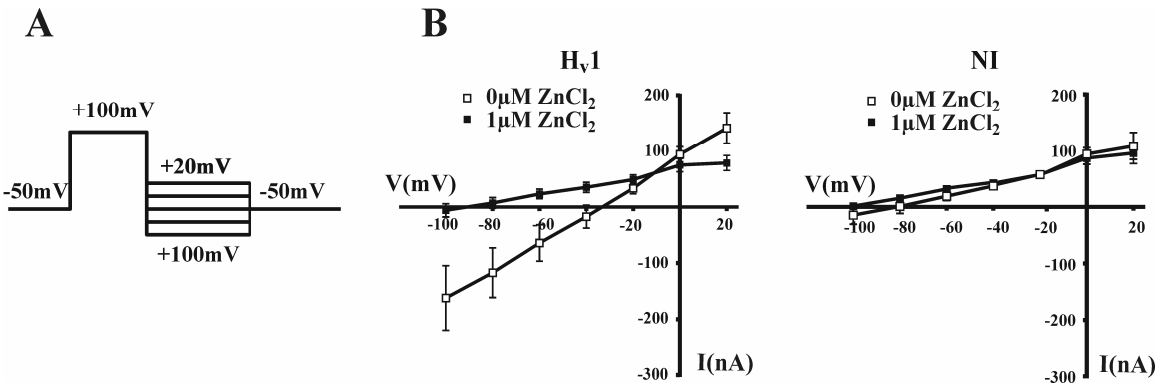

Figure 24: *Plots of tail current amplitude against membrane potential under conditions with and without 1µM $ZnCl_2$* (A) Simplified scheme of the applied voltage step protocol. (B) Plots of tail current amplitude against membrane potential. H_v1 expressing oocytes (H_v1) and noninjected oocytes (NI) were perfused with ND96 solution with (closed squares) or without (open squares) 1 µM $ZnCl_2$.

5.4.4 Co-expression of H_v1 decreases ENaC mediated I_{amil} in *X. laevis* oocytes

To address the question whether there is a relationship of H_v1 and aldosterone regulated salt reabsorption, ENaC was co-expressed with H_v1 in *X. laevis* oocytes. TEVC measurements demonstrated that H_v1 has an inhibitory effect on ENaC function over the entire range of tested voltages (Figure 25 A). In an initial experiment 20 ng H_v1 cRNA were injected into each oocyte to test its effect on I_{amil} (Figure 25 A). Afterwards the amount of injected H_v1 cRNA per oocyte was titrated down to 5ng per oocyte. The I-V curve for I_{amil} shows that the expression of H_v1 using 20 ng H_v1 cRNA for injection leads to a major inhibition of I_{amil}, whereas the expression after injection of 10 ng and 5ng H_v1 cRNA respectively showed a moderate effect on I_{amil} (Figure 25 B). We conclude from these results that the amount of H_v1 cRNA is crucial for the amplitude of the decrease of I_{amil}. Since it is known that zinc blocks the proton conductance of H_v1(Ramsey, Moran et al. 2006; Sasaki, Takagi et al. 2006), I tested whether the application of $ZnCl_2$ would

reestablish ENaC mediated I_{amil} which was previously inhibited by H_v1. Treatment of co-expressing *X. laevis* oocytes with $ZnCl_2$ in a range from 0.05- 100 µM does not abolish the effect of H_v1 on ENaC currents (Figure 25 C). Even the incubation of oocytes in a zinc-containing bath solution over night showed similar results (Data not shown). Furthermore, the I-V relations shown in figure 25 C reveal that addition of $ZnCl_2$ to the bath solution increases I_{amil} in oocytes that express ENaC alone. This data is consistent with the observation of other investigators that showed that I_{amil} can be induced by the addition of extracellular zinc (Sheng, Perry et al. 2004) (Figure 25 C). The fact that the inhibitory effect of H_v1 on ENaC is not reversed by addition of extracellular zinc leads to the assumption that inhibition of ENaC by H_v1 is independent of its proton conductance.

Figure 25

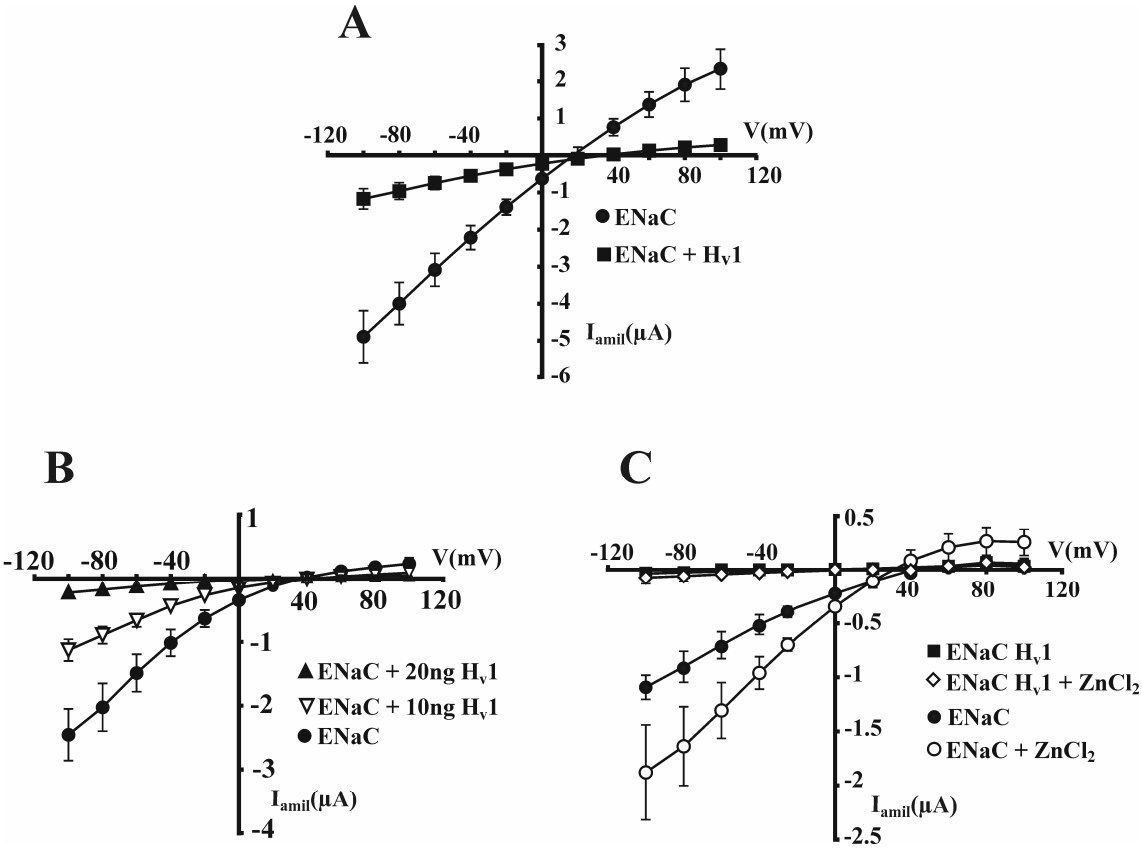

Figure 25: *Co-expression of ENaC with H_v1. Current-voltage relationships of I_{amil} measured by TEVC.*
(A) Co-expression of H_v1 (20 ng H_v1 cRNA / oocyte) with ENaC (0.05 ng / SU / oocyte) showed a remarkable decrease in I_{amil} at the range of voltages applied: -100 mV to 100 mV. Data are means ± SEM; n = 17. (B) 20 ng and 10 ng H_v1 cRNA were co-injected with ENaC respectively. Data are means ± SEM, n = 4. (C) Oocytes were incubated +/- 1 µM $ZnCl_2$.

5.4.5 H_v1 decreases ROMK2 activity in *X. laevis* oocytes

To address the question whether the effect of H_v1 on ENaC is specific H_v1 was co-expressed with the potassium channel ROMK2 in *X. laevis* oocytes. The expression of ROMK2 in *X. laevis* oocytes is well established and ROMK2 mediated K^+ currents can be determined using a simple protocol. Whole cell potassium currents (I_K) were measured at a clamped membrane potential of – 50 mV and blocked by the substitution of $MgCl_2$ with $BaCl_2$ in the bath solution (ND96). Currents recorded while perfusing with the control solution were subtracted from those obtained after switching to the substituted solution. Subsequently the results were normalized to those obtained from noninjected control oocytes. Initially ROMK2 was chosen to serve as a negative control and it was expected that H_v1 would probably not affect its function. Nevertheless, the results of the TEVC measurements showed that H_v1 decreases ROMK2 mediated I_K significantly in three independent experiments (Figure 26 A). These results could lead to the interpretation that the inhibitory effect of H_v1 co-expression is a *X. laevis* oocyte artifact. Nevertheless, ROMK2 is also one of the key players in the aldosterone regulated salt reabsorption in the ASDN which could be regulated by H_v1 similar to ENaC. To further test whether the effects of H_v1 on ROMK2 and ENaC are due to artifacts of the *X. laevis* oocyte expression system another transport protein, the type IIb Na^+/P_i cotransporter (NaPi-IIb) (Forster, Wagner et al. 1997) was co-expressed with H_v1. NaPi-IIb was cloned from flounder because of its 5- to 10-fold higher expression in *X. laevis* oocytes (Forster, Wagner et al. 1997) compared with its mammalian cousins (Bacconi, Ravera et al. 2007). Function of NaPi-IIb can be tested by using TEVC recordings at a clamped membrane potential of -50 mV. Since it is well established that extracellular P_i induces inward currents in the presence of extracellular Na^+, TEVC recordings of Napi-IIb mediated currents were obtained by using ND96 solution supplemented with phosphate (P_i). At a stable membrane potential of -60 mV co-expression of H_v1 does not affect the P_i current in oocytes expressing NaPi-IIb (Figure 26 B). The fact that H_v1 did not influence the function of NaPi-IIb in *X. laevis* oocytes is compatible with the assumption that the effect of H_v1 on ENaC and ROMK2 is not an artifact occurring in the used expression system,

but is rather a specific effect targeting to the modulation of the activity of ion channels that are involved in the Na^+ reabsorption in aldosterone target cells.

Figure 26

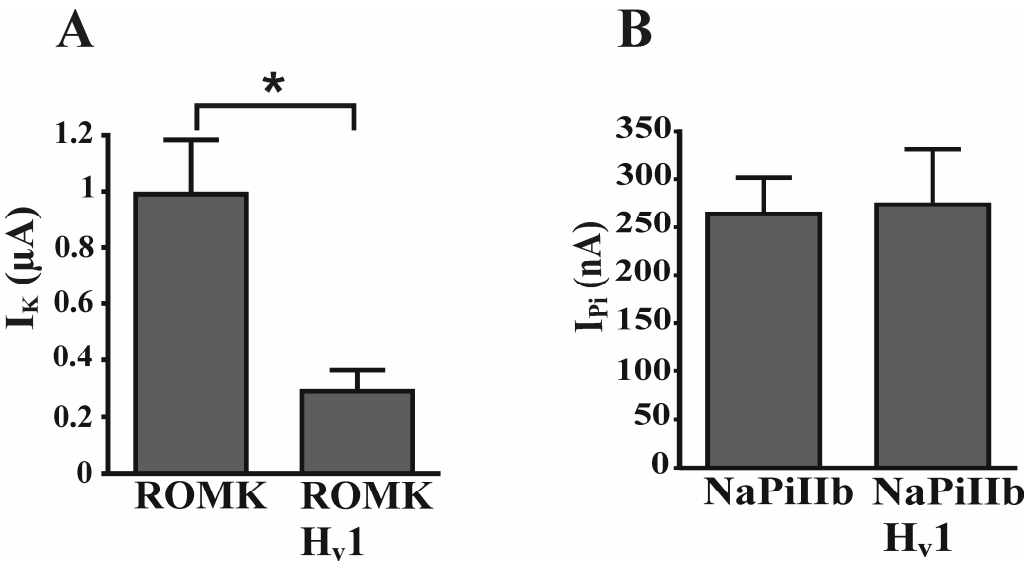

Figure 26: *Effect of H_v1 coexpression on ROMK2 and NaPi-IIb.* (A) Coexpression of H_v1 in *X. laevis* oocytes with the potassium channel ROMK2 reduced ROMK2 mediated potassium currents at -60 mV significantly. Data are means ± SEM; n = 14-16; **P* < 0.001. I_K obtained from noninjected control oocytes were subtracted. (B) Coexpression of H_v1 with the Na^+ dependent P_i cotransporter NaPi-IIb did not affect phosphate currents at -60 mV membrane potential (n = 10-11; $P \geq 0.05$).

6 Discussion

6.1 Usp2-45 increases ENaC activity by deubiquitylation

As rate-limiting luminal Na^+ influx pathway of aldosterone target epithelia, ENaC plays a central role for the regulation of Na^+ absorption. It belongs to the ENaC/DEG gene family, the members of which show a high degree in functional heterogeneity and a wide tissue distribution (Kellenberger and Schild 2002). ENaC is expressed in a variety of osmoregulatory tissues in vertebrates, like the frog skin, urinary bladder, lungs, sweat glands and kidney (Garty and Palmer 1997; Kellenberger and Schild 2002; Snyder 2002) where it is crucial for the regulation of water and ion homeostasis of the body (Uchiyama and Konno 2006). The fact that Na^+ reabsorption is such an important task is in line with the observation that ENaC is regulated by a complex network of pathways which is modulated by many diverse contributions. More and more mechanisms and regulatory cross-talks that impact on ENaC function have been discovered in the last few years (Rotin, Staub et al. 2000; Kamynina, Debonneville et al. 2001). The mineralocorticoid hormone aldosterone is modulating the transcription of genes that are involved in the regulation of transepithelial Na^+ transport (Wald, Goldstein et al. 1996; Naray-Fejes-Toth and Fejes-Toth 2000; Staruschenko, Nichols et al. 2004; Staruschenko, Patel et al. 2004; Soundararajan, Zhang et al. 2005) and is a major regulator of ENaC activity and trafficking (Verrey 1998; Booth, Johnson et al. 2002; Connell and Davies 2005; Fuller and Young 2005; Rozansky 2006). The inputs that impact on transepithelial Na^+ transport in the short term (up to 3 h) appear to converge onto a dominating repressor system that involves ENaC ubiquitylation and deubiquitylation. Deubiquitylation of target proteins has lately gained great importance as a regulatory mechanism although it has already been described at the time of the ubiquitin system discovery (Hershko, Ciechanover et al. 1980; Amerik and Hochstrasser 2004). A number of studies using overexpression systems and cells that express ENaC endogenously showed that ENaC is ubiquitylated through the E3 ligase Nedd4-2 (Staub, Gautschi et al. 1997; Staub, Abriel et al. 2000; Debonneville and Staub 2004; Wang, Traub et al. 2006). ENaC ubiquitylation was found to take place in the apical membrane (Wiemuth, Ke et al. 2007; Zhou, Patel et al. 2007) of epithelial cells but

it remains uncertain whether mono-, poly- or multiubiquitylation of ENaC induces its internalization (Butterworth, Edinger et al. 2007; Zhou, Patel et al. 2007). Our list of early aldosterone-regulated mRNAs of mouse connecting and collecting tubules revealed that indeed two of the most prominent upregulated genes encode proteins that appear to be directly involved in the ubiquitylation and deubiquitylation of proteins, namely Sgk1 and Usp2. Sgk1, already known as an early aldosterone-regulated gene product that regulates ENaC (Snyder, Cheng et al. 1998; Chen, Bhargava et al. 1999; Naray-Fejes-Toth, Canessa et al. 1999; Naray-Fejes-Toth and Fejes-Toth 2000; Verrey, Pearce et al. 2000), was 4-fold up-regulated in our screen. The serine/threonine protein kinase Sgk1 inhibits the function of Nedd4-2 by phosphorylation which leads to the decrease of ENaC ubiquitylation and trafficking (Snyder 2002; Pearce 2003). Nevertheless, a deubiquitylating step avoiding trafficking of ubiquitylated ENaC towards degradation is also required (Hurley, Lee et al. 2006; Butterworth, Edinger et al. 2007; Lu, Pribanic et al. 2007). Usp2, which was 2.2 fold upregulated in our gene screen, is a member of the ubiquitin specific protease family and possibly able to facilitate the deubiquitylation of ENaC. To test this hypothesis, I investigated the potential role of Usp2 on ENaC. An induction of ENaC mediated currents by the short Usp2 isoform (Usp2-45) but not by the long one (Usp2-69) was detected using TEVC recordings of I_{amil} in ENaC expressing *X. laevis* oocytes (Figure 12). That only Usp2-45 influences ENaC activity goes in line with the fact that Usp2-69 is expressed just at low levels in the kidney (unpublished observation PF, VF) (Gousseva and Baker 2003). The human homologue of Usp2-69, Usp2a, was found to deubiquitylate antiapoptotic proteins in prostate cancer cells and represents a therapeutic target in prostate cancer (Priolo, Tang et al. 2006). In contrast the short isoform Usp2-45 was not yet investigated in terms of its physiological function. Around 100 different Usps are found in mammalians (Hemelaar, Galardy et al. 2004; Nijman, Luna-Vargas et al. 2005), so that an increase in ENaC mediated currents could be also mediated by any other ubiquitin protease, that is expressed in the kidney. We randomly selected Usp15, a widely expressed ubiquitin specific protease that is also present in the mouse kidney (Angelats, Wang et al. 2003) to test its function on ENaC in *X. laevis* oocytes. Its co-expression with ENaC did not increase but rather decrease I_{amil} which indicates that the effect of Usp2-45 is specific (Figure 13). The decrease in I_{amil}

mediated by Usp15 is probably the result of the deubiquitylation of other proteins which are involved in ENaC mRNA or protein stability, transcription, translation or trafficking.
As expected we observed that the stimulation of ENaC by Sgk1 was not further increased by co-expression of Usp2-45 (Figure 14) taking into account that the action of Sgk1 decreases the amount of ubiquitylated ENaC. Thus, assuming that Sgk1 prevents that ENaC is ubiquitylated and therefore increases its amount at the cell membrane, Usp2-45 is then not able to additionally increase its surface expression by deubiquitylation. These results strongly support the hypothesis that Usp2-45 cuts off ubiquitin moieties that have been ligated onto ENaC by the ubiquitin ligase Nedd4-2.
Since it was not clarified at that point whether Usp2-45 actually increases ENaC function by its protease activity we tested the action of a protease dead mutant on ENaC. The substitution of one crucial amino acid in the catalytic core entirely abolished the action of Usp2-45 on ENaC (Figure 15). These results support the hypothesis that ENaC is deubiquitylated by Usp2-45 dependent on the integrity of its protease motif.
To examine whether the stimulatory effect of Usp2-45 on ENaC function is not an artefact only occurring in the *X. laevis* oocyte expression system, we tested its function on endogenous ENaC in cultured mpkCCD$_{c14}$ cells. The over-expression of Usp2-45 increased the basal (no aldosterone) transepithelial I_{amil} in mpkCCD$_{c14}$ cells significantly compared to the control and to cells transfected with the protease dead mutant (Figure 16). The fact that transepithelial I_{amil} are similar in Usp2-45 and mock-transfected cells after aldosterone stimulation is not surprising, since it is expected that ENaC is mostly deubiquitylated due to the action of Sgk1 that was shown to be rapidly induced in mpkCCD$_{c14}$ cells by aldosterone (data not shown). Taken together these results strongly suggest that Usp2-45, a gene product that is rapidly induced by aldosterone in vivo, deubiquitylates ENaC, the main player of transepithelial Na^+ transport. Further biochemical and functional experiments done on *X. laevis* oocytes and the Hek273 cell expression systems were carried out by Dorothée Daidiée and Dr. Miguel Van Bemmelen in the laboratory of Prof. Olivier Staub. Their results reinforce the conclusion that ENaC is deubiquitylated by Usp2-45 and therefore prevented from endocytosis and degradation (see Adam, Fakitsas et al. 2007). Considering that Sgk1 indirectly regulates ENaC ubiquitylation via phosphorylation of Nedd4-2, Usp2 is apparently the first gene product identified that is induced by aldosterone and directly acts on ENaC. However, it is

expected that still other aldosterone induced gene-products, possibly also identified in our screen, act via different pathways on ENaC expression and function. The question whether the deubiquitylation event takes place in the plasma membrane or in transport vesicles inside the cells could not be answered yet. Nevertheless it became clear that Usp2-45 increases ENaC function dramatically by deubiquitylation in overexpression systems. Recently Butterworth et al uncovered that also UCH-L3, another deubiquitylating enzyme regulates the apical membrane recycling of ENaC (Butterworth, Edinger et al. 2007). It can be assumed that several deubiquitylating enzymes are involved in ENaC deubiquitylation at the various points of the recycling pathway from endosomal vesicles back towards the apical membrane (Butterworth, Edinger et al. 2007). However, transcription of Usp2 was not only found to be regulated by aldosterone but also by other hormones like androgens and parathyroid hormone, indicating that the Usp2 gene products are involved in the mediation of diverse essential hormonally regulated functions (Miles, Sluka et al. 2002; Graner, Tang et al. 2004).

Figure 27

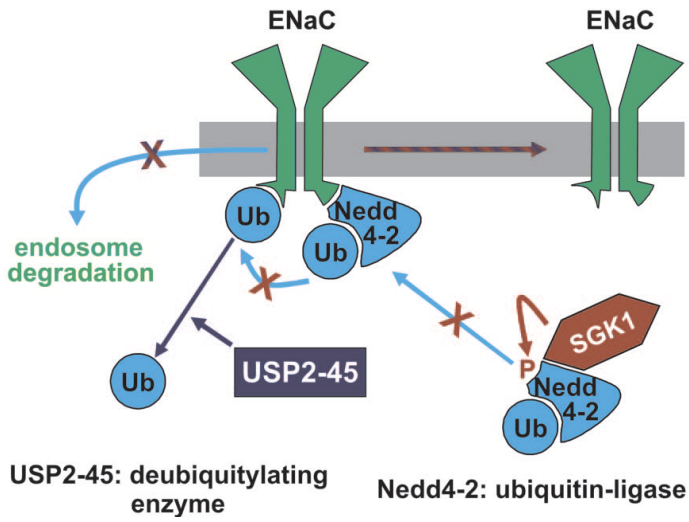

Figure 27: *Graphic illustration of the convergent effect of Sgk1 and Usp2-45.* Both enzymes decrease the amount of ubiquitylated ENaC and hence increase the amount of active channel proteins in the membrane. This figure was adopted from Adam, Fakitsas et al. 2007.

6.2 Does Usp53 act on Na^+ transport?

Considering, that ENaC and other channels and transporters involved in aldosterone regulated Na^+ absorption in the ASDN are ubiquitylated (Coppi and Guidotti 1997; Staub, Gautschi et al. 1997), a second deubiquitylating enzyme, Usp53 that is significantly upregulated in the gene screen obtained immediately our attention. Usp53 is also a member of the family of deubiquitylating enzymes but lacks an essential histidine residue located nine amino acids N-terminal of the histidine at the catalytic site (Hu, Li et al. 2002; Quesada, Diaz-Perales et al. 2004). Hence, Usp53 was classified as a non-protease homologue according to the MEROPS data base nomenclature (Quesada, Diaz-Perales et al. 2004; http://merops.sanger.ac.uk/). A protease activity assay done by Quesada et al revealed that Usp53 has indeed no proteolytic function on the tested substrate. After checking the NCBI database (http://www.ncbi.nlm.nih.gov/Database/) we found that Usp53 protein exists in two different isoforms, that we named Usp53fl for Usp53 full length and Usp53t for the truncated form. Usp53t annotated in the database with the accession number AAH22221 lacks the first 392 amino acids at the N-terminus which includes the complete catalytic site (Figure 17 A). Therefore it was not surprising that this truncated form of Usp53 does not affect ENaC mediated Na^+ currents in co-expressing *X. laevis* oocytes. However, the co-expression of Usp53fl with ENaC does not change I_{amil} either (Figure 18). Neither Usp53fl nor Usp53t influence ENaC function; although both forms could be expressed at a reasonable protein level in oocytes which was tested by Western blot using an antibody against Usp53 (Figure 17 B). Subsequently I tested whether Usp53 has an impact on the Na^+-K^+-ATPase which is known to be involved in the transepithelial Na^+ transport by pumping Na^+ out of the cell at the basolateral side and thereby establishing the driving force for Na^+ reabsorption in the kidney (Greger 2000). The outcome of the experiment performed was quite unexpected since Usp53t, despite lacking its whole protease domain increased the exogenous Na^+-K^+-pump current in a number of batches of *X. laevis* oocytes significantly. However repeating this experiment could not confirm the first observations but there is still a tendency that Usp53t increases Na^+-K^+-ATPase currents (Figure 19 B). Usp53fl in contrast does not influence the pump current at all (Figure 19 A) which implies that the regulation is not based on a

deubiquitylation event. The fact that also Usp2-45 does not impact on the Na^+-K^+-ATPase (Figure 19 C) suggests the hypothesis, that the effect of Usp2-45 on ENaC is rather specific. Since Usp53t has no ubiquitin specific protease function the mechanism by which it activates Na^+ pump function remains entirely unknown. The observation that Usp53 is endogenously expressed in mpkCCD$_{c14}$ cells on mRNA level supports the idea that this Usp has important tasks in the control of Na^+ absorption or differentiation. One hour after aldosterone treatment the mRNA abundance of Usp53 increased ~0.5 fold (Figure 20). The fact that aldosterone-induced Usps stimulate the function of ENaC and of the Na^+-K^+-ATPase supports the hypothesis, that ubiquitylation and deubiquitylation plays a central role in transepithelial Na^+ transport regulation.

The characterization of Usp53 generates in the moment more questions than answers. The results of TEVC recordings are unclear. Even though our Usp53 antibody detects Usp53 protein in Western blot it was not possible to perform localization studies using immunofluorescence on kidney sections with this antibody. These technical limitations and other factors made me stopping the investigation of Usp53 function. Nevertheless I continued my work on the characterization of another early aldosterone regulated gene product: H_v1, a voltage gated proton channel.

6.3 H_v1 influences important players of the Na^+ reabsorption in the ASDN

The analysis of the lists of early aldosterone induced mRNAs showed that one of these encodes a protein comprising an ion channel domain structure. Interestingly this protein turned out to be a member of the VSPs and was characterized recently in the HEK cell expression system as a voltage gated proton channel (Ramsey, Moran et al. 2006; Sasaki, Takagi et al. 2006).

H_v1 is expressed in aldosterone target cells

Since it was rather surprising to find a voltage gated proton channel within aldosterone regulated gene products we were curious to investigate its function in the context of aldosterone regulated salt reabsorption in the kidney. The lack of an H_v1 antibody, giving a specific signal in Western blot prevented the testing of the impact of short term aldosterone treatment on the protein expression level of H_v1 in the ASDN. Nevertheless the up-regulation of mRNA levels in CNT/CCDs could be verified by quantitative real-time RT PCR (P.F. data not shown). Interestingly H_v1 was found to be predominantly expressed in immune tissues and just to a very small extent in the kidney (Ramsey, Moran et al. 2006; Sasaki, Takagi et al. 2006). Nonetheless the accomplishment of immunofluorescence studies on mouse kidney sections suggested that H_v1 protein is expressed in aldosterone target cells in the kidney of non-treated mice. The localization was detected by an anti-H_v1 antibody. Viewing of the images and discussion with Prof. Jan Loffing supported the suggestion that the staining at the apical pole of principal cells in the CD (Figure 21 A, B) is most likely specific and that the rather sporadic staining of β intercalated cells is possibly unspecific (Figure 21 C, D, E, F). Treatment of mice with aldosterone 1h before tissue fixation did lead to a visible enhancement or redistribution of H_v1 signal in the kidney (data not shown). The fact that H_v1 is also endogenously expressed in $mpkCCD_{c14}$ cells on mRNA level (Figure 22) strengthens our supposition that H_v1 plays a role in the aldosterone regulated salt reabsorption across principal cells.

That aldosterone treatment increases H_v1 mRNA expression in these cells confirmes the results obtained with the beforehand performed gene screen. The big inter-experimental variations, that lead to rather large error bars (Figure 22) are probably due to the variable differentiation status of the $mpkCCD_{c14}$ cells. Experiments to investigate the subcellular localization of H_v1 in CCD cells need still to be done. Nevertheless these results give evidence that the voltage gated proton channel H_v1 is rapidly up-regulated by aldosterone which leads to the assumption that it could play an important role in the regulation of transepithelial Na^+ transport in the ASDN.

Characterization of H_v1 in *Xenopus laevis* oocytes

First, several experiments using H_v1 expressing *X. laevis* oocytes were performed to test whether the channel is functionally active in this particular system. After the expression of H_v1 protein in *X. laevis* oocytes was verified by Western blot (Figure 23 A) functional experiments were performed using electrophysiology. Consistent with observations of Ramsey and colleges and Sasaki et al in the HEK cell expression system, H_v1 expressing oocytes exhibit inward tail currents during repolarisation (Figure 23 B). Sasaki et al and Ramsey et al observed that E_{rev} shifts ~50 mV per pH unit difference between pH_i and pH_o indicating that H_v1 is acting as a proton channel considering the Nernst potential for protons (Ramsey, Moran et al. 2006; Sasaki, Takagi et al. 2006). We did not observe consistent pH dependence in *X. laevis* oocytes expressing H_v1 (Figure 23 C), suggesting that H_v1 is not expressed at the surface membrane in *X. laevis* oocytes. Zinc, a common blocker for proton channels caused a flattening of the I-V curve and a shift of E_{rev} towards more negative potentials. These results are not in line with observations done in HEK cells (Ramsey, Moran et al. 2006; Sasaki, Takagi et al. 2006) and are rather induced by endogenous *X. laevis* oocyte procedures. Taken together these results suggest that H_v1 is not functional at the surface membrane of *X. laevis* oocytes and could be expressed in intracellular compartments.

H_v1 affects ENaC and ROMK currents

Until recently the molecular identity of voltage gated proton channels was still unknown or rather speculative. H_v1 is the first voltage gated proton channel that was molecularly identified (Ramsey, Moran et al. 2006; Sasaki, Takagi et al. 2006; Okamura 2007). Ten years ago Gekle and co-workers performed studies on Madin-Darby canine kidney (MDCK) cells showing that aldosterone induces a Zn^{2+} sensitive proton conductance, which is dependent on the membrane potential (Gekle, Silbernagl et al. 1997). This goes in line with the identification of H_v1 as an aldosterone induced gene product in our screen that is considered to mediate Zn^{2+}-sensitive proton currents (Ramsey, Moran et al. 2006; Sasaki, Takagi et al. 2006). A large variety of cells have been reported to express voltage gated H^+ channels including different types of mammalian epithelia (Decoursey 2003) as well as cultured cells like HEK-cells and MDCK cells. By performance of real-time RT PCR we found H_v1 endogenously expressed on the mRNA level in mpkCCD$_{c14}$ cells, too (Figure 22).

It has been shown that intracellular acidification reduces ENaC activity in *X. laevis* oocytes (Chalfant, Denton et al. 1999). Since ENaC currents are directly modified by changes of pH_i but not of pH_o it had been suggested that amino acids at the intracellular N- and C-termini of the ENaC subunits are involved in that regulation (Chalfant, Denton et al. 1999). Chuard and colleagues studied the reciprocal relationship between pH_i and transepithelial Na^+ transport in A6 cells and suggested that pH_i mediates the dialogue between the apical and basolateral side of polarized epithelial cells (Chuard and Durand 1992). The action of pH_i as a regulator of Na^+ transport had been reviewed by L.G. Palmer in 2001 (Palmer 2001). He suggested that pH_i could serve as a second messenger for rapid effects of aldosterone (Palmer 2001). It has been proposed that aldosterone increases pH_i via a nongenomic effect that affects the activity of the Na^+/H^+ exchanger (Oberleithner, Weigt et al. 1987; Cooper and Hunter 1996). One hypothesis is that aldosterone itself is regulating epithelial transport through modulation of pH_i (Palmer 2001), since alkalinisation of the intracellular compartment is supporting the Na^+ and K^+ transport (Palmer 2001). One suggested situation, in which such a regulation may make sense, is the occurance of metabolic stress. The excessive usage of ATP for instance by the Na^+-K^+-ATPase to support high Na^+ transport can cause intracellular acidosis (Frindt,

Silver et al. 1995). Under these circumstances Na^+ and K^+ transport would be down-regulated and therefore the cell is saved from excessive usage of metabolic resources (Palmer 2001).

We investigated the function of the new identified aldosterone regulated gene product H_v1 on Na^+ transport by coexpression of ENaC in *X. laevis* oocytes. Since H_v1 is an early aldosterone regulated gene product our expectation was that H_v1 would rather have an activating effect on I_{amil} considering that aldosterone increases the Na^+ reabsorption in the ASDN. We hypothesised, that the local depolarisation of the apical membrane mediated by the Na^+ transport of ENaC would favour the efflux of protons through H_v1 into the tubular lumen, which is in line with the observation that aldosterone increases the acidification of the tubular fluid in the collecting ducts (Koeppen and Helman 1982). The resulting local alkalinisation of the cytosol would have a stimulatory effect on ENaC function (Palmer 2001). This situation could be amplified by the transcriptional activation of H_v1 by aldosterone. An increased H_v1 abundance on the apical membrane could then activate ENaC function via two additive mechanisms. (1) Removing protons from the local environment of ENaC would be activated by the local alkalinisation (Figure 28). (2) The efflux of protons would counteract the depolarisation of the membrane and so favour the influx of positively charged Na^+ ions via ENaC. This situation would basically be more weightily when $pH_o/pH_i > 1$ (Figure 28).

Figure 28

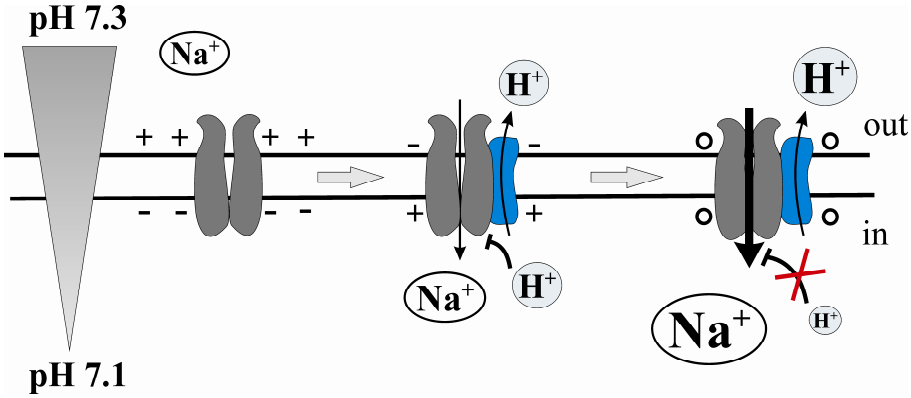

Figure 28: *Graphic illustration of a possible mechanism by which H_v1 could increase ENaC function in the apical membrane of an epithelial cell.* H_v1 localised close to ENaC on the apical membrane of aldosterone target cells could influence ENaC mediated Na^+ transport. Local depolarisation of the apical membrane through Na^+ influx mediated by ENaC causes the activation of H_v1 which mediates the efflux of protons. This induces local alkalinisation of the cytosol and stimulates ENaC, subsequently leading to an enhanced Na^+ reabsorption in the ASDN.

However, in our experiments we observed that H_v1 co-expression inhibits ENaC function in the oocyte expression system (Figure 25, 29). ENaC mediated currents were substantially decreased by H_v1 co-expression over the entire range of tested membrane voltages (Figure 25). Nevertheless, considering that H_v1 would mediate a proton *inward* current in the oocytes these results would be consistent with the observations that low pH_i decreases ENaC function (Chuard and Durand 1992; Chalfant, Denton et al. 1999; Ramsey, Moran et al. 2006; Sasaki, Takagi et al. 2006). Since it is known that aldosterone action is acidifying the tubular fluid in the collecting duct it is expected that the ratio pH_o/pH_i is < 1 in the ASDN after aldosterone action. The proton gradient in this situation would support the influx of protons through H_v1 but the depolarized membrane potential would rather oppose it (Figure 29). However, a proton influx could mediate ENaC inhibition and therefore protect the cell from excessive Na^+ uptake. However, our observation that $ZnCl_2$ did not affect the inhibition of ENaC by H_v1 in *X. laevis* oocytes was then rather unexpected, since it means that H_v1 mediated inhibition of ENaC function is not dependent on its proton conductance (Figure 25 C). The reason for the failure to block H_v1 mediated ENaC inhibition by $ZnCl_2$ application suggested that the inhibiting

action of H_v1 is not at the surface membrane. This latter hypothesis is coherent with the fact that we could not show in our experiments on *X. laevis* oocytes that H_v1 is indeed conducting protons through the plasma membrane.

Figure 29

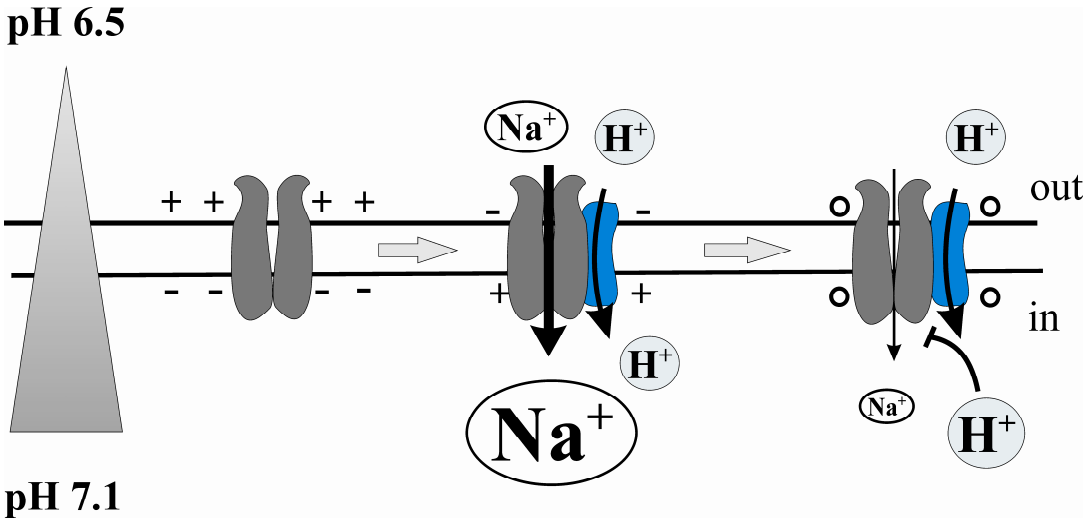

Figure 29: *Graphical scheme of a possible mechanism by which H_v1 would decrease ENaC function in the apical membrane of an epithelial cell.* ENaC action locally depolarises the membrane, H_v1 is activated and mediates a proton influx. This influx is permitted by the acidic pH in the extracellular fluid. ENaC function is shut down by the acidification of the microenvironment.

Considering the possibilities mentioned above that imply that H_v1 would be expressed at the apical surface does not lead to a clarifying hypothesis as regards its potential role. There are pros and cons for the two possible functional mechanisms. On the one hand, the fact, that intracellular acidification is inhibiting ENaC function supports the results obtained in oocytes co-expressing ENaC if considering H_v1 mediates a proton influx and therefore increases at least local intracellular acidification. On the other hand, it is questionable why an aldosterone induced gene product could have an inhibitory effect on ENaC and ROMK2 decreasing the transepithelial Na^+ transport in aldosterone target tissues. We could speculate that this mechanism is a negative regulatory feedback system

to protect the cell from excessive Na^+ intake when the apical membrane depolarizes to a certain extend that is triggered by too much Na^+ influx.

Several groups reported that a decrease in pH_i also negatively affects apical and basolateral K^+ channels that are responsible for K^+ recycling in aldosterone target cells and therefore also are crucial players in transepithelial Na^+ transport (Fakler, Schultz et al. 1996; Urbach, Van Kerkhove et al. 1996; Choe, Zhou et al. 1997). Considering that H_v1 is acidifying the microenvironment inside the oocyte by conducting protons, our observation that H_v1 co-expression decreases ROMK2 mediated K^+ currents is consistent with these studies. Considering that several researchers already proposed that intracellular pH acts as a second messenger system (Gekle, Silbernagl et al. 1997; Palmer 2001), H_v1 could mediate the translation of changes in membrane potentials into intracellular signals (in this case pH) that are able to regulate specific target proteins.

A third possible mechanism of action for the regulation of ENaC or ROMK2 by H_v1 could be a direct interaction between the two molecules. Changes in transmembrane voltages could induce intra-molecular movements within H_v1. These movements could directly impact on the modulation of ENaC function based on the model of voltage gated K^+ channel regulation (Jiang, Ruta et al. 2003). The fact that H_v1 was shown to be expressed at the apical pole of principal cells is a first sign that ENaC and H_v1 could be expressed in close proximity *in vivo*. Whether ENaC directly interacts with H_v1 has to be investigated by co-immunoprecipitation.

Nevertheless, the decrease of ENaC and ROMK2 function by H_v1 co-expression can also be due to artefacts that occur in the *X. laevis* oocyte expression system.

7 Future perspectives

Usp2-45

Usp2-45 is a new aldosterone regulated gene product that we have shown to deubiquitylate ENaC. Its action on the regulation of Na^+ conductance was documented in over-expression systems such as *X. laevis* oocytes and mammalian cell lines. The next logical question is therefore whether ENaC is an Usp2-45 *in vivo* target as well. To address this question it is important to examine the localization of Usp2-45 *in vivo*. Our hypothesis and expectation would be that Usp2-45 co-localizes with ENaC in aldosterone target cells in the mouse kidney. ENaC is not only present at the plasma membrane but also located in intracellular compartments. Aldosterone induces ENaC translocation from the intracellular compartment towards the plasma membrane (Loffing, Zecevic et al. 2001). One important question is at which point of trafficking Usp2-45 co-localizes with ENaC. Knowledge on this particular point would suggest at what level deubiquitylation takes place. It appears possible that Usp2-45 deubiquitylates ENaC directly at the plasma membrane. It is also possible that deubiquitylation takes place at the level of intracellular transport vesicles, for instance in early endosomes.

The exact molecular mechanism of the deubiquitylation of ENaC is not yet fully clarified. One suggestion is that Usp2-45 acts as a single protein on ENaC but it is also imaginable that Usp2-45 interacts with Nedd4-2 (the ubiquitin specific ligase acting on ENaC) or other proteins to deubiquitylate ENaC. An elegant way to show an interaction between Usp2-45 and possible partners would be a co-crystallization. Current investigations aim towards the structural clarification of Usp2-45 with and without possible interacting partners. The result could give more information about a specific site of interaction on Usp2-45 which might be crucial for its substrate specificity. A very important aspect is whether Usp2-45 has a physiologically relevant effect on aldosterone regulated Na^+ reabsorption, a question that could be tested on an Usp2-45 knock out mouse model.

Usp53

Transcription of Usp53 was found to be significantly up-regulated by aldosterone. However, functional investigations did not show a significant impact of its expression on Na^+ transport molecules in *X. laevis* oocytes. A possibly useful other approach would be to do further tests on differentiated distal nephron cell cultures, for instance cultured $mpkCCD_{c14}$ cells, that over-express Usp53. It would be of particular interest to detect its subcellular localization in a cell line as well as *in vivo*. Functional studies with mammalian cell lines, including Usp53 knockdowns, would give more information on the functional role of Usp53 in the regulation of transepithelial Na^+ transport.

H_v1

The most exciting finding concerning H_v1 was certainly that this voltage gated proton channel inhibits ENaC function in *X. laevis* oocytes despite the fact that it was found to be induced by aldosterone. Until now it could not be clarified whether H_v1 reduces ENaC function by influencing its surface expression or its open probability at the plasma membrane. Therefore future experiments could aim to visualize possible changes in ENaC surface expression in oocytes co-expressing H_v1. So far it is still unknown which mechanism could underlie the inhibitory action of H_v1 on ENaC and ROMK2. In this respect it would be crucial to investigate a possible interaction between $H_v1$and ENaC or ROMK2. The hypothesis that H_v1 could inhibit ENaC function by modulation of the intracellular proton concentration has not been tested yet, since it is not possible to control the intracellular pH within the oocytes. In this respect a cut open oocyte system would be a useful tool for having access to the cytosolic side of the oocyte and to apply defined conditions to it. By mutating specific amino acid residues within the H_v1 protein the mechanism of ENaC regulation could be uncovered in an elegant way.

H_v1 expression was detected in the ASDN by real-time RT PCR and our immunofluorescence data suggest that H_v1 protein is expressed in the apical pole of principal cells in the CD. Nevertheless, these results did not give clear enough

information on the exact subcellular localization. Investigations aiming to identify the subcellular protein localization in cultured kidney cells would be necessary to show whether and where the proton channel co-localizes with ENaC or ROMK2. Knowing the precise localization also could give additional information about the mechanism of ENaC and ROMK2 modulation. Co-localization of ENaC and H_v1 in intracellular vesicles for instance would confute the regulation of ENaC open probability by H_v1.

Since the experiments I have performed in *X. laevis* oocyte expression system were essentially of electrophysiological nature, alternative mechanisms leading to ENaC and ROMK2 inhibition involving rather intracellular effects possibly also independent of a proton conductance are not excluded. To address this question, cell biological experiments, in particular of subcellular localization should be performed. Possibly however the *X. laevis* oocytes over-expression system is not an optimal system to reconstitute the role of a proton conductance in the aldosterone-regulated Na^+ reabsorption and K^+ secrection. Alternative in vitro systems are for instance HEK cells in which exogenous surface-expression of H_v1 was successful (Ramsey, Moran et al. 2006; Sasaki, Takagi et al. 2006) or a cell line such as $mpkCCD_{c14}$ cells that express a polarized CCD principal cell type Na^+ transport.

Finally, an H_v1 knockout mouse model would be crucial to obtain information about the physiological role of H_v1 in the context of aldosterone regulated salt reabsorption in the kidney and therefore blood pressure maintenance.

8 References

Abriel, H. and J. D. Horisberger (1999). "Feedback inhibition of rat amiloride-sensitive epithelial sodium channels expressed in Xenopus laevis oocytes." J Physiol **516 (Pt 1)**: 31-43.

Abriel, H., J. Loffing, et al. (1999). "Defective regulation of the epithelial Na+ channel by Nedd4 in Liddle's syndrome." J Clin Invest **103**(5): 667-73.

Abriel, H. and O. Staub (2005). "Ubiquitylation of ion channels." Physiology (Bethesda) **20**: 398-407.

Adam, G., P. Fakitsas, et al. (2007). "Early aldosterone-induced gene product regulates the epithelial sodium channel by deubiquitylation." J Am Soc Nephrol **18**(4): 1084-92.

Adam, G., J. Ousingsawat, et al. (2005). "Increase in intracellular Cl- concentration by cAMP- and Ca2+-dependent stimulation of M1 collecting duct cells." Pflugers Arch **449**(5): 470-8.

Aitken, A. (2002). "Functional specificity in 14-3-3 isoform interactions through dimer formation and phosphorylation. Chromosome location of mammalian isoforms and variants." Plant Mol Biol **50**(6): 993-1010.

Alvarez de la Rosa, D., C. M. Canessa, et al. (2000). "Structure and regulation of amiloride-sensitive sodium channels." Annu Rev Physiol **62**: 573-94.

Amerik, A. Y. and M. Hochstrasser (2004). "Mechanism and function of deubiquitinating enzymes." Biochim. Biophys. Acta **1695**(1-3): 189-207.

Angelats, C., X. W. Wang, et al. (2003). "Isolation and characterization of the mouse ubiquitin-specific protease Usp15." Mamm Genome **14**(1): 31-46.

Asher, C., H. Wald, et al. (1996). "Aldosterone-induced increase in the abundance of Na+ channel subunits." Am J Physiol **271**(2 Pt 1): C605-11.

Bacconi, A., S. Ravera, et al. (2007). "Temperature dependence of steady-state and presteady-state kinetics of a type IIb Na+/P i cotransporter." J Membr Biol **215**(2-3): 81-92.

Beguin, P., G. Crambert, et al. (2001). "CHIF, a member of the FXYD protein family, is a regulator of Na,K-ATPase distinct from the gamma-subunit." Embo J **20**(15): 3993-4002.

Benos, D. J. and B. A. Stanton (1999). "Functional domains within the degenerin/epithelial sodium channel (Deg/ENaC) superfamily of ion channels." J Physiol **520 Pt 3**: 631-44.

Bens, M., V. Vallet, et al. (1999). "Corticosteroid-dependent sodium transport in a novel immortalized mouse collecting duct principal cell line." J Am Soc Nephrol **10**(5): 923-34.

Berdiev, B. K., E. Cormet-Boyaka, et al. (2007). "Molecular proximity of cystic fibrosis transmembrane conductance regulator and epithelial sodium channel assessed by fluorescence resonance energy transfer." J Biol Chem **282**(50): 36481-8.

Berdiev, B. K., B. Jovov, et al. (2004). "ENaC subunit-subunit interactions and inhibition by syntaxin 1A." Am J Physiol Renal Physiol **286**(6): F1100-6.

Berdiev, B. K., V. G. Shlyonsky, et al. (2000). "Gating of amiloride-sensitive Na(+) channels: subunit-subunit interactions and inhibition by the cystic fibrosis transmembrane conductance regulator." Biophys J **78**(4): 1881-94.

Beron, J., L. Mastroberardino, et al. (1995). "Aldosterone modulates sodium kinetics of Na,K-ATPase containing an alpha 1 subunit in A6 kidney cell epithelia." Mol Biol Cell **6**(3): 261-71.

Bhalla, V., D. Daidie, et al. (2005). "Serum- and glucocorticoid-regulated kinase 1 regulates ubiquitin ligase neural precursor cell-expressed, developmentally down-regulated protein 4-2 by inducing interaction with 14-3-3." Mol Endocrinol **19**(12): 3073-84.

Bhalla, V., R. Soundararajan, et al. (2006). "Disinhibitory pathways for control of sodium transport: regulation of ENaC by SGK1 and GILZ." Am J Physiol Renal Physiol **291**(4): F714-21.

Bize, V. and J. D. Horisberger (2007). "Sodium self-inhibition of human epithelial sodium channel: selectivity and affinity of the extracellular sodium sensing site." Am J Physiol Renal Physiol **293**(4): F1137-46.
Booth, R. E., J. P. Johnson, et al. (2002). "Aldosterone." Adv Physiol Educ **26**(1-4): 8-20.
Boron W F, B. E. L. (2005). Medical Physiology, updated edition. Philadelphia, Pennsilvania, Elsevier Saunders.
Brennan, F. E. and P. J. Fuller (2006). "Mammalian K-ras2 is a corticosteroid-induced gene in vivo." Endocrinology **147**(6): 2809-16.
Broer, S. (2003). "Xenopus laevis Oocytes." Methods Mol Biol **227**: 245-58.
Butterworth, M. B., R. S. Edinger, et al. (2007). "The deubiquitinating enzyme, UCH-L3 regulates the apical membrane recycling of the epithelial sodium channel (ENaC)." J Biol Chem.
Byerly, L. and Y. Suen (1989). "Characterization of proton currents in neurones of the snail, Lymnaea stagnalis." J Physiol **413**: 75-89.
Caldwell, R. A., R. C. Boucher, et al. (2005). "Neutrophil elastase activates near-silent epithelial Na+ channels and increases airway epithelial Na+ transport." Am J Physiol Lung Cell Mol Physiol **288**(5): L813-9.
Canessa, C. M. (2007). "Structural biology: unexpected opening." Nature **449**(7160): 293-4.
Canessa, C. M., J. D. Horisberger, et al. (1993). "Epithelial sodium channel related to proteins involved in neurodegeneration." Nature **361**(6411): 467-70.
Canessa, C. M., L. Schild, et al. (1994). "Amiloride-sensitive epithelial Na+ channel is made of three homologous subunits." Nature **367**(6462): 463-7.
Catterall, W. A. (1986). "Molecular properties of voltage-sensitive sodium channels." Annu Rev Biochem **55**: 953-85.
Chalfant, M. L., J. S. Denton, et al. (1999). "Intracellular H+ regulates the alpha-subunit of ENaC, the epithelial Na+ channel." Am J Physiol **276**(2 Pt 1): C477-86.
Chang, S. S., S. Grunder, et al. (1996). "Mutations in subunits of the epithelial sodium channel cause salt wasting with hyperkalaemic acidosis, pseudohypoaldosteronism type 1." Nat Genet **12**(3): 248-53.
Chen, H. I. and M. Sudol (1995). "The WW domain of Yes-associated protein binds a proline-rich ligand that differs from the consensus established for Src homology 3-binding modules." Proc Natl Acad Sci U S A **92**(17): 7819-23.
Chen, S. Y., A. Bhargava, et al. (1999). "Epithelial sodium channel regulated by aldosterone-induced protein sgk." Proc Natl Acad Sci U S A **96**(5): 2514-9.
Cherny, V. V. and T. E. DeCoursey (1999). "pH-dependent inhibition of voltage-gated H(+) currents in rat alveolar epithelial cells by Zn(2+) and other divalent cations." J Gen Physiol **114**(6): 819-38.
Choe, H., H. Zhou, et al. (1997). "A conserved cytoplasmic region of ROMK modulates pH sensitivity, conductance, and gating." Am J Physiol **273**(4 Pt 2): F516-29.
Chraibi, A. and J. D. Horisberger (2002). "Na self inhibition of human epithelial Na channel: temperature dependence and effect of extracellular proteases." J Gen Physiol **120**(2): 133-45.
Chraibi, A., V. Vallet, et al. (1998). "Protease modulation of the activity of the epithelial sodium channel expressed in Xenopus oocytes." J Gen Physiol **111**(1): 127-38.
Chuard, F. and J. Durand (1992). "Coupling between the intracellular pH and the active transport of sodium in an epithelial cell line from Xenopus laevis." Comp Biochem Physiol Comp Physiol **102**(1): 7-14.
Chung O, U. T. (2006). Das Renin-Angiotensin-System www.klinikundforschung.de/sup/heft5/renin_angi.htm.
Condliffe, S. B., M. D. Carattino, et al. (2003). "Syntaxin 1A regulates ENaC via domain-specific interactions." J Biol Chem **278**(15): 12796-804.

Connell, J. M. and E. Davies (2005). "The new biology of aldosterone." J Endocrinol **186**(1): 1-20.
Cooper, G. J. and M. Hunter (1996). "Role of de novo protein synthesis and calmodulin in rapid activation of Na(+)-H+ exchange of aldosterone in frog diluting segment." J Physiol **491 (Pt 1)**: 219-23.
Cooper, M. and G. Boner (2004). "Dual blockade of the renin-angiotensin system in diabetic nephropathy." Diabet Med **21 Suppl 1**: 15-8.
Coppi, M. V. and G. Guidotti (1997). "Ubiquitination of Na,K-ATPase alpha1 and alpha2 subunits." FEBS Lett **405**(3): 281-4.
Crambert, G., U. Hasler, et al. (2000). "Transport and pharmacological properties of nine different human Na, K-ATPase isozymes." J Biol Chem **275**(3): 1976-86.
Cucu, D., J. Simaels, et al. (2003). "External Ni2 + and ENaC in A6 cells: Na+ current stimulation by competition at a binding site for amiloride and Na+." J Membr Biol **194**(1): 33-45.
Dada, L. A., L. C. Welch, et al. (2007). "Phosphorylation and ubiquitination are necessary for Na,K-ATPase endocytosis during hypoxia." Cell Signal **19**(9): 1893-8.
Debonneville, C., S. Y. Flores, et al. (2001). "Phosphorylation of Nedd4-2 by Sgk1 regulates epithelial Na(+) channel cell surface expression." Embo J **20**(24): 7052-9.
Debonneville, C. and O. Staub (2004). "Participation of the ubiquitin-conjugating enzyme UBE2E3 in Nedd4-2-dependent regulation of the epithelial Na+ channel." Mol Cell Biol **24**(6): 2397-409.
Decoursey, T. E. (2003). "Voltage-gated proton channels and other proton transfer pathways." Physiol Rev **83**(2): 475-579.
DeCoursey, T. E. and V. V. Cherny (1998). "Temperature dependence of voltage-gated H+ currents in human neutrophils, rat alveolar epithelial cells, and mammalian phagocytes." J Gen Physiol **112**(4): 503-22.
Duffey, M. E. and D. C. Devor (1990). "Intracellular pH and membrane potassium conductance in rabbit distal colon." Am J Physiol **258**(2 Pt 1): C336-43.
Eaton, D. C., K. L. Hamilton, et al. (1984). "Intracellular acidosis blocks the basolateral Na-K pump in rabbit urinary bladder." Am J Physiol **247**(6 Pt 2): F946-54.
Elinder, F., J. Nilsson, et al. (2007). "On the opening of voltage-gated ion channels." Physiol Behav **92**(1-2): 1-7.
Erlij, D., P. De Smet, et al. (1994). "Effect of insulin on area and Na+ channel density of apical membrane of cultured toad kidney cells." J Physiol **481 (Pt 3)**: 533-42.
Escoubet, B., C. Coureau, et al. (1997). "Noncoordinate regulation of epithelial Na channel and Na pump subunit mRNAs in kidney and colon by aldosterone." Am J Physiol **272**(5 Pt 1): C1482-91.
Eskandari, S., P. M. Snyder, et al. (1999). "Number of subunits comprising the epithelial sodium channel." J Biol Chem **274**(38): 27281-6.
Fakler, B., J. H. Schultz, et al. (1996). "Identification of a titratable lysine residue that determines sensitivity of kidney potassium channels (ROMK) to intracellular pH." Embo J **15**(16): 4093-9.
Faletti, C. J., N. Perrotti, et al. (2002). "sgk: an essential convergence point for peptide and steroid hormone regulation of ENaC-mediated Na+ transport." Am J Physiol Cell Physiol **282**(3): C494-500.
Firsov, D., I. Gautschi, et al. (1998). "The heterotetrameric architecture of the epithelial sodium channel (ENaC)." Embo J **17**(2): 344-52.
Firsov, D., L. Schild, et al. (1996). "Cell surface expression of the epithelial Na channel and a mutant causing Liddle syndrome: a quantitative approach." Proc Natl Acad Sci U S A **93**(26): 15370-5.
Forster, I. C., C. A. Wagner, et al. (1997). "Electrophysiological characterization of the flounder type II Na+/Pi cotransporter (NaPi-5) expressed in Xenopus laevis oocytes." J Membr Biol **160**(1): 9-25.

Frindt, G., R. B. Silver, et al. (1995). "Feedback regulation of Na channels in rat CCT. III. Response to cAMP." Am J Physiol **268**(3 Pt 2): F480-9.
Fuchs, W., E. H. Larsen, et al. (1977). "Current-voltage curve of sodium channels and concentration dependence of sodium permeability in frog skin." J Physiol **267**(1): 137-66.
Fuller, P. J. and M. J. Young (2005). "Mechanisms of mineralocorticoid action." Hypertension **46**(6): 1227-35.
Fyfe, G. K. and C. M. Canessa (1998). "Subunit composition determines the single channel kinetics of the epithelial sodium channel." J Gen Physiol **112**(4): 423-32.
Fyfe, G. K., A. Quinn, et al. (1998). "Structure and function of the Mec-ENaC family of ion channels." Semin Nephrol **18**(2): 138-51.
Garty, H., E. D. Civan, et al. (1985). "Effects of internal and external pH on amiloride-blockable Na+ transport across toad urinary bladder vesicles." J Membr Biol **87**(1): 67-75.
Garty, H. and L. G. Palmer (1997). "Epithelial sodium channels: function, structure, and regulation." Physiol Rev **77**(2): 359-96.
Gekle, M., S. Silbernagl, et al. (1997). "The mineralocorticoid aldosterone activates a proton conductance in cultured kidney cells." Am J Physiol **273**(5 Pt 1): C1673-8.
Goldschimdt, I., F. Grahammer, et al. (2004). "Kidney and colon electrolyte transport in CHIF knockout mice." Cell Physiol Biochem **14**(1-2): 113-20.
Gonzalez-Rodriguez, E., H. P. Gaeggeler, et al. (2007). "IGF-1 vs insulin: respective roles in modulating sodium transport via the PI-3 kinase/Sgk1 pathway in a cortical collecting duct cell line." Kidney Int **71**(2): 116-25.
Good, D. W. (2007). "Nongenomic actions of aldosterone on the renal tubule." Hypertension **49**(4): 728-39.
Gordon, R. D. (1995). "Heterogeneous hypertension." Nat Genet **11**(1): 6-9.
Gormley, K., Y. Dong, et al. (2003). "Regulation of the epithelial sodium channel by accessory proteins." Biochem J **371**(Pt 1): 1-14.
Goulet, C. C., K. A. Volk, et al. (1998). "Inhibition of the epithelial Na+ channel by interaction of Nedd4 with a PY motif deleted in Liddle's syndrome." J Biol Chem **273**(45): 30012-7.
Gousseva, N. and R. T. Baker (2003). "Gene structure, alternate splicing, tissue distribution, cellular localization, and developmental expression pattern of mouse deubiquitinating enzyme isoforms Usp2-45 and Usp2-69." Gene Expr **11**(3-4): 163-79.
Graner, E., D. Tang, et al. (2004). "The isopeptidase USP2a regulates the stability of fatty acid synthase in prostate cancer." Cancer Cell **5**(3): 253-61.
Greger, R. (2000). "Physiology of renal sodium transport." Am J Med Sci **319**(1): 51-62.
Guipponi, M., G. Vuagniaux, et al. (2002). "The transmembrane serine protease (TMPRSS3) mutated in deafness DFNB8/10 activates the epithelial sodium channel (ENaC) in vitro." Hum Mol Genet **11**(23): 2829-36.
Haglund, K. and I. Dikic (2005). "Ubiquitylation and cell signaling." Embo J **24**(19): 3353-9.
Hansson, J. H., C. Nelson-Williams, et al. (1995). "Hypertension caused by a truncated epithelial sodium channel gamma subunit: genetic heterogeneity of Liddle syndrome." Nat Genet **11**(1): 76-82.
Harris, M., A. Garcia-Caballero, et al. (2008). "Preferential assembly of ENaC subunits in Xenopus oocyte: Role of furin- mediated endogenous proteolysis." J Biol Chem.
Harvey, B. J. and J. Ehrenfeld (1988). "Epithelial pH and ion transport regulation by proton pumps and exchangers." Ciba Found Symp **139**: 139-64.
Hemelaar, J., P. J. Galardy, et al. (2004). "Chemistry-based functional proteomics: mechanism-based activity-profiling tools for ubiquitin and ubiquitin-like specific proteases." J Proteome Res **3**(2): 268-76.
Hershko, A., A. Ciechanover, et al. (1980). "Proposed role of ATP in protein breakdown: conjugation of protein with multiple chains of the polypeptide of ATP-dependent proteolysis." Proc Natl Acad Sci U S A **77**(4): 1783-6.

Horisberger, J. D. and A. Chraibi (2004). "Epithelial sodium channel: a ligand-gated channel?" Nephron Physiol **96**(2): p37-41.
Horisberger, J. D., P. Jaunin, et al. (1991). "Coexpression of alpha 1 with putative beta 3 subunits results in functional Na+/K+ pumps in Xenopus oocytes." Proc Natl Acad Sci U S A **88**(19): 8397-400.
Hu, M., P. Li, et al. (2002). "Crystal structure of a UBP-family deubiquitinating enzyme in isolation and in complex with ubiquitin aldehyde." Cell **111**(7): 1041-54.
Hughey, R. P., J. B. Bruns, et al. (2004). "Epithelial sodium channels are activated by furin-dependent proteolysis." J Biol Chem **279**(18): 18111-4.
Hurley, J. H., S. Lee, et al. (2006). "Ubiquitin-binding domains." Biochem J **399**(3): 361-72.
Ichimura, T., H. Yamamura, et al. (2005). "14-3-3 proteins modulate the expression of epithelial Na+ channels by phosphorylation-dependent interaction with Nedd4-2 ubiquitin ligase." J Biol Chem **280**(13): 13187-94.
Jaisser, F., J. D. Horisberger, et al. (1992). "The beta subunit modulates potassium activation of the Na-K pump." Ann N Y Acad Sci **671**: 113-9.
Jasti, J., H. Furukawa, et al. (2007). "Structure of acid-sensing ion channel 1 at 1.9 A resolution and low pH." Nature **449**(7160): 316-23.
Jiang, Y., V. Ruta, et al. (2003). "The principle of gating charge movement in a voltage-dependent K+ channel." Nature **423**(6935): 42-8.
Kaissling, B. and M. Le Hir (1982). "Distal tubular segments of the rabbit kidney after adaptation to altered Na- and K-intake. I. Structural changes." Cell Tissue Res **224**(3): 469-92.
Kamynina, E., C. Debonneville, et al. (2001). "A novel mouse Nedd4 protein suppresses the activity of the epithelial Na+ channel." Faseb J **15**(1): 204-214.
Kamynina, E., C. Debonneville, et al. (2001). "Liddle's syndrome: a novel mouse Nedd4 isoform regulates the activity of the epithelial Na(+) channel." Kidney Int **60**(2): 466-71.
Kellenberger, S., I. Gautschi, et al. (1998). "Mutations causing Liddle syndrome reduce sodium-dependent downregulation of the epithelial sodium channel in the Xenopus oocyte expression system." J Clin Invest **101**(12): 2741-50.
Kellenberger, S. and L. Schild (2002). "Epithelial sodium channel/degenerin family of ion channels: a variety of functions for a shared structure." Physiol Rev **82**(3): 735-67.
Kleyman, T. R., M. M. Myerburg, et al. (2006). "Regulation of ENaCs by proteases: An increasingly complex story." Kidney Int **70**(8): 1391-2.
Koefoed-Johnsen, V. and H. H. Ussing (1958). "The nature of the frog skin potential." Acta Physiol Scand **42**(3-4): 298-308.
Koeppen, B. M. and S. I. Helman (1982). "Acidification of luminal fluid by the rabbit cortical collecting tubule perfused in vitro." Am J Physiol **242**(5): F521-31.
Kolb, H. A. (1990). "Ion channels in opossum kidney cells." Ren Physiol Biochem **13**(1-2): 26-36.
Kosari, F., S. Sheng, et al. (1998). "Subunit stoichiometry of the epithelial sodium channel." J Biol Chem **273**(22): 13469-74.
Kunzelmann, K. (1999). "The cystic fibrosis transmembrane conductance regulator and its function in epithelial transport." Rev Physiol Biochem Pharmacol **137**: 1-70.
Kunzelmann, K. and R. Schreiber (1999). "CFTR, a regulator of channels." J Membr Biol **168**(1): 1-8.
Kunzelmann, K., R. Schreiber, et al. (2002). "Mechanisms for the inhibition of amiloride-sensitive Na+ absorption by extracellular nucleotides in mouse trachea." Pflugers Arch **444**(1-2): 220-6.
Lang, F., G. Capasso, et al. (2005). "Renal tubular transport and the genetic basis of hypertensive disease." Clin Exp Nephrol **9**(2): 91-9.
Lee, C. T., Y. L. Ma, et al. (2007). "Serum- and glucocorticoid-inducible kinase1 enhances contextual fear memory formation through down-regulation of the expression of Hes5." J Neurochem **100**(6): 1531-42.

Letz, B. and C. Korbmacher (1997). "cAMP stimulates CFTR-like Cl- channels and inhibits amiloride-sensitive Na+ channels in mouse CCD cells." Am J Physiol **272**(2 Pt 1): C657-66.
Liang, X., K. W. Peters, et al. (2006). "14-3-3 isoforms are induced by aldosterone and participate in its regulation of epithelial sodium channels." J Biol Chem **281**(24): 16323-32.
Liddle, G. W., D. P. Island, et al. (1963). "Nonpituitary neoplasms and Cushing's syndrome. Ectopic "adrenocorticotropin" produced by nonpituitary neoplasms as a cause of Cushing's syndrome." Arch Intern Med **111**: 471-5.
Lifton, R. P. (1996). "Molecular genetics of human blood pressure variation." Science **272**(5262): 676-80.
Ling, B. N., J. B. Zuckerman, et al. (1997). "Expression of the cystic fibrosis phenotype in a renal amphibian epithelial cell line." J Biol Chem **272**(1): 594-600.
Loffing, J., D. Loffing-Cueni, et al. (2000). "Localization of epithelial sodium channel and aquaporin-2 in rabbit kidney cortex." Am J Physiol Renal Physiol **278**(4): F530-9.
Loffing, J., M. Zecevic, et al. (2001). "Aldosterone induces rapid apical translocation of ENaC in early portion of renal collecting system: possible role of SGK." Am J Physiol Renal Physiol **280**(4): F675-82.
Lu, C., S. Pribanic, et al. (2007). "The PY motif of ENaC, mutated in Liddle syndrome, regulates channel internalization, sorting and mobilization from subapical pool." Traffic **8**(9): 1246-64.
Ma, H. P., S. Saxena, et al. (2002). "Anionic phospholipids regulate native and expressed epithelial sodium channel (ENaC)." J Biol Chem **277**(10): 7641-4.
Maehama, T., G. S. Taylor, et al. (2001). "PTEN and myotubularin: novel phosphoinositide phosphatases." Annu Rev Biochem **70**: 247-79.
Mall, M., M. Bleich, et al. (1998). "The amiloride-inhibitable Na+ conductance is reduced by the cystic fibrosis transmembrane conductance regulator in normal but not in cystic fibrosis airways." J Clin Invest **102**(1): 15-21.
Mall, M., M. Bleich, et al. (1999). "CFTR-mediated inhibition of epithelial Na+ conductance in human colon is defective in cystic fibrosis." Am J Physiol **277**(3 Pt 1): G709-16.
Mastroberardino, L., B. Spindler, et al. (1998). "Ras pathway activates epithelial Na+ channel and decreases its surface expression in Xenopus oocytes." Mol Biol Cell **9**(12): 3417-27.
McNicholas, C. M. and C. M. Canessa (1997). "Diversity of channels generated by different combinations of epithelial sodium channel subunits." J Gen Physiol **109**(6): 681-92.
Miles, R. R., J. P. Sluka, et al. (2002). "Parathyroid hormone (hPTH 1-38) stimulates the expression of UBP41, an ubiquitin-specific protease, in bone." J Cell Biochem **85**(2): 229-42.
Miller, C. (2006). "Biophysics. Lonely voltage sensor seeks protons for permeation." Science **312**(5773): 534-5.
Morgan, D. and T. E. DeCoursey (2003). "Diversity of voltage gated proton channels." Front Biosci **8**: s1266-79.
Murata, Y., H. Iwasaki, et al. (2005). "Phosphoinositide phosphatase activity coupled to an intrinsic voltage sensor." Nature **435**(7046): 1239-43.
Murata, Y. and Y. Okamura (2007). "Depolarization activates the phosphoinositide phosphatase Ci-VSP, as detected in Xenopus oocytes coexpressing sensors of PIP2." J Physiol **583**(Pt 3): 875-89.
Naray-Fejes-Toth, A. (1999). "Sgk: A New Player (Star?) in the Early Action of Aldosterone." News Physiol Sci **14**: 274-275.
Naray-Fejes-Toth, A., C. Canessa, et al. (1999). "sgk is an aldosterone-induced kinase in the renal collecting duct. Effects on epithelial na+ channels." J Biol Chem **274**(24): 16973-8.
Naray-Fejes-Toth, A. and G. Fejes-Toth (2000). "The sgk, an aldosterone-induced gene in mineralocorticoid target cells, regulates the epithelial sodium channel." Kidney Int **57**(4): 1290-4.

Naray-Fejes-Toth, A., P. M. Snyder, et al. (2004). "The kidney-specific WNK1 isoform is induced by aldosterone and stimulates epithelial sodium channel-mediated Na+ transport." Proc Natl Acad Sci U S A **101**(50): 17434-9.

Nijman, S. M., M. P. Luna-Vargas, et al. (2005). "A genomic and functional inventory of deubiquitinating enzymes." Cell **123**(5): 773-86.

O'Reilly, M., E. Marshall, et al. (2006). "Dietary electrolyte-driven responses in the renal WNK kinase pathway in vivo." J Am Soc Nephrol **17**(9): 2402-13.

Oberleithner, H., M. Weigt, et al. (1987). "Aldosterone activates Na+/H+ exchange and raises cytoplasmic pH in target cells of the amphibian kidney." Proc Natl Acad Sci U S A **84**(5): 1464-8.

Okamura, Y. (2007). "Biodiversity of voltage sensor domain proteins." Pflugers Arch **454**(3): 361-71.

Palmer, L. G. (1982). "Ion selectivity of the apical membrane Na channel in the toad urinary bladder." J Membr Biol **67**(2): 91-8.

Palmer, L. G. (1985). "Modulation of apical Na permeability of the toad urinary bladder by intracellular Na, Ca, and H." J Membr Biol **83**(1-2): 57-69.

Palmer, L. G. (1987). "Ion selectivity of epithelial Na channels." J Membr Biol **96**(2): 97-106.

Palmer, L. G. (2001). "Intracellular pH as a regulator of Na + transport." J Membr Biol **184**(3): 305-11.

Palmer, L. G. and G. Frindt (1987). "Effects of cell Ca and pH on Na channels from rat cortical collecting tubule." Am J Physiol **253**(2 Pt 2): F333-9.

Paunescu, T. G., N. Da Silva, et al. (2004). "Expression of the 56-kDa B2 subunit isoform of the vacuolar H(+)-ATPase in proton-secreting cells of the kidney and epididymis." Am J Physiol Cell Physiol **287**(1): C149-62.

Pearce, D. (2003). "SGK1 regulation of epithelial sodium transport." Cell Physiol Biochem **13**(1): 13-20.

Pochynyuk, O., Q. Tong, et al. (2006). "Regulation of the epithelial Na+ channel (ENaC) by phosphatidylinositides." Am J Physiol Renal Physiol **290**(5): F949-57.

Pochynyuk, O., Q. Tong, et al. (2007). "Binding and direct activation of the epithelial Na+ channel (ENaC) by phosphatidylinositides." J Physiol **580**(Pt. 2): 365-72.

Priolo, C., D. Tang, et al. (2006). "The isopeptidase USP2a protects human prostate cancer from apoptosis." Cancer Res **66**(17): 8625-32.

Qi, J., K. W. Peters, et al. (1999). "Regulation of the amiloride-sensitive epithelial sodium channel by syntaxin 1A." J Biol Chem **274**(43): 30345-8.

Quesada, V., A. Diaz-Perales, et al. (2004). "Cloning and enzymatic analysis of 22 novel human ubiquitin-specific proteases." Biochem Biophys Res Commun **314**(1): 54-62.

Ramsey, I. S., M. M. Moran, et al. (2006). "A voltage-gated proton-selective channel lacking the pore domain." Nature **440**(7088): 1213-6.

Record, R. D., M. Johnson, et al. (1996). "Aldosterone and insulin stimulate amiloride-sensitive sodium transport in A6 cells by additive mechanisms." Am J Physiol **271**(4 Pt 1): C1079-84.

Renard, S., E. Lingueglia, et al. (1994). "Biochemical analysis of the membrane topology of the amiloride-sensitive Na+ channel." J Biol Chem **269**(17): 12981-6.

Romeo, E., M. H. Dave, et al. (2006). "Luminal kidney and intestine SLC6 amino acid transporters of B0AT-cluster and their tissue distribution in Mus musculus." Am J Physiol Renal Physiol **290**(2): F376-83.

Rossier, B. C. (2004). "The epithelial sodium channel: activation by membrane-bound serine proteases." Proc Am Thorac Soc **1**(1): 4-9.

Rotin, D. (2000). "Regulation of the epithelial sodium channel (ENaC) by accessory proteins." Curr Opin Nephrol Hypertens **9**(5): 529-34.

Rotin, D., O. Staub, et al. (2000). "Ubiquitination and endocytosis of plasma membrane proteins: role of Nedd4/Rsp5p family of ubiquitin-protein ligases." J Membr Biol **176**(1): 1-17.

Rozansky, D. J. (2006). "The role of aldosterone in renal sodium transport." Semin Nephrol **26**(2): 173-81.
Sands, Z., A. Grottesi, et al. (2005). "Voltage-gated ion channels." Curr Biol **15**(2): R44-7.
Sasaki, M., M. Takagi, et al. (2006). "A voltage sensor-domain protein is a voltage-gated proton channel." Science **312**(5773): 589-92.
Saxena, S., M. W. Quick, et al. (1999). "Interaction of syntaxins with the amiloride-sensitive epithelial sodium channel." J Biol Chem **274**(30): 20812-7.
Saxena, S. K., C. M. George, et al. (2006). "Epithelial sodium channel is regulated by SNAP-23/syntaxin 1A interplay." Biochem Biophys Res Commun **343**(4): 1279-85.
Saxena, S. K. and S. Kaur (2006). "Regulation of epithelial ion channels by Rab GTPases." Biochem Biophys Res Commun **351**(3): 582-7.
Saxena, S. K., M. Singh, et al. (2006). "Rab4 GTP/GDP modulates amiloride-sensitive sodium channel (ENaC) function in colonic epithelia." Biochem Biophys Res Commun **340**(2): 726-33.
Schild, L. (1996). "The ENaC channel as the primary determinant of two human diseases: Liddle syndrome and pseudohypoaldosteronism." Nephrologie **17**(7): 395-400.
Schild, L. (2004). "The epithelial sodium channel: from molecule to disease." Rev Physiol Biochem Pharmacol **151**: 93-107.
Schild, L., Y. Lu, et al. (1996). "Identification of a PY motif in the epithelial Na channel subunits as a target sequence for mutations causing channel activation found in Liddle syndrome." Embo J **15**(10): 2381-7.
Schreiber, R., A. Hopf, et al. (1999). "The first-nucleotide binding domain of the cystic-fibrosis transmembrane conductance regulator is important for inhibition of the epithelial Na+ channel." Proc Natl Acad Sci U S A **96**(9): 5310-5.
Schulz, N., M. H. Dave, et al. (2007). "Differential localization of vacuolar H+-ATPases containing a1, a2, a3, or a4 (ATP6V0A1-4) subunit isoforms along the nephron." Cell Physiol Biochem **20**(1-4): 109-20.
Sheng, S., C. J. Perry, et al. (2004). "Extracellular Zn2+ activates epithelial Na+ channels by eliminating Na+ self-inhibition." J Biol Chem **279**(30): 31687-96.
Shi, H., C. Asher, et al. (2002). "Interactions of beta and gamma ENaC with Nedd4 can be facilitated by an ERK-mediated phosphorylation." J Biol Chem **277**(16): 13539-47.
Shimkets, R. A., R. Lifton, et al. (1998). "In vivo phosphorylation of the epithelial sodium channel." Proc Natl Acad Sci U S A **95**(6): 3301-5.
Shimkets, R. A., D. G. Warnock, et al. (1994). "Liddle's syndrome: heritable human hypertension caused by mutations in the beta subunit of the epithelial sodium channel." Cell **79**(3): 407-14.
Skou, J. C. (1982). "The effect of pH, of ATP and of modification with pyridoxal 5-phosphate on the conformational transition between the Na+-form and the K+-form of the (Na+ +K+)-ATPase." Biochim Biophys Acta **688**(2): 369-80.
Snyder, P. M. (2002). "The epithelial Na+ channel: cell surface insertion and retrieval in Na+ homeostasis and hypertension." Endocr Rev **23**(2): 258-75.
Snyder, P. M. (2005). "Minireview: regulation of epithelial Na+ channel trafficking." Endocrinology **146**(12): 5079-85.
Snyder, P. M., C. Cheng, et al. (1998). "Electrophysiological and biochemical evidence that DEG/ENaC cation channels are composed of nine subunits." J Biol Chem **273**(2): 681-4.
Snyder, P. M., F. J. McDonald, et al. (1994). "Membrane topology of the amiloride-sensitive epithelial sodium channel." J Biol Chem **269**(39): 24379-83.
Snyder, P. M., D. R. Olson, et al. (2004). "cAMP and serum and glucocorticoid-inducible kinase (SGK) regulate the epithelial Na(+) channel through convergent phosphorylation of Nedd4-2." J Biol Chem **279**(44): 45753-8.
Snyder, P. M., D. R. Olson, et al. (2002). "Serum and glucocorticoid-regulated kinase modulates Nedd4-2-mediated inhibition of the epithelial Na+ channel." J Biol Chem **277**(1): 5-8.

Snyder, P. M., M. P. Price, et al. (1995). "Mechanism by which Liddle's syndrome mutations increase activity of a human epithelial Na+ channel." Cell **83**(6): 969-78.
Soundararajan, R., T. T. Zhang, et al. (2005). "A novel role for glucocorticoid-induced leucine zipper protein in epithelial sodium channel-mediated sodium transport." J Biol Chem **280**(48): 39970-81.
Spindler, B., L. Mastroberardino, et al. (1997). "Characterization of early aldosterone-induced RNAs identified in A6 kidney epithelia." Pflugers Arch **434**(3): 323-31.
Staruschenko, A., E. Adams, et al. (2005). "Epithelial Na+ channel subunit stoichiometry." Biophys J **88**(6): 3966-75.
Staruschenko, A., J. L. Medina, et al. (2004). "Fluorescence resonance energy transfer analysis of subunit stoichiometry of the epithelial Na+ channel." J Biol Chem **279**(26): 27729-34.
Staruschenko, A., A. Nichols, et al. (2004). "Rho small GTPases activate the epithelial Na(+) channel." J Biol Chem **279**(48): 49989-94.
Staruschenko, A., P. Patel, et al. (2004). "Ras activates the epithelial Na(+) channel through phosphoinositide 3-OH kinase signaling." J Biol Chem **279**(36): 37771-8.
Staub, O., H. Abriel, et al. (2000). "Regulation of the epithelial Na+ channel by Nedd4 and ubiquitination." Kidney Int **57**(3): 809-15.
Staub, O., S. Dho, et al. (1996). "WW domains of Nedd4 bind to the proline-rich PY motifs in the epithelial Na+ channel deleted in Liddle's syndrome." Embo J **15**(10): 2371-80.
Staub, O., I. Gautschi, et al. (1997). "Regulation of stability and function of the epithelial Na+ channel (ENaC) by ubiquitination." Embo J **16**(21): 6325-36.
Staub, O. and D. Rotin (2006). "Role of ubiquitylation in cellular membrane transport." Physiol Rev **86**(2): 669-707.
Staub, O. and F. Verrey (2005). "Impact of Nedd4 proteins and serum and glucocorticoid-induced kinases on epithelial Na+ transport in the distal nephron." J Am Soc Nephrol **16**(11): 3167-74.
Staub, O., H. Yeger, et al. (1997). "Immunolocalization of the ubiquitin-protein ligase Nedd4 in tissues expressing the epithelial Na+ channel (ENaC)." Am J Physiol **272**(6 Pt 1): C1871-80.
Stockand, J. D., B. J. Spier, et al. (1999). "Regulation of Na(+) reabsorption by the aldosterone-induced small G protein K-Ras2A." J Biol Chem **274**(50): 35449-54.
Strautnieks, S. S., R. J. Thompson, et al. (1996). "A novel splice-site mutation in the gamma subunit of the epithelial sodium channel gene in three pseudohypoaldosteronism type 1 families." Nat Genet **13**(2): 248-50.
Stryer, L. (1999). "Biochemie." Spektrum, Akademischer Verlag **4. Auflage**.
Stutts, M. J., C. M. Canessa, et al. (1995). "CFTR as a cAMP-dependent regulator of sodium channels." Science **269**(5225): 847-50.
Subramanya, A. R., C. L. Yang, et al. (2006). "WNK kinases regulate sodium chloride and potassium transport by the aldosterone-sensitive distal nephron." Kidney Int **70**(4): 630-4.
Sudol, M., H. I. Chen, et al. (1995). "Characterization of a novel protein-binding module--the WW domain." FEBS Lett **369**(1): 67-71.
Summa, V., S. M. Camargo, et al. (2004). "Isoform specificity of human Na(+), K(+)-ATPase localization and aldosterone regulation in mouse kidney cells." J Physiol **555**(Pt 2): 355-64.
Summa, V., D. Mordasini, et al. (2001). "Short term effect of aldosterone on Na,K-ATPase cell surface expression in kidney collecting duct cells." J Biol Chem **276**(50): 47087-93.
Tahmasebi, M., J. R. Puddefoot, et al. (1999). "The tissue renin-angiotensin system in human pancreas." J Endocrinol **161**(2): 317-22.
Terlau, H. and W. Stuhmer (1998). "Structure and function of voltage-gated ion channels." Naturwissenschaften **85**(9): 437-44.

Thomas, C. P. and O. A. Itani (2004). "New insights into epithelial sodium channel function in the kidney: site of action, regulation by ubiquitin ligases, serum- and glucocorticoid-inducible kinase and proteolysis." Curr Opin Nephrol Hypertens **13**(5): 541-8.
Thomas, R. C. and R. W. Meech (1982). "Hydrogen ion currents and intracellular pH in depolarized voltage-clamped snail neurones." Nature **299**(5886): 826-8.
Thomas, W., V. McEneaney, et al. (2007). "Rapid responses to steroid hormones in the kidney." Nephron Physiol **107**(1): p1-9.
Tiwari, S., L. Nordquist, et al. (2007). "Trafficking of ENaC subunits in response to acute insulin in mouse kidney." Am J Physiol Renal Physiol **293**(1): F178-85.
Tombola, F., M. M. Pathak, et al. (2006). "How does voltage open an ion channel?" Annu Rev Cell Dev Biol **22**: 23-52.
Tong, Q. and J. D. Stockand (2005). "Receptor tyrosine kinases mediate epithelial Na(+) channel inhibition by epidermal growth factor." Am J Physiol Renal Physiol **288**(1): F150-61.
Uchiyama, M. and N. Konno (2006). "Hormonal regulation of ion and water transport in anuran amphibians." Gen Comp Endocrinol **147**(1): 54-61.
Urbach, V., E. Van Kerkhove, et al. (1996). "Cross-talk between ATP-regulated K+ channels and Na+ transport via cellular metabolism in frog skin principal cells." J Physiol **491 (Pt 1)**: 99-109.
Ussing, H. H. and K. Zerahn (1951). "Active transport of sodium as the source of electric current in the short-circuited isolated frog skin." Acta Physiol Scand **23**(2-3): 110-27.
Vallet, V., A. Chraibi, et al. (1997). "An epithelial serine protease activates the amiloride-sensitive sodium channel." Nature **389**(6651): 607-10.
Verrey, F. (1998). "Early aldosterone effects." Exp Nephrol **6**(4): 294-301.
Verrey, F. (1999). "Early aldosterone action: toward filling the gap between transcription and transport." Am J Physiol **277**(3 Pt 2): F319-27.
Verrey, F., D. Pearce, et al. (2000). "Pleiotropic action of aldosterone in epithelia mediated by transcription and post-transcription mechanisms." Kidney Int **57**(4): 1277-82.
Verrey, F., V. Summa, et al. (2003). "Short-term aldosterone action on Na,K-ATPase surface expression: role of aldosterone-induced SGK1?" Ann N Y Acad Sci **986**: 554-61.
Wald, H., O. Goldstein, et al. (1996). "Aldosterone induction and epithelial distribution of CHIF." Am J Physiol **271**(2 Pt 2): F322-9.
Wald, H., M. M. Popovtzer, et al. (1997). "Differential regulation of CHIF mRNA by potassium intake and aldosterone." Am J Physiol **272**(5 Pt 2): F617-23.
Wall, S. M. (2005). "Recent advances in our understanding of intercalated cells." Curr Opin Nephrol Hypertens **14**(5): 480-4.
Walter F. Boron, E. L. B. (2005). "Medical Physiology, updated edition." Elsevier Saunders.
Wang, H., L. M. Traub, et al. (2006). "Clathrin-mediated endocytosis of the epithelial sodium channel. Role of epsin." J Biol Chem **281**(20): 14129-35.
Wang, J., P. Barbry, et al. (2001). "SGK integrates insulin and mineralocorticoid regulation of epithelial sodium transport." Am J Physiol Renal Physiol **280**(2): F303-13.
Wang, W. and G. Giebisch (1991). "Dual effect of adenosine triphosphate on the apical small conductance K+ channel of the rat cortical collecting duct." J Gen Physiol **98**(1): 35-61.
Wang, W. H., A. Schwab, et al. (1990). "Regulation of small-conductance K+ channel in apical membrane of rat cortical collecting tubule." Am J Physiol **259**(3 Pt 2): F494-502.
Warnock, D. G. (1998). "Liddle syndrome: an autosomal dominant form of human hypertension." Kidney Int **53**(1): 18-24.
Wiemuth, D., Y. Ke, et al. (2007). "Epithelial sodium channel (ENaC) is multi-ubiquitinated at the cell surface." Biochem J **405**(1): 147-55.
Wilker, E. and M. B. Yaffe (2004). "14-3-3 Proteins--a focus on cancer and human disease." J Mol Cell Cardiol **37**(3): 633-42.
Wilkinson, K. D. (2000). "Ubiquitination and deubiquitination: targeting of proteins for degradation by the proteasome." Semin Cell Dev Biol **11**(3): 141-8.

Williams, G. H. (2005). "Aldosterone biosynthesis, regulation, and classical mechanism of action." Heart Fail Rev **10**(1): 7-13.
Winter, C., N. Schulz, et al. (2004). "Nongenomic stimulation of vacuolar H+-ATPases in intercalated renal tubule cells by aldosterone." Proc Natl Acad Sci U S A **101**(8): 2636-41.
Yaffe, M. B. (2002). "How do 14-3-3 proteins work?-- Gatekeeper phosphorylation and the molecular anvil hypothesis." FEBS Lett **513**(1): 53-7.
Young, M. and J. W. Funder (2000). "Aldosterone and the heart." Trends Endocrinol Metab **11**(6): 224-6.
Yu, F. H., V. Yarov-Yarovoy, et al. (2005). "Overview of molecular relationships in the voltage-gated ion channel superfamily." Pharmacol Rev **57**(4): 387-95.
Yue, G., B. Malik, et al. (2002). "Phosphatidylinositol 4,5-bisphosphate (PIP2) stimulates epithelial sodium channel activity in A6 cells." J Biol Chem **277**(14): 11965-9.
Zecevic, M., D. Heitzmann, et al. (2004). "SGK1 increases Na,K-ATP cell-surface expression and function in Xenopus laevis oocytes." Pflugers Arch **448**(1): 29-35.
Zhang, Y. H., D. Alvarez de la Rosa, et al. (2005). "Insulin-induced phosphorylation of ENaC correlates with increased sodium channel function in A6 cells." Am J Physiol Cell Physiol **288**(1): C141-7.
Zhou, R., S. V. Patel, et al. (2007). "Nedd4-2 catalyzes ubiquitination and degradation of cell surface ENaC." J Biol Chem **282**(28): 20207-12.

9 Acknowledgements

Financial support:

- URPP “Integrative Human Physiology” PhD Fellowship for 2 years salary
- URPP “Integrative Human Physiology” consumable grant

Further I would like to thank

Prof. François Verrey, my thesis supervisor and boss, for the guidance through the years of my thesis.

Prof. Dr Olivier Staub, Prof. Dr Thomas Lutz the members of my thesis comitee, that accepted the task of going with me as pioneers through the whole ZIHP procedures including meetings exams and discussions.

Panos Fakitsas for collaboration and the performance of the gene screen;

Dr. Simone M. R. Carmargo and Dustin Singer who contributed with their work to the completion of my thesis: Dr. Carmargo performed the retroviral transduction of the mouse cells and Dustin Singer performed the mouse kidney fixations.

Our collaborators: Prof. Dr Olivier Staub and members of his group that performed next to functional tests in oocytes also the experiments in cultured HEK cells.

Ian Forster for great support concerning all kind of issues around the electrophysiology (including the Ussing Chamber).

Vicky and Dustin for proofreading and helpful advices.

All current and former members of the Verrey group, and specially Simone, Tamara, Dustin, Thomas, Brigitte for helpful discussions and advises and great support in good and bad times.

Sonja and Marta for many great evenings and other activities that we could enjoy together.

Meiner Familie, die mich immer unterstützt hat, speziell meiner Mama, die es schafft mich immer wieder aufzubauen und zu motivieren.

Meinem Schatz Stephan, der mir immer unterstützend zur Seite steht und mir Kraft gibt.